SCHOOL OF ENGINEERING

ELECTRIC POWER SYSTEMS RESEARCH GROUP

INVESTIGATING THE IMPACT OF ASSET CONDITION ON DISTRIBUTION NETWORK RECONFIGURATION AND ITS CAPACITY VALUE

A THESIS PRESENTED FOR THE DEGREE OF DOCTOR OF PHILOSOPHY

ILIAS SARANTAKOS

JULY 2019

Abstract

Generally, decisions regarding Distribution Network (DN) operations are based only on operational parameters, such as voltages, currents and power flows. Asset condition is a key parameter that is usually not considered by Network Management Systems (NMSs) in their optimization process. The work in this thesis seeks to quantify the extent to which asset condition information can positively influence network operation and planning; specifically through Distribution Network Reconfiguration (DNR).

Asset condition can be translated into Health Indices (HIs) and failure rates, allowing an NMS – or an optimization algorithm – to make better informed decisions. This is realized via appropriate asset condition assessment and failure rate models. The effect on optimal DNR is evaluated – focusing on substation condition and reliability; the idea of load transfer from one feeder or substation to a more reliable one is key in the proposed methodology. Condition-based risk is considered in the DNR problem, and the impact of transformer ageing on network reconfiguration is examined as well. The effect of asset condition assessment and ageing – which depends on the type of network branches (overhead lines or underground cables) – on the optimal distribution switch automation is also investigated. Finally, a probabilistic method is developed to quantify the contribution of DNR to network security considering asset condition and ageing.

The results show that savings can be in the order of tens of thousands of U.S. dollars for a single DN; this corresponds approximately to 10% of the annual cost of active power losses. This can mean hundreds of thousands – or even millions – of U.S. dollars of savings for a single DN operator. Regarding the optimal placement of automated switches, neglecting the effect of asset ageing can result in an underestimation of expected outage cost by as much as $223,000 over a 20-year period. Finally, ignoring the contribution of DNR to security of supply can double the estimation of network risk; in addition to that, disregarding asset condition and ageing results in a reinforcement deferral overestimation of two years.

Declaration

I hereby declare that this thesis is a record of work undertaken by myself, that it has not been the subject of any previous application for a degree, and that all sources of information have been duly acknowledged.

Parts of this thesis have been published by the author:

CHAPTER 4

I. Sarantakos, D. Greenwood, J. Yi, S. Blake, and P. Taylor, "A Method to Include Component Condition and Substation Reliability into Distribution System Reconfiguration", *International Journal of Electrical Power and Energy Systems*, 2019, DOI: 10.1016/j.ijepes.2019.01.040.

Acknowledgements

Δόξα τω Θεώ! Ευχαριστώ το Θεό, την Παναγία μας, τον πνευματικό μου π. Θεμιστοκλή (που χωρίς την ευχή του, τίποτα καλό δε μπορώ να κάνω), τους Αγγέλους μας, τον Άγιο Προφήτη Ηλία, τους Αγίους Τρεις Ιεράρχες (τους Προστάτες της Παιδείας και των Γραμμάτων), τον Άγιο Ελευθέριο και τη μητέρα του Αγία Ανθία, τον Άγιο Παΐσιο, τον Άγιο Αρσένιο, την Αγία Αντιγόνη, τον Άγιο Ιωάννη της Κροστάνδης, τον Άγιο Μελέτιο, τον Άγιο Cuthbert, τον Άγιο Bede, και όλους τους Αγίους, τους π. Δημήτριο, π. Δημήτριο, π. Ειρηναίο, π. Αντώνιο, π. Αθηναγόρα, π. Ευάγγελο, π. Ραφαήλ, π. Θωμά, π. Μιχαήλ, π. Ανδρέα, π. Andrew, π. Ιωακείμ, και π. Αντώνιο. Ευχαριστώ την αγάπη μου, την Αντιγόνη για την αγάπη της, που πάντα με άκουγε σε αυτά που είχα να της πω και με συμβούλευε και με ενθάρρυνε πολύ, και για όλη τη φροντίδα της· χωρίς τη σύζυγό μου, οπωσδήποτε, δε θα τα είχα καταφέρει. Ευχαριστώ τους γονείς, τους παππούδες, τις γιαγιάδες, και τα αδέλφια μας, για όλα όσα έχουν κάνει για εμένα. Τέλος, ευχαριστώ τους κολλητούς μου Παρασκευά (και την οικογένειά του), Γρηγόρη, Σοφία, Θωμά, και τους φίλους μου Ευθύμη, Κωνσταντίνο, και Παύλο. Δεν αναφέρθηκα σε πολλούς· με συγχωρείτε και σας ευχαριστώ.

I would like to express my gratitude to my supervisors, Professor Phil Taylor, Dr Pádraig Lyons, Dr Simon Blake, Dr Jialiang Yi, and – last but not least – Dr David Greenwood (in order of appearance!). Apparently, I had a number of supervisors; thank God, David – when he was about to leave (and abandon me) as well – changed his mind and finally stayed here. I honestly thank all of you for your guidance and patience; without your help and support, this work would have been impossible.

I would also like to acknowledge the support of my industrial supervisors and partners, Scott Rowland, Dr Graeme Coapes, Dr Serdar Çelik, and Dr Liang Tao from Siemens; their advice and help has been really important to me.

Finally, I would like to acknowledge my colleagues and friends, Stalin Muñoz (for all the time that we spent together, for our discussions, and for

his help), Varvara Alimisi, Manolis Loukarakis, Peter Davison, Haris Patsios, Neal Wade, Damian Giaouris, Iván Castro León, Pengfei Wang, Nikolas Spiliopoulos, Luke Burl, Timur Sayfutdinov, Natalia Zografou (for the many discussions we have had and her help), and George Gkizas; many thanks folks.

List of Publications

JOURNAL PAPERS

I. Sarantakos, D. Greenwood, J. Yi, S. Blake, and P. Taylor, "A Method to Include Component Condition and Substation Reliability into Distribution System Reconfiguration", *International Journal of Electrical Power and Energy Systems*, 2019, DOI: 10.1016/j.ijepes.2019.01.040.

I. Sarantakos, D. Greenwood, and P. Taylor, "A Probabilistic Method to Quantify the Contribution of Network Reconfiguration to Security of Supply Considering Asset Condition and Ageing", *IEEE Transactions on Power Systems*, 2019 (Under Revision).

CONFERENCE PROCEEDINGS

D. Greenwood, **I. Sarantakos**, P. Davison, C. Patsios, A. Ahmad, and M. Black, "Enhancing the Understanding of Distribution Network Losses", *CIRED*, Madrid, Spain, 2019.

I. Sarantakos, P. Lyons, S. Blake, P. Taylor, L. Tao, S. Celik, and S. Rowland, "Incorporating Asset Management into Power System Operations", *CIRED*, Glasgow, UK, 2017.

S. Blake, **I. Sarantakos**, and P. Taylor, "Effects of Network Reinforcement Options on Energy Losses", *CIRED*, Glasgow, UK, 2017.

Acronyms

Acronym	Definition
ACSR	Aluminium Conductor Steel Reinforced
AM	Asset Management
CB	Circuit Breaker
CDF	Customer Damage Function
CI	Customer Interruptions
CLNR	Customer-Led Network Revolution
CML	Customer Minutes Lost
CNAIM	Common Network Asset Indices Methodology
CoF	Consequences of Failure
DG	Distributed Generation
DGA	Dissolved Gas Analysis
DN	Distribution Network
DNO	Distribution Network Operator
DPSO	Discrete Particle Swarm Optimization
DSR	Demand Side Response
ECC	Equivalent Conventional Capacity
ECOST	Expected Customer Interruption Cost
EENS	Expected Energy Not Supplied
EFC	Equivalent Firm Capacity
ELCC	Effective Load Carrying Capability
ENS	Energy Not Supplied
ESS	Energy Storage System
FFA	Furfuraldehyde
GA	Genetic Algorithm
GB	Great Britain
HI	Health Index
HV	High Voltage
IEC	International Electrotechnical Commission
IEEE	Institute of Electrical and Electronics Engineers
LOLP	Loss of Load Probability
LP	Load Point
LV	Low Voltage
MINLP	Mixed-Integer Nonlinear Programming

MV	Medium Voltage
NaFIRS	National Fault and Interruption Reporting Scheme
NMS	Network Management System
NOP	Normally Open Point
Ofgem	Office of Gas and Electricity Markets
OHL	Overhead Line
PoF	Probability of Failure
PSO	Particle Swarm Optimization
RBTS	Roy Billinton Test System
RCM	Reliability-centered Maintenance
RCS	Remote Controlled Switch
RTTR	Real-Time Thermal Rating
S/S	Substation
SAIDI	System Average Interruption Duration Index
SOP	Soft Open Point
SP	Supply Point
TNR	Total Network Risk
TPC	Taiwan Power Company
TSC	Total Supply Capability
TTF	Time to Failure
TTR	Time to Repair
TTS	Time to Switch
TX	Transformer
UGC	Underground Cable

Nomenclature

A, B, C	Failure rate model parameters (*Brown et al.*)	
age	Current age of the asset	[yr]
$A_{k,t}$	Availability of branch k at time t	
C	Failure rate model constant (CNAIM)	
CI	Network risk cost of customer interruptions	[$]
C_{jp}	Interruption cost of LP p due to failure event j	[$/kW]
CML	Network risk cost of customer minutes lost	[$]
$Cost_{\mathrm{LoL}}$	Cost of loss of life of primary S/S transformers	[$]
$Cost_{P_{\mathrm{loss}}}$	Annual cost of active power losses	[$/yr]
$Cost_{P_{\mathrm{loss,daily}}}$	Cost of active power losses for a one-day period	[$]
$C_{P_{\mathrm{loss}}}$	Cost coefficient for losses	[$/kW]
D	Difference operator, in difference equations	
Dt	Time step	[min]
D_t	Power of the demand group at time t	[MVA],[MW]
DF	Probability of second failure before first is restored	
ECOST	Total ECOST of the network ($ECOST_1$ + $ECOST_2$)	[$/yr]
$ECOST_1$	ECOST for failures in primary DN	[$/yr]
$ECOST_2$	ECOST for failures at S/Ss and upstream network	[$/yr]
$ECOST_{jp}$	ECOST of load point p due to failure event j	[$/yr]
EENS	Expected energy not supplied	[MWh/yr]
EL	Expected life of an asset	[yr]
ENS_t	ENS during time period t	[MWh]
EP	Energy Price	[$/kWh]
F	% of failures that result in an interruption of supply	
HI	(Current) Health Index of an asset	
HI_{EL}	Asset HI when expected life is reached, equal to 5.5	
HI_{f}	Future HI	
HI_{init}	Initial HI (related to age)	

HI_{new}	HI of a new asset, equal to 0.5	
I	Current	[A]
IC	Installation Cost	[$]
I_k	Current of branch k	[A]
$I_{k,max}$	Current rating of branch k	[A]
IR	Interest rate	
K	TX Load Factor (load current / rated current)	
k_{11}, k_{21}, k_{22}	Thermal model constants	
K_{FR}	Failure rate model constant (CNAIM)	
L	Total ageing over the time period considered	[days]
LF	Load Factor	
LG	Load growth rate (per year)	
LLF	Loss Load Factor	
L_p	Average load of load point p	[MW]
MC	Maintenance Cost (total)	[$]
MC_{unit}	Maintenance Cost of an RCS	[$]
$MTTF$	Mean time to failure	[h]
N_{br}	Number of branches	
N_{bus}	Number of buses	
NC	Number of customers	
N_{days}	Number of days in the Monte Carlo simulation	
$N_{ev,p}$	Number of possible failure events for LP p	
N_f	Number of feeders	
N_{hours}	Number of hours in the Monte Carlo simulation	
N_{LP}	Number of load points	
N_S	Number of RCSs	
N_{years}	RCS life period	
p	Index of load points	
P	Active Power	[W]
P_c	Probability that a CB fails to open when required	

Pen	Overall penalty term for the objective function	[$/yr]
Pen_1	Penalty term for loop constraints	[$/yr]
Pen_2	Penalty term for operational constraints	[$/yr]
P_{loss}	Active power losses (calculated at peak load)	[W]
Q	Reactive Power	[VAr]
r	Repair time	[h]
R	Resistance	[Ω]
r''	Maintenance outage time	[h]
$R1$	% of customers restored via automated switching	
$R2$	% of customers restored after manual switching	
r_{af}	Ageing reduction factor	
R_c	Rating of one incoming circuit	[MVA]
r_{jp}	Interruption duration of LP p due to failure event j	[h]
R_k	Resistance of branch k	[Ω]
R_L	Ratio of losses at rated current to no-load losses	
RT	Restoration time	[h],[min]
SC	Capital cost of an RCS	
$S_{j,max}$	Rating of the first branch of feeder F_j	[MVA]
S_t^j	Apparent power of the first branch of feeder F_j at t	[MVA]
ST	Switching time	[h],[min]
TNR	Total Network Risk	[$]
Total Cost 1	Loss Cost + $ECOST_1$	[$/yr]
Total Cost 2	Loss Cost + $ECOST_1$ + $ECOST_2$	[$/yr]
TTF	Time to failure	[h]
TTR	Time to repair	[h]
TTS	Time to switch	[h]
UCI	Unit cost to DNO per interrupted customer	[$]
$UCML$	Unit cost to DNO per customer minute lost	[$]
V	Voltage	[V]
V_{max}	Maximum voltage limit	[V]

V_{min}	Minimum voltage limit	[V]
W	Relative ageing rate	
x	State vector	
X_t	Available capacity of incoming circuits at time t	[MVA]
y	Winding exponent	
Y_t	Available contribution of feeders of adjacent S/Ss	[MVA]
z	Oil exponent	
Z_t	Loss of load at time t	[MVA]
β_1	Initial ageing rate	[yr^{-1}]
β_2	Forecast ageing rate	[yr^{-1}]
Δt	Duration of each time interval t	[h]
$\Delta\theta_h$	Hot-spot-to-top-oil gradient at the load considered	[K]
$\Delta\theta_{hr}$	Hot-spot-to-top-oil (in tank) gradient at rated current	[K]
$\Delta\theta_{or}$	Top-oil (in tank) temperature rise at rated losses	[K]
θ_a	Ambient temperature	[°C]
θ_h	Hot-spot temperature	[°C]
θ_o	Top-oil temperature (in tank) at the load considered	[°C]
λ	(Overall) Failure rate	[f/yr]
λ''	Maintenance outage rate	[out/yr]
λ_A	Active failure rate	[f/yr]
λ_{cb}	Condition-based failure rate	[f/yr]
λ_j	Failure rate for failure event j	[f/yr]
λ_{ncb}	Non-condition-based failure rate	[f/yr]
λ_P	Permanent (total) failure rate	[f/yr]
τ_o	Average oil time constant	[min]
τ_w	Winding time constant	[min]
$\Omega_{br}^{F_j}$	Set of branches of feeder F_j	
$\Omega_{bus}^{F_i}$	Set of buses of feeder F_i	
$\Omega_{bus}^{F_j}$	Set of buses of feeder F_j	

Table of Contents

List of Figures

List of Tables

Chapter 1. Introduction

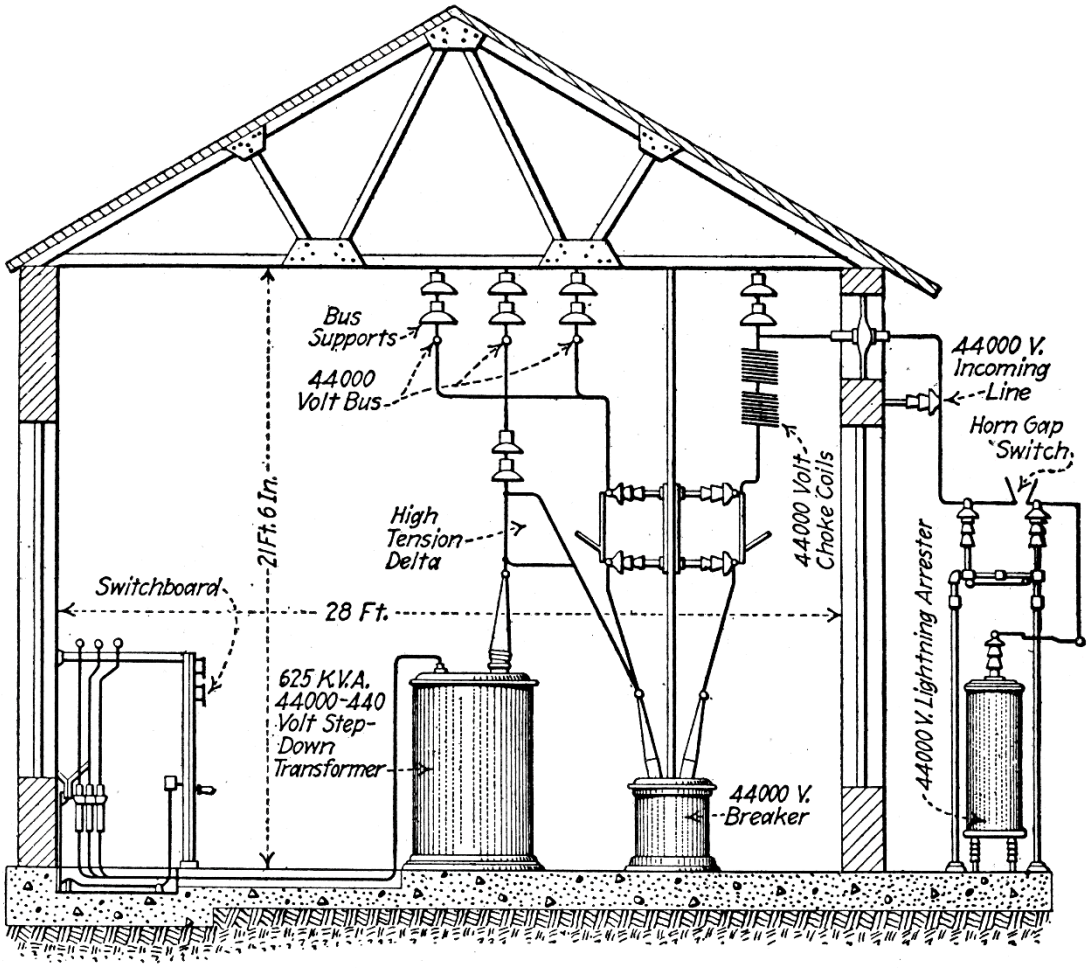

1.1. BACKGROUND

The privatization of the electrical power industry and ageing equipment in distribution networks (DNs) requires Distribution Network Operators (DNOs) to continually consider new and innovative approaches to the management of their assets. Asset Management (AM) is a process that seeks to find the optimal balance between expenditure, performance and risk. More specifically, the objective of AM decisions for a DNO is to minimize the life-cycle costs of its assets, while maintaining high levels of reliability at an acceptable level of risk [1, 2]. Maintaining this balance is becoming increasingly difficult due to the proliferation of renewables-based distributed generation (DG) with their associated power output variability, evolving loads such as electric vehicles and heat pumps, and the increasingly old power system components [3, 4].

The regulatory changes over the last few decades have put great pressure on DNOs to reduce their expenditure; power utilities have done so by postponing investments, reducing internal expertise, and decreasing maintenance frequency. So far, this has not had an effect on the reliability of DNs, but it may have a detrimental impact in the coming years, with the potential for the quality of supply to decline quickly [5].

Concurrently, DNs have the highest share of customer service interruptions in power systems [6, 7]. Typical national fault statistics for the UK [8] are presented in Figure 1.1, which illustrates the proportions of the total number of incidents, of customer interruptions (CIs), and of customer minutes lost (CMLs), by voltage level. The British gas and electricity regulator (Office of Gas and Electricity Markets) rewards or penalizes DNOs according to their performance with respect to the aforementioned metrics [9]. These measures result in the DNOs concentrating their efforts on improving performance in these indices, particularly at Medium Voltage (MV) level. It should be noted that 20 kV, 11 kV, and 6.6 kV are classified as High Voltage (HV) in the UK (as far as electricity distribution is concerned); however this thesis refers to these voltages as MV, as this is the case in

most other countries. The conventional approach to improving fault performance in a DN is reinforcement and asset replacement, which can be very costly.

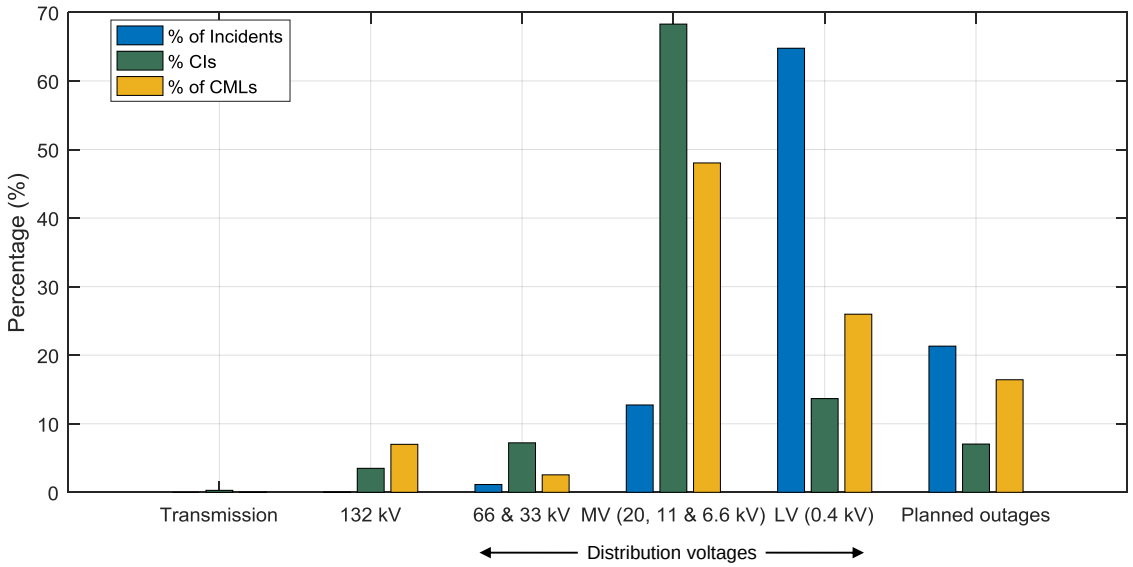

Figure 1.1: Customer interruptions at different voltage levels.

As mentioned earlier, the main dilemma for DNOs today is between cost and quality of supply. This means that power utilities should allocate their financial resources in the best possible way, in order to improve the reliability of their networks. Asset condition information is a key parameter that can contribute considerably to achieving this objective.

Current practice is that DN operations and planning do not take asset condition into account. However, the proliferation of smart grid technologies such as active network management, condition monitoring and AM decision support tools and methodologies [10], such as the DNO Common Network Asset Indices Methodology (CNAIM) [11], will provide DNOs with opportunities to incorporate asset condition information into network operations and planning, by integrating these technologies.

Typically, network operation and planning decisions are made by an optimization process, which takes account of voltages, currents, and power flows. Besides, AM strategies (asset maintenance, refurbishment, and replacement programs) make use of condition data in order to optimize asset life-cycle costs. These two worlds do not collaborate with each other;

however, using appropriate AM methodologies, asset condition data can be converted into Health Indices (HIs) and failure rates, which can be used to inform the optimization process. This concept is illustrated diagrammatically in Figure 1.2.

The work in this thesis demonstrates how asset condition can be included in a number of DN operation and planning problems, which involve Distribution Network Reconfiguration (DNR). This is primarily achieved by making decisions for the network, which take account of not only the operational parameters of the DN, but also the condition of the assets, through their corresponding HIs.

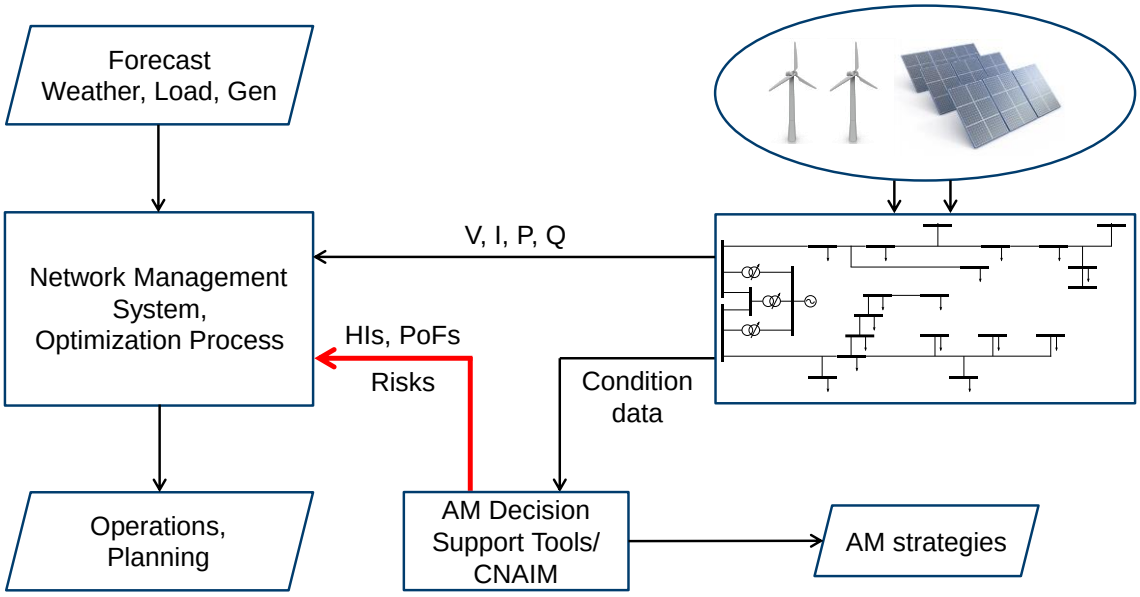

Figure 1.2: The inclusion of asset condition into network operation and planning.

1.2. Overview of Asset Condition

Network reliability models generally use average component failure rates [12]. However, there are a number of methodologies and AM decision support tools that relate specific asset condition parameters to a single value, which indicates its overall condition [13]. The condition parameters can be assessed and assigned a score using maintenance or condition monitoring data, which will become more prevalent in smart networks and modern substations (S/Ss). HIs, and their associated condition-based failure

rates can then be derived and along with the Consequences of Failure (CoF), the risk can be calculated.

In the UK, the Office of Gas and Electricity Markets (Ofgem) approved in 2017 a common methodology (CNAIM) [11] across all DNOs for the evaluation, forecasting, and regulatory reporting of asset condition and associated risks. This will encourage DNOs to collect and utilize condition data in a more systematic way. Consequently, DNOs will have better knowledge and understanding of the condition of their assets, which could facilitate the application of the proposed work to a DN.

In this methodology, several condition parameters, such as age, observed and measured condition information, can be combined in an appropriate way and yield a single value, which indicates the overall condition of an asset. This figure is called asset HI and can be of great importance in AM and network operation decisions. The present work uses the term 'Health Index' instead of 'Health Score', which is used by CNAIM. Based on the HI of the asset, the corresponding probability of failure (PoF) can be calculated. PoF is the first key parameter of this methodology. The second is CoF, which can be broken down into four categories, namely financial, safety, environmental and network performance. PoF and CoF are combined in order to derive a single figure for asset risk, expressed in monetary terms. The aforementioned process, which describes how the condition-based risk of an asset is calculated, is illustrated in Figure 1.3.

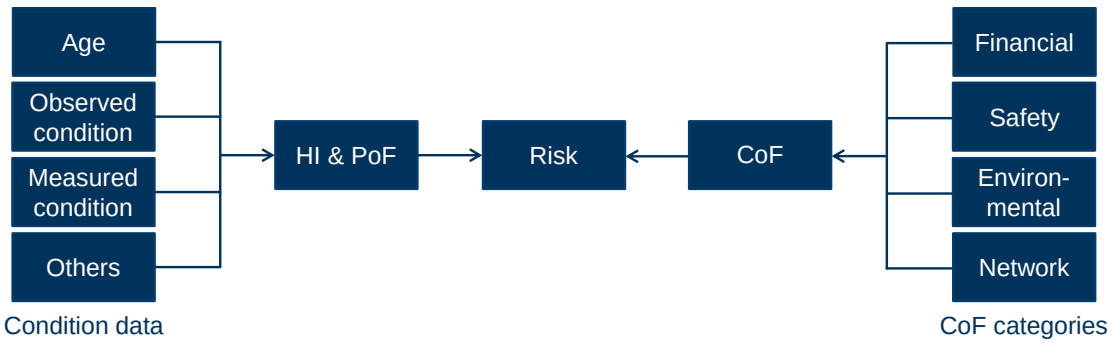

Figure 1.3: CNAIM process overview.

As an illustrative example of this methodology, the PoF – HI curve of a circuit breaker (CB) located at a primary S/S, is illustrated in Figure 1.4. It should be noted that in this thesis, the terms 'PoF' and 'failure rate' are used interchangeably.

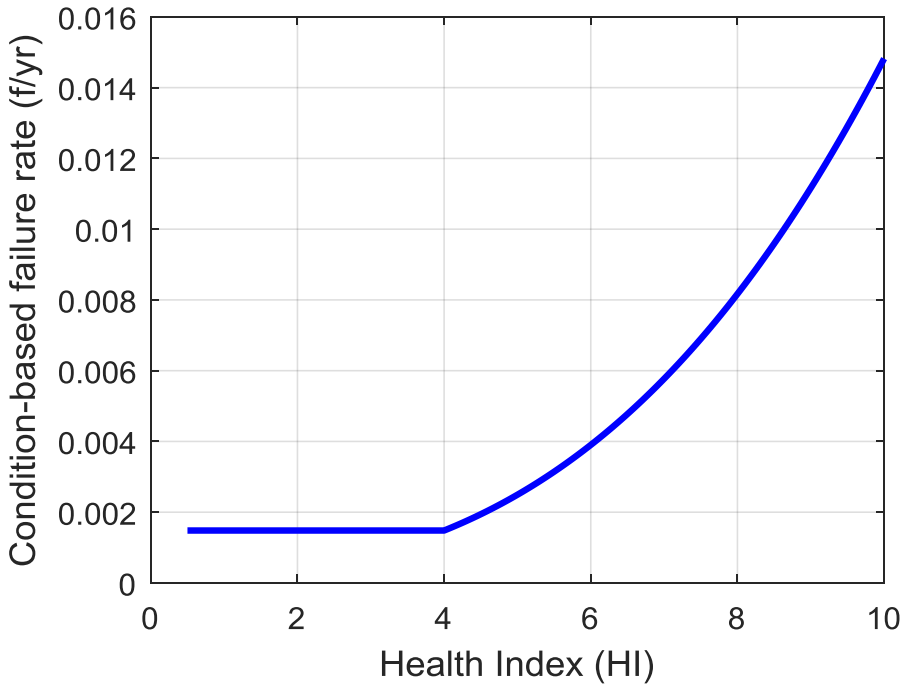

Figure 1.4: Condition-based PoF – HI curve of a CB located at a primary substation.

1.3. Distribution Network Reconfiguration

Distribution Network Reconfiguration can be defined as the procedure of changing the configuration of the network using the branch switches. There are two types of switches: normally open and normally closed. The state of these devices determines the topology of the network. For each possible topology, all of the constraints should be satisfied, including the radiality of the network. DNs are typically constructed as meshed systems, but they are operated in radial configuration. This is primarily to reduce the number of network components exposed to a failure on any single feeder, in the case of a fault on the network [6].

Different combinations of open and closed switches result in different network configurations. To illustrate that, an example network is shown in

Figure 1.5. Each network topology is associated with specific values of network variables, such as voltages, currents, and power flows. These variables, in turn, determine the values of a number of network functions, such as active power losses, voltage deviation, and load balance. These can be the objective functions of an optimal DNR problem. The network configuration (i.e. the combination of open and closed switches) that optimizes a given objective function is called the optimal network configuration.

Optimal DNR is a combinatorial nonlinear optimization problem [14] and the size of its search space can become extremely large, even for relatively small DNs. The network in Figure 1.5, for example, has hundreds of billions of possible radial configurations. The first work on this topic was from *Merlin* and *Back* [15], in 1975 and since then, significant research has been conducted. An extensive literature review on this topic can be found in Chapter 3.

Minimization of active power losses has been the most common objective in the relevant literature. To the best of the author's knowledge, reconfiguration to improve network reliability had not been investigated until 2001, when a paper by *Brown et al.* [16] extended the use of DNR to optimize reliability. There are several strategies available (except DNR) to power utilities to enhance the reliability of their networks, some of which are mentioned below [7]:

1) Protection devices: the first step to increase network reliability is to place fuses on all laterals; this is critical as a fault on an unfused lateral will cause an outage to all load points of a feeder, whereas a fault on a fused lateral will only lead to a disconnection of the load point(s) downstream of the fuse.
2) Reclosers: these devices can be employed to enable self-clearance of temporary faults on overhead lines.
3) Sectionalizing switches: the key motivation of switching – in order to improve reliability – is the capability it can provide to isolate a fault

and restore a number of disconnected customers before the repair is completed.

4) Automation: this process can substantially decrease the time required to perform switching actions (fault isolation and restoration) leading to reduced outage durations.
5) Faster crew response: after a fault occurs, the operator dispatches a crew to locate the fault; then isolate it by opening the appropriate disconnect switches (they might also restore some load points by closing specific normally open points). After switching is completed, the repair of the faulted component(s) is carried out by the crew, and finally the network returns to its initial state. In order to achieve improved crew response times, the following reliability improvement projects might be an option: a) outage management systems, b) faulted circuit indicators, c) automatic fault location devices, and d) increased number of crews and dispatch centers.

The main advantage of DNR (considering manual switching) compared to other solutions is its little or even zero capital expenditure. The main idea behind this technique is to transfer customers currently experiencing poor reliability to adjacent feeders, or even S/Ss, with a higher level of reliability [7].

Available literature on reliability reconfiguration makes use of average failure rates without considering the condition of the assets. Nevertheless, as mentioned earlier, DNOs in the UK are already required to regularly report asset HIs to Ofgem; this fact that can accommodate the transition to condition-based reliability in network reconfiguration problems.

Another significant factor than can have a material impact on DNR – and is currently neglected – is S/S reliability. Typically, in DNR studies, when multiple S/Ss are considered, their reliability is not taken into account, or they are assumed to be totally reliable. This means that the reliability of two load points supplied from two different S/Ss can have significantly

different values, if S/S reliability is taken into account – especially if their condition is considered.

The work in this thesis primarily focuses on reliability-based DNR, considering asset condition and S/S reliability, and further elaborates on them in Chapters 3 and 4.

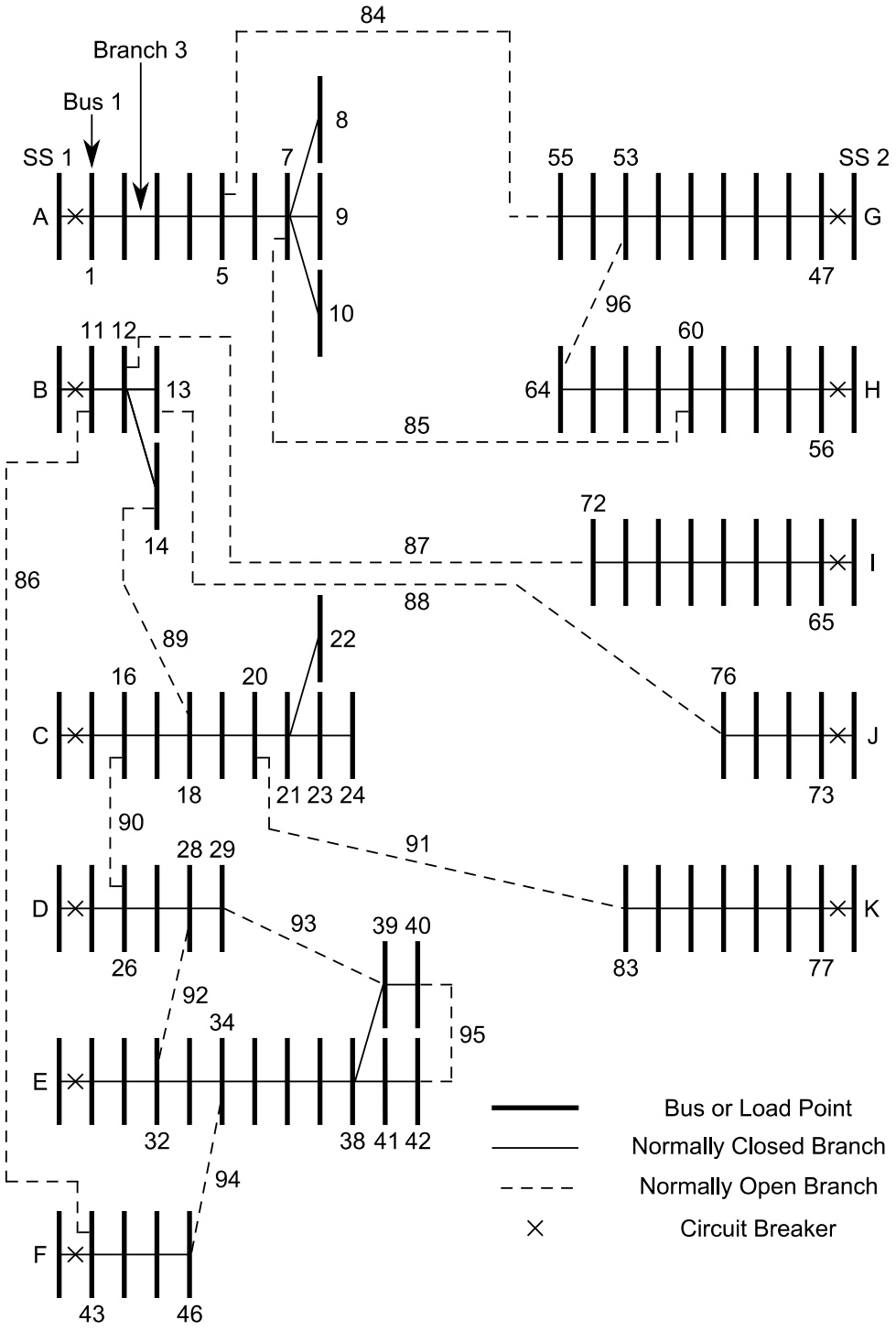

Figure 1.5: A DN from Taiwan Power Company (used as an example network).

1.4. Distribution Switch Automation

In terms of distribution automation, we typically refer to automated S/Ss and feeder switches [7]. This section gives an overview of the switch automation problem (i.e. the optimal automated switch placement). Automation – as also previously mentioned – can significantly reduce the time required to isolate a fault and restore interrupted customers, which in turn can result in critical reliability improvement, in terms of interruption duration. In order to demonstrate the importance of the problem and make it more comprehensible, the process that is followed after a fault on a main feeder section, is illustrated in Figure 1.6.

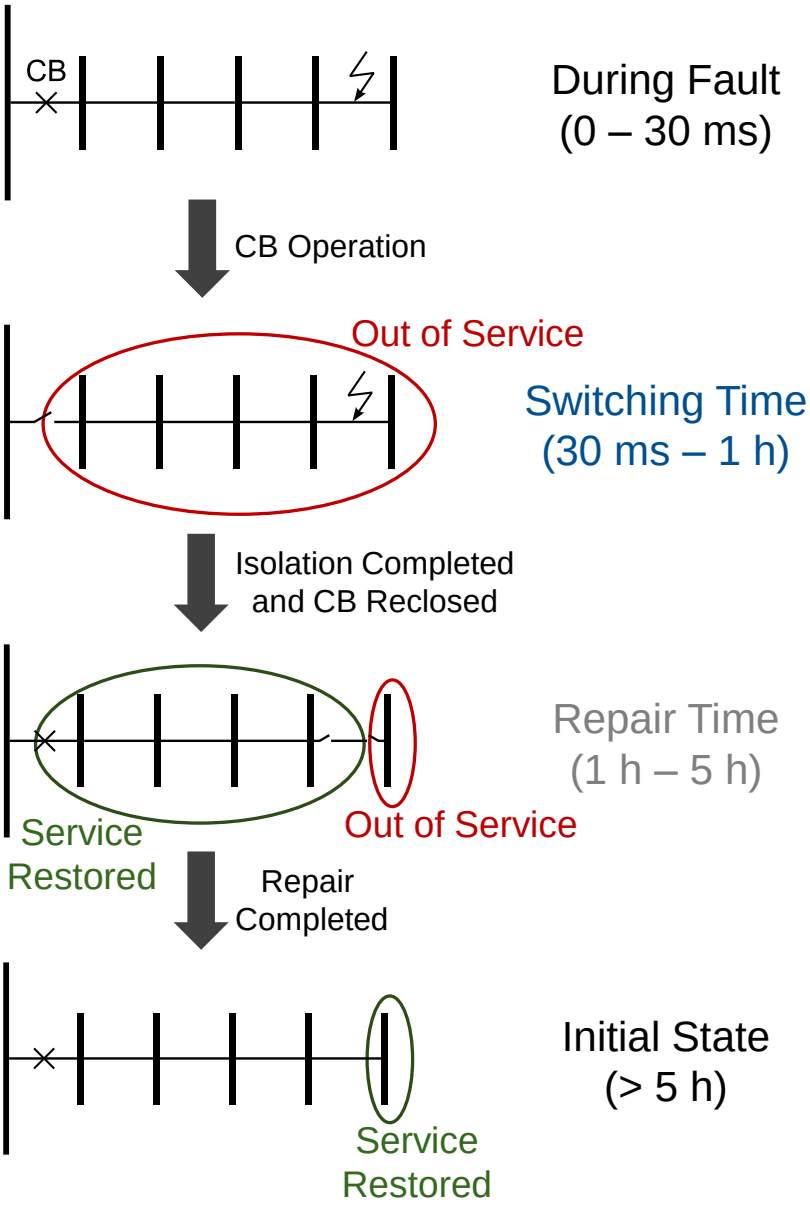

Figure 1.6: Process after an active fault on a main feeder section (the diagram refers to manual switching; times are taken from [17]).

In the case of an active failure (i.e. fault that causes CBs to operate) along the main feeder, the CB operates in order to clear the fault. Consequently, all load points (LPs) of the feeder are interrupted until the CB is reclosed. This can be done after the fault has been detected and isolated (by opening the relevant disconnect switches); the time required to perform these actions is called switching time. After the CB has been reclosed, the power supply, between the supply point and the point of isolation, is restored. The LPs located downstream of the faulted branch are restored after the repair process has been completed, unless they can be transferred onto another feeder through a normally open point (NOP) [6].

If it is assumed that each bus (LP) in Figure 1.6 supplies 200 customers, then for the fault illustrated, the number of disconnected customers is as shown in Figure 1.7. In this case the customer loss is equal to 1,000×1 + 200×4 = 1,800 customer·hours. Manual switching duration was 1 hour in this example; it can take longer, depending on the location of the fault and other conditions. If there was an automated switch upstream of the failure in the faulted branch with a switching time of 2 minutes, then the corresponding customer loss would be 1,027 customer·hours. Therefore, automation can play a very important role in reducing the duration of customer interruptions.

Specifically, automated switches can contribute to the reduction of outage duration in the following manner: 1) if an automated switch is placed in a normally closed branch, it reduces significantly the time to isolate a failure; and 2) if the switch is installed in a normally open branch, it reduces the time to (post-fault) reconfigure the network, i.e. supply specific LPs via an alternative route [18].

The decision of which switches to automate in a DN in order to optimize a specific reliability index, taking the investment cost into account, is the problem of optimal placement of automated switches. This problem will be studied in more detail in Chapter 5.

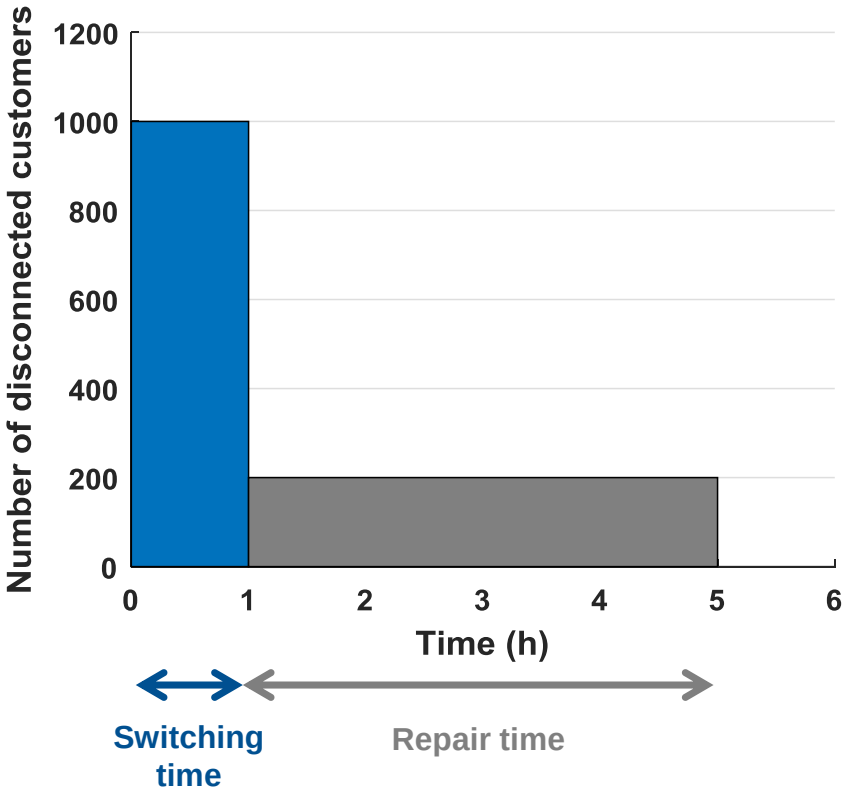

Figure 1.7: Customer interruptions following an active failure on a main feeder section.

1.5. SECURITY OF SUPPLY AND DNR

Security of supply generally refers to the N-k principle, which means that a network with N components should be capable of supplying its customers, even in the case of unavailability of k components. The present security of supply standard in the UK (Engineering Recommendation P2/6 [19]) states that for a group demand between 12 and 60 MW, only one incoming circuit (at a primary S/S) should be considered sufficient to supply the peak load. Figure 1.8 shows a primary S/S (S/S 1), which supplies its load, through two 16 MVA transformers. Without considering load transfer capability to adjacent S/Ss (S/S 2 and S/S 3), the maximum load that could be supplied following the first circuit outage (i.e. after losing a line or transformer) is 16 MVA. Therefore, if the peak demand rises to a value greater than that, network reinforcement is required. A conventional reinforcement is illustrated in Figure 1.8, which is the addition of a new circuit alongside the existing ones. The network used for illustration of this concept is the RBTS Bus 4 DN [17].

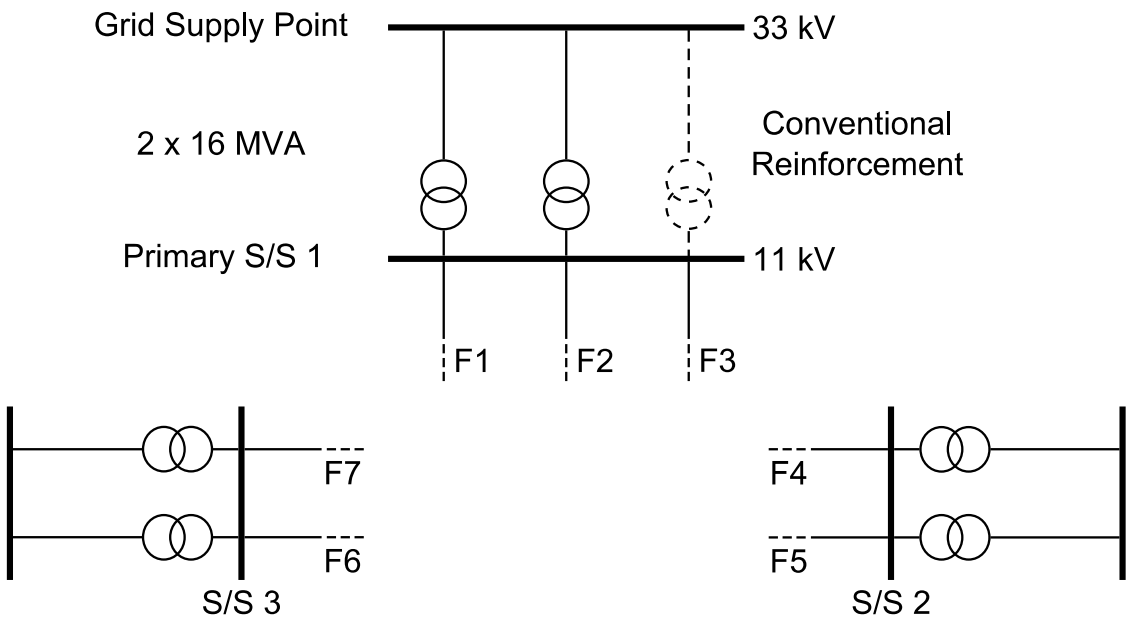

Figure 1.8: The RBTS Bus 4 DN, with conventional network reinforcement at S/S 1 to accommodate increased demand.

Postponing network investment can be achieved by a number of means such as (DG), energy storage systems (ESSs), demand side response (DSR), real-time thermal ratings (RTTRs), and DNR. Each of these solutions can contribute a specific amount to the security of supply of a DN, and based on that, decisions regarding reinforcement can be made [20-23].

When compared to the aforementioned solutions, DNR (considering manual switching) can contribute to network security for little or no capital expenditure [7]. Therefore, it is of great value to formally quantify the capacity contribution that can be made by DNR. P2/6 states that this contribution should be taken into account, when examining the need for reinforcement. However, this standard does not provide a methodology to quantify this value. In other words, the reconfiguration capability cannot play a part in a DNO's compliance with P2/6, which may lead to investment decisions being made much earlier than strictly necessary.

The capacity value (or capacity credit) of an asset can be defined as the additional load that can be accommodated because of the asset contribution, while maintaining the same reliability level. In the literature the terms 'contribution to adequacy of supply' (e.g. [24-26]) and 'contribution to

security of supply' (e.g. [21, 22, 27]) are both used to express the capacity value of an asset. The difference is that the latter papers consider component outages.

Three reliability-based methods for capacity value calculation, which have been widely employed in the relevant literature [24, 26] are described below. The concept of these metrics is illustrated in Figure 1.9. At this point, it should be mentioned that the reliability evaluation of the system requires the selection of a specific reliability index – here expected energy not supplied (EENS) has been chosen. In Figure 1.9, two characteristic reliability levels are shown for all metrics: i) EENS of original system (base case), i.e. without any additional asset providing capacity contribution; and ii) EENS of system considering the aforementioned asset.

1) Effective load carrying capability (ELCC) [28]: The specified reliability index is iteratively calculated for the system with the asset, which contributes to the security of supply, and the load is gradually increased. Of course, as the system load increases, it is expected that the reliability level will deteriorate. The amount of load, for which the reliability index is equal to the corresponding value for the base case, is the ELCC. This is illustrated in Figure 1.9a. According to *Dent et al.* [29], ELCC is the most appropriate metric for distribution system planning.
2) Equivalent firm capacity (EFC): The selected reliability index is iteratively evaluated for the original system, but with a perfectly reliable generator (for transmission) or circuit (for distribution) connected to the network. As the capacity of the ideal generator/circuit increases, the reliability of the system improves (see Figure 1.9b); the capacity, for which the system reaches the reliability level mentioned in (ii) above (i.e. EENS of system with the asset providing capacity contribution), is the EFC.
3) Equivalent conventional capacity (ECC): The philosophy of ECC is the same as the one for EFC; however, in this case a real (not perfectly reliable) generator is applied to the system. Because this

method depends on the (arbitrary) reliability parameters of the conventional generator, ECC might not exist (curve A in Figure 1.9c); this would indicate that the real generator connected to the system is not capable of contributing as much as the asset under consideration (ii). For this reason, *Amelin* [24] recommends the first two metrics – ELCC and EFC – for capacity value calculation. If the benchmark unit can provide the required capacity contribution for a specific capacity (curve B in Figure 1.9c), then the ECC is defined in the same way as the EFC.

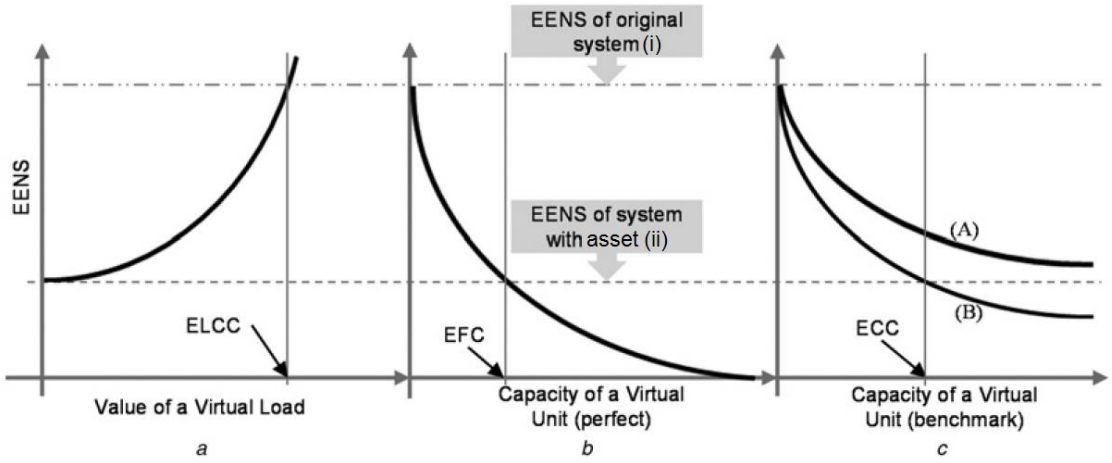

Figure 1.9: Concept of the three classic capacity value assessment methodologies [26].

A paper by *Xiao et al.* [30] has defined total supply capability (TSC) as the maximum load that a DN can accommodate, while satisfying the N-1 criterion and other operational constraints; they propose an optimization-based algorithm to calculate TSC. References [31, 32] – following this approach – consider network reconfiguration in their optimization problems. These papers, however, neglect demand variation (simplified load profiles are taken into account only by *Chen et al.* [31]) and its inherent uncertainty. Network reliability is also disregarded, which has a critical impact on the evaluated TSC. In addition to that, asset condition and ageing significantly influence network reliability assessment [10-12]. Therefore, this study investigates a probabilistic and reliability-based approach to quantify the capacity value of DNR, which is presented in Chapter 6.

1.6. RESEARCH OBJECTIVES

The primary aim of the research presented in this thesis is to investigate the impact of asset condition on DNR and its capacity value. The main research objectives are:

1) Describe how asset condition can be translated into HIs and failure rates, which can allow a network management system (NMS) – or an optimization algorithm – to make better informed decisions.
2) Develop a method to include asset condition and substation reliability into DNR.
3) Investigate how transformer ageing affects optimal network reconfiguration.
4) Examine the impact of asset ageing on optimal switch automation.
5) Devise a method to quantify the contribution of DNR to the security of supply of the network, considering asset condition and ageing.

1.7. THESIS OUTLINE

The rest of this thesis is organized as follows: In Chapter 2, a number of asset condition assessment methodologies and corresponding failure rate models are reviewed. Two of them are selected for the research presented in this thesis, which are then thoroughly described. This chapter also provides a technique to compute the overall failure rate of an asset – based on fault statistics – considering the contribution of failures related to age or wear. Finally, Chapter 2 examines the impact of transformer loading on the ageing of the asset.

Chapters 3 and 4 investigate the impact of asset condition on DNR, mainly focusing on S/S condition and reliability. The main idea is to transfer LPs experiencing poor reliability to more reliable neighbouring feeders, which can be supplied by a different S/S. Chapter 3 presents the initial research conducted by the author on this topic, and Chapter 4 further develops and improves the work in the former chapter. Chapter 3 also explores the linkage between transformer ageing and network reconfiguration.

Chapter 5 incorporates asset condition assessment and ageing – which depends on the type of the feeders (overhead lines or underground cables) – into the optimal switch automation problem.

Chapter 6 presents a probabilistic method to quantify the contribution of DNR to network security. This evaluation is realized using the effective load carrying capability (ELCC) method, within a sequential Monte Carlo framework; this is essential to capture the time dependency of certain variables as well as their inherent uncertainty. Moreover, this chapter employs condition-based reliability assessment of the network; and integrates the combined effect of load growth and asset ageing into the network security study.

Chapter 7 presents critical discussion of the research carried out and the broader implications of this work; it also identifies opportunities for further research in this area.

Finally, Chapter 8 explains how the main research objectives – set out in Chapter 1 – are met, and draws the conclusions.

Chapter 2. Asset Condition

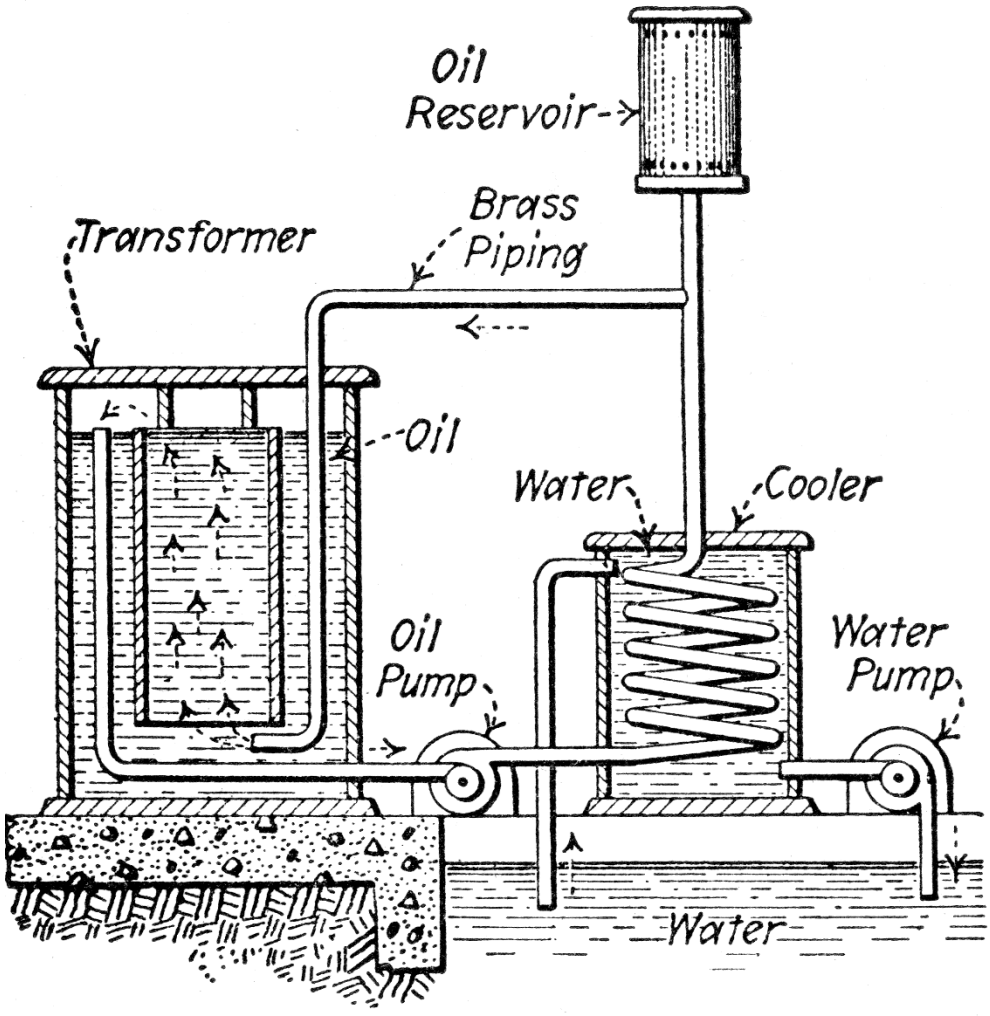

2.1. INTRODUCTION

The primary aim of the research presented in this thesis is to integrate asset condition into network operation and planning problems. This chapter begins with a review of a number of asset condition assessment methodologies and associated failure rate modelling techniques. The fundamental concept behind these methods is presented, and subsequently two of them are selected (according to appropriate criteria) for the work in this thesis, which are then explained in detail. Moreover, a technique is proposed in order to derive the overall failure rate of an asset, in case the output of the model is only the condition-based failure rate. Finally, the impact of transformer loading (a critical operation variable) on the ageing process of the asset is examined. This analysis clearly indicates the potential value of the linkage between asset condition and network operation.

2.2. LITERATURE REVIEW

As a result of the deregulation of the electricity industry, DNOs are facing the need to maintain a high level of reliability at the lowest possible cost. AM is critical to achieve this balance. In recent years, utilities have introduced reliability-centered maintenance (RCM) into their AM plans [33]. The RCM approach [34] achieves improved maintenance cost-effectiveness by concentrating on the maintenance efforts that are the most effective for the performance of the plant. In the case of a DNO, this process prioritizes the network assets according to their condition and criticality, which are evaluated appropriately. This way a utility optimizes the allocation of its available resources for maintenance by spending on the most critical assets [35]. A typical risk matrix that can be used for asset prioritization is shown in Table 2.1. For example, CNAIM uses 5 HI bands, which represent an average PoF of 4, 4.75, 6, 7.25, and 10, respectively; in terms of criticality bands, there are four, which correspond to 70%, 100%, 150%, and 250% of average overall CoF for the asset category.

Table 2.1: A typical risk matrix, which classifies network assets according to their HI and criticality; there are 5 HI and criticality bands (from bottom to top, HI bands represent worse condition; from left to right, criticality bands correspond to higher failure impact)

	C1 - Very Low	C2 - Low	C3 - Average	C4 - High	C5 - Very High
HI 5	Medium	High	Very High	Extreme	Extreme
HI 4	Medium	Medium	High	Very High	Extreme
HI 3	Low	Medium	Medium	High	Very High
HI 2	Very Low	Low	Medium	Medium	High
HI 1	Very Low	Very Low	Low	Medium	Medium

Asset condition and asset criticality are two key factors that are used by many AM decision support methodologies, which will be mentioned below. Asset condition can be expressed by an HI, and this value can be converted into a (condition-based) PoF. Asset criticality can be described by CoF. These two factors can be combined to yield a value that expresses risk. The results of this analysis can generally support AM decisions, such as maintenance planning as well as optimal timing for refurbishment and replacement activities. This concept forms the basis for a number of modern AM decision support tools [11, 36-39].

In this chapter, asset condition will only be examined, as CoF are separately analyzed in Chapters 3 and 4. As already mentioned in Chapter 1, an HI represents the condition of an asset in a comprehensive way and can significantly assist asset managers in their decision-making process. Figure 2.1 illustrates the process that is generally followed by many AM methodologies in order to derive the asset HI. The process begins with assessment of selected condition parameters by assigning a score to each of them. A default score can be assigned to parameters, for which no information is available [11]. Subsequently, according to the weight of each condition parameter, an overall score can be derived. This value is called asset HI. Based on that, some methodologies classify the asset into one of a number of predefined HI categories, accompanied by a qualitative description for its condition, PoF, and expected remaining life [40-42]; a number of alternative methodologies also convert the asset HI into a failure rate [11, 12, 36, 38, 43].

It should be noted that condition parameters are scored independently by inspection or condition monitoring data. However, if there is unavailability of data for some condition parameters, a default score can be given; this might be an unsatisfactory estimate, if there is correlation between two condition parameters. Two possible ways to deal with that, would be to make use of the available condition information to assess the specific condition parameter or employ historical condition monitoring data of the same asset type.

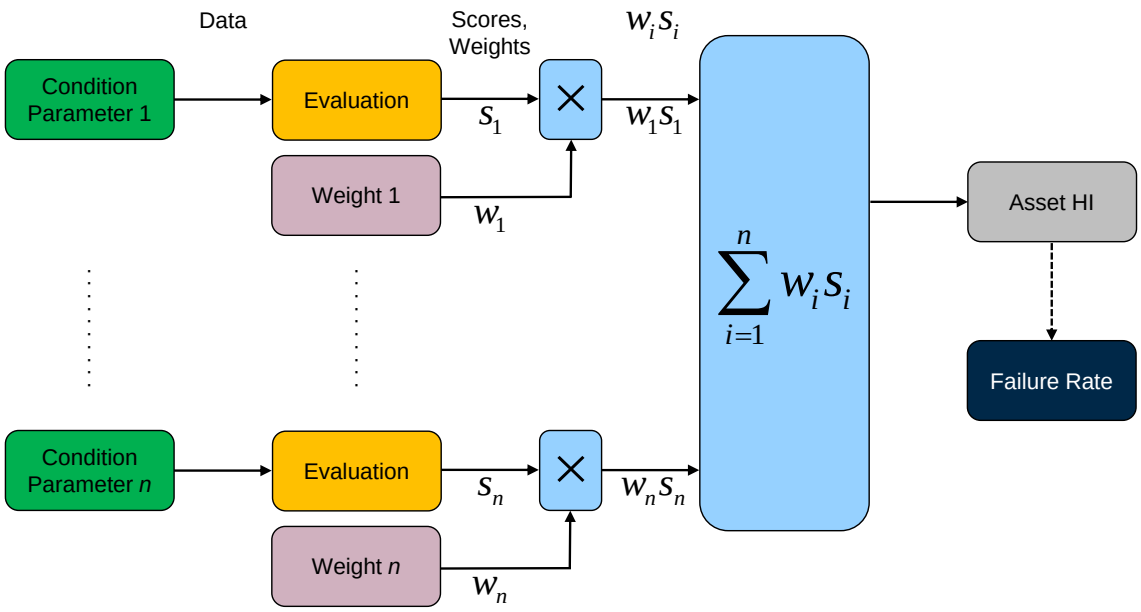

Figure 2.1: Concept of HI calculation. A number of condition parameters are assessed and according to their corresponding weights, an overall condition score is computed. Some methodologies also derive a failure rate based on the asset HI.

In order to be able to incorporate a condition assessment methodology in the work presented in this thesis, it needs to satisfy the following requirements: 1) it should be reproducible; many methodologies are described qualitatively (most of them constitute intellectual property), and thus cannot be implemented, 2) it must cover all basic asset types; some methods deal only with a specific asset type (mainly transformers), and 3) it should relate the asset HI to the corresponding condition-based failure rate. From all of the above-mentioned methodologies, only CNAIM [11] and *Brown et al.* [12] satisfy the criteria stated. Consequently, these are the methodologies, which

have been chosen for asset condition assessment and condition-based failure rate calculation in this thesis, and are presented in section 2.3.

2.3. CONDITION ASSESSMENT & FAILURE RATE MODELLING

2.3.1. METHODOLOGY 1

The first methodology is the CNAIM, which has been developed by a team of dedicated engineers from all of the UK DNOs. In 2017, the electricity regulator approved this methodology and now, all DNOs in the UK are required to classify their assets in specific HI and criticality bands and compute the corresponding risks, in order to regularly report on them.

It should be noted that CNAIM can be used only to compute condition-based failure rates. It is then necessary to determine the contribution of failures that are not based on condition as well, in order to be able to derive the overall failure rate. Therefore, it is proposed that typical national fault statistical data [8] be employed to derive the contributions of failures related to age or wear to the overall numbers of failures, for each asset type. In this way, the overall failure rate of an asset can be calculated, which is considered to consist of a part that is condition-based (variable) and the remainder, which is not related to age or wear (constant). For example, some faults that are not related to age or wear are due to the following: lightning, snow, wind, trees, birds, theft, etc. Moreover, CNAIM provides the capability to forecast the future HI of an asset.

2.3.1.1. HEALTH INDEX AND CONDITION-BASED FAILURE RATE

CNAIM evaluates specific condition parameters (depending on asset type) and assigns a score to each of them, using inspection or condition monitoring data. These individual scores are combined to produce a single value – called the HI – which indicates the overall condition of the asset. The HI can then be used to calculate the associated condition-based failure rate:

$$\lambda_{cb} = K_{FR} \cdot \left[1 + (C \cdot HI) + \frac{(C \cdot HI)^2}{2!} + \frac{(C \cdot HI)^3}{3!} \right]. \quad (2.1)$$

Equation (2.1) is based on the first three terms of the Taylor series for an exponential function; this formulation has the advantage of capturing the rapid increase of λ_{cb} as asset health deteriorates, but at a more controlled rate than a full exponential function. The C value defines the shape of the curve, and the K value scales the PoF to a failure rate. C has the same value for all asset types and has been chosen such that λ_{cb} at the worst HI is ten times higher than λ_{cb} of a new asset. K for each asset type has been determined by examining [11]:

1) The observed number of functional failures per annum.
2) The HI distribution for the asset population.
3) Numbers of assets within the population.

The calibration of K – for each asset type – has been implemented employing data accounting for the national asset population so that the overall expected number of functional failures in Great Britain (GB) is the same with the actual number of GB functional failures. K and C values for each asset type can be found in [11].

CNAIM is a deterministic methodology and apparently, there is uncertainty associated with the process of evaluating condition data, calculating HIs, and deriving condition-based failure rates. Monte Carlo simulation would be an effective (but time-consuming) way to deal with this problem; for example, the uncertainty could be introduced in the scores of the condition parameters, which would then propagate to HIs, and eventually λ_{cb}. The framework of the methodology (for capacity value assessment) presented in Chapter 6 can facilitate the incorporation of uncertainty, since it employs a sequential Monte Carlo simulation. In Chapter 4, a sensitivity analysis of λ_{cb} on optimal network configuration is performed.

HIs range from 0.5 to 10 for current asset condition, and the scale is extended up to 15 in order to forecast the future HI; a lower HI corresponds

to a better condition. The condition-based failure rates with respect to HI are illustrated in Figure 2.2 for the asset types used in this work. As the figure shows, CNAIM considers a constant λ_{cb}, until HI is equal to 4; beyond this threshold, λ_{cb} increases according to (2.1). Table 2.2 shows an illustrative example for a 45-year old transformer located at a primary S/S. The condition parameters used to evaluate the HI of the transformer and the associated scores are presented in the table. For example, a description of 'minor corrosion or evidence of low level oil leaks' for the 'Main Tank Condition' observed condition parameter, corresponds to a score of 1.4; and a description of 'some moderate levels of partial discharge recorded (e.g. 'Amber' result from Transient Earth Voltage measuring device or between 10% and 30% of the manufacturers recommendation' for the 'Partial Discharge' measured condition parameter, corresponds to a score of 1.1. The condition parameters for all asset types and detailed guidance on how to evaluate them can be found in [11].

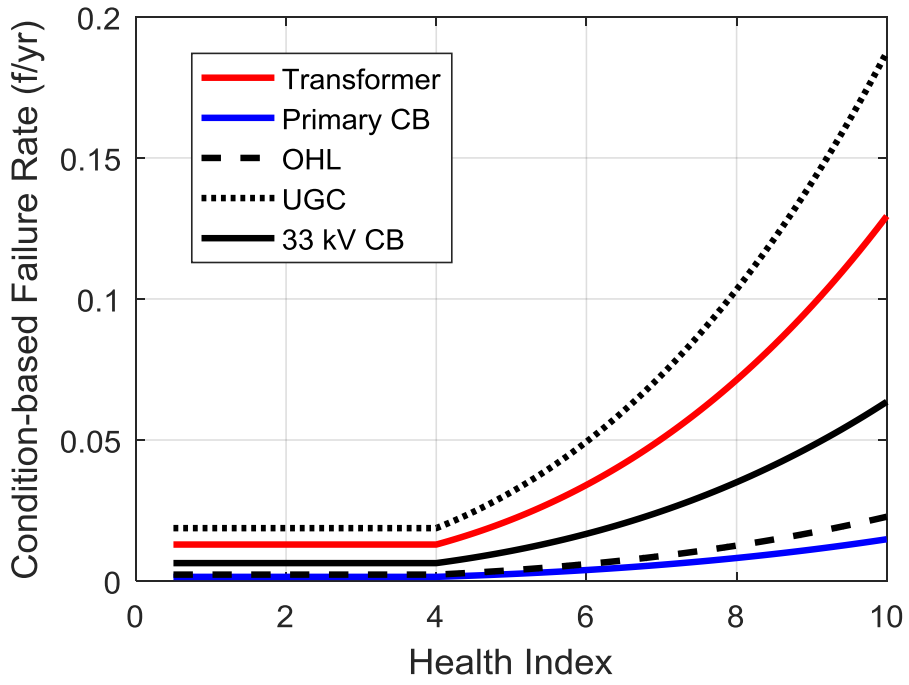

Figure 2.2: Condition-based failure rate curves with respect to asset HI; the illustrated curves correspond to transformers, circuit breakers, overhead lines, and underground cables (failure rate for lines/cables in f/yr·km).

Table 2.2: An illustrative condition assessment for a 45-year old transformer located at a primary S/S; HI and condition-based failure rate are computed as well

Parameter	Value	Comments
Transformer HI	**6.17**	Initial HI × HI Factor
Condition-based Failure Rate	**0.0366**	Equation (2.1)
Age	45	
Initial HI	3.02	Related to Age
HI Factor	2.04	Related to Condition
Expected Life	60	
Initial Ageing Rate	0.04	
Forecast Ageing Rate	0.056	
Observed Condition Factor	**1.67**	
Main Tank Condition	1.4	Some Deterioration
Coolers / Radiator Condition	1.2	Some Deterioration
Bushings Condition	1.2	Some Deterioration
Kiosk Condition	1.1	Some Deterioration
Cable Boxes Condition	1.1	Some Deterioration
Measured Condition Factor	**1.27**	
Partial Discharge	1.1	Medium
Temperature Readings	1.2	Moderately High
Oil Test Factor	**1.1**	
Oil Condition Score	570	
Moisture Score	2	15 - 25 ppm
Acidity Score	2	0.10 - 0.15 mg KOH/g
Breakdown Strength Score	2	40 - 50 kV
DGA Test Factor	**1.2**	
% Change	90	Significant
DGA Score	760	Previous DGA Score = 400
Hydrogen	2	20 - 40 ppm
Methane	2	10 - 20 ppm
Ethylene	2	10 - 20 ppm
Ethane	2	10 - 20 ppm
Acetylene	4	5 - 20 ppm
FFA Test Factor	**1**	
S (FFA value in ppm)	3	

2.3.1.2. FUTURE HEALTH INDEX CALCULATION

Another strength of this methodology is its ability to compute future HIs, which is of particular importance for planning studies. The process of forecasting the future HI of an asset is described below.

The initial HI is given by the following equation, which expresses the generic relationship between HI and age, making use of the expected life of the asset.

$$HI_{\text{init}} = HI_{\text{new}} \cdot e^{(\beta_1 \cdot age)}, \tag{2.2}$$

where

$$\beta_1 = \frac{\ln\left(\frac{HI_{\text{EL}}}{HI_{\text{new}}}\right)}{EL}. \tag{2.3}$$

The forecast ageing rate (β_2) is calculated using the current HI and the age of the asset

$$\beta_2 = \frac{\ln\left(\frac{HI}{HI_{\text{new}}}\right)}{age}, \tag{2.4}$$

and is capped such that:

$$\beta_2 \leq 2\beta_1. \tag{2.5}$$

The future HI can now be calculated as follows:

$$HI_{\text{f}} = HI \cdot e^{\left(\frac{\beta_2}{r_{\text{af}}} \cdot year\right)}, \tag{2.6}$$

where r_{af} is the ageing reduction factor, which is introduced in this methodology in order to moderate the effect of escalating increase in the condition-based failure rate of an asset, when it reaches a high HI. The ageing reduction factor practically decelerates the ageing rate (as can be seen in (2.6)) of an asset by a variable factor that depends on the current HI, and is illustrated in Figure 2.3; and *year* is the future year, for which the HI has to be calculated.

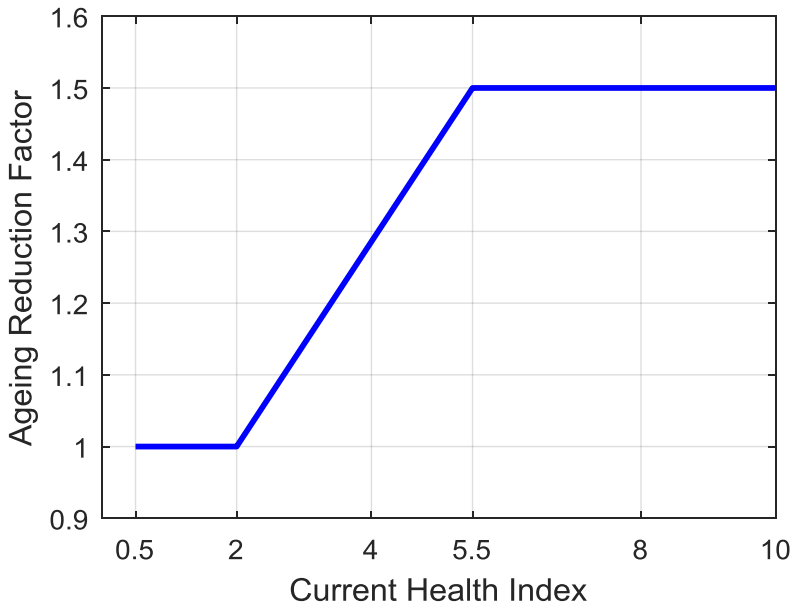

Figure 2.3: Ageing Reduction Factor; for assets that are close to their end of life, the forecasting process may lead to overestimation of the condition-based failure rate, because of the use of the exponential function.

Taking as an example the 45-year old transformer from Table 2.2, the future HI can be given according to:

$$HI_{\mathrm{f}} = 6.17 \cdot e^{0.03723 \cdot year}, \tag{2.7}$$

which is illustrated, along with the condition-based failure rate, for the next 15 years in Figure 2.4.

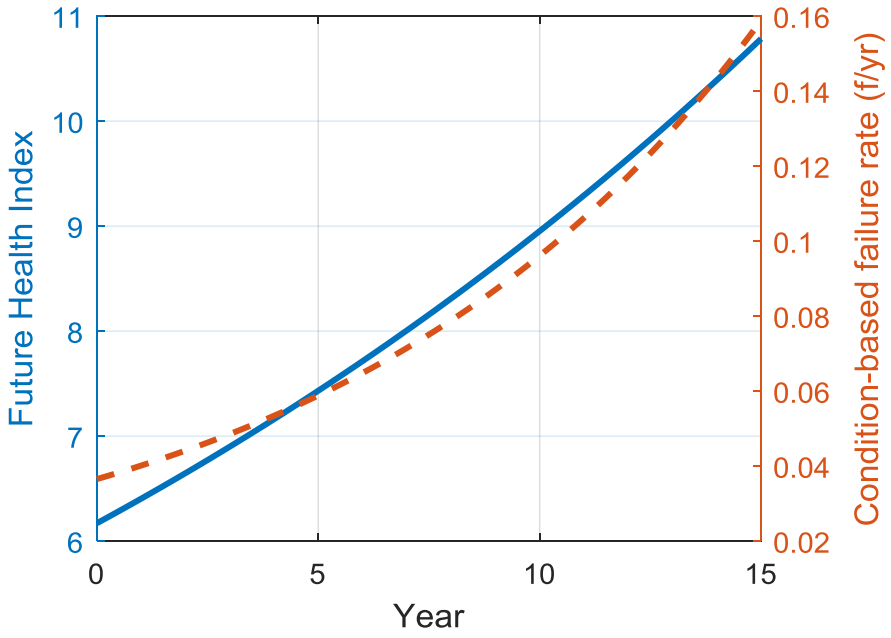

Figure 2.4: Future HI and condition-based failure rate for a 45-year old transformer at a primary S/S (Table 2.2) for the next 15 years.

2.3.1.3. OVERALL FAILURE RATE CALCULATION

As already mentioned, CNAIM can be used to derive only condition-based failure rates. Thus, it is proposed in this thesis that the failure rate of an asset comprises two components: 1) condition-based, which has been described and it is variable; and 2) non-condition-based, which does not depend on age or condition and is constant (this failure rate component accounts for faults, e.g. due to lightning, snow, wind, trees, birds, theft, etc.). The overall failure rate can then be expressed as:

$$\lambda = \lambda_{cb} + \lambda_{ncb}. \tag{2.8}$$

The percentages of failures not related to age or wear for primary transformers, primary CBs, 33 kV CBs, underground cables (UGCs), and overhead lines (OHLs) (33 kV & 11 kV), according to the National Fault and Interruption Reporting Scheme (NaFIRS) for the UK [8], are presented in Table 2.3. In order to calculate λ_{ncb} for each asset type, each percentage is multiplied by the corresponding overall failure rate from [17]. Figure 2.5 illustrates the overall failure rates (with respect to HI) for the above-mentioned asset types. It should also be noted that as far as OHLs/UGCs are concerned, the same condition-based failure rate model has been used for both voltage levels, as 11 kV lines/cables are not (yet) covered by CNAIM.

Table 2.3: Contribution of failures that are not related to age or wear for different asset types (failure rate for lines/cables in f/yr·km)

Asset Type	Percentage of λ_{ncb}	λ_{ncb} (f/yr)
Primary Transformer	71.20 %	0.0107
Primary CB	73.54 %	0.0044
33 kV CB	66.84 %	0.0013
UGC (33 kV & 11 kV)	46.00 %	0.0184
33 kV OHL	89.25 %	0.0411
11 kV OHL	83.45 %	0.0542

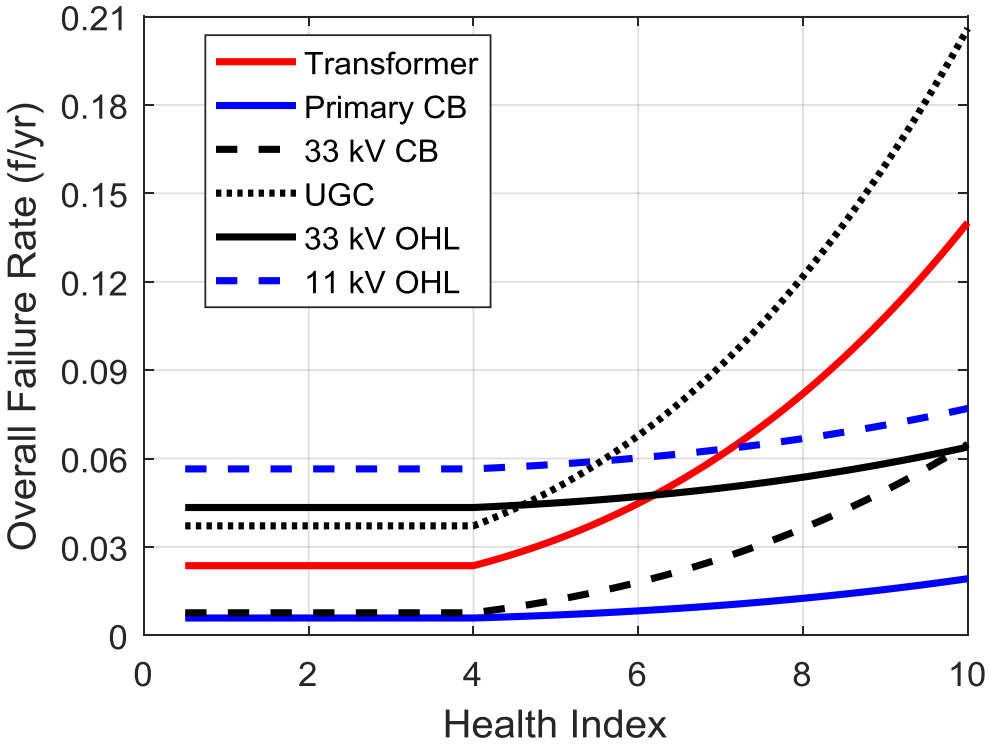

Figure 2.5: Overall failure rate curves with respect to asset HI (failure rate for lines/cables in f/yr·km).

2.3.2. METHODOLOGY 2

The second failure rate model has been developed by *Brown et al.* [12] and provides a method to map maintenance data to an HI and then convert this into a PoF. Asset HIs are derived as described in Figure 2.1 and the output of this model can be considered as an overall failure rate. Table 2.4 presents the condition parameters that need to be evaluated in order to calculate the HI of a transformer. In this methodology, HIs range from 0 to 1, which correspond to the best and the worst condition, respectively.

In contrast to CNAIM, the method by *Brown et al.*: 1) does not provide the condition parameters that should be assessed for asset types other than transformers, and 2) does not give a process to compute the future HI of an asset. Therefore, this methodology can be applied, if it is only required to derive the failure rate of an asset (except transformers) based on its HI, and there is no need for future HI calculation. However, *Brown et al.* provide failure rate model parameters for several asset types, one of which is busbars, which is not covered by CNAIM. These parameters are shown in

Table 2.5 and can be used along with (2.9) to convert an asset HI into a failure rate. The resultant curves are illustrated in Figure 2.6.

$$\lambda(HI) = Ae^{B \cdot HI} + C. \tag{2.9}$$

Table 2.4: Condition assessment for transformers according to *Brown et al.* [12]

Criterion	Weight	Score
Age (years of operation)	8	
Condition of internal solid insulation	2	
Oil type	1	
Condition of core	2	
Condition of inaccessible parts	1	
Condition of tank	1	
Condition of cooling system	1	
Condition of tap changer	2	
Condition of accessible parts	1	
Condition of bushings	2	
Experience with this transformer type	4	
Transformer loading history	3	
Number of extraordinary mechanical stresses	3	
Number of extraordinary dielectric stresses	2	
Noise level	1	
Core and winding losses	2	
Gas in oil analysis (current results)	5	
Gas in oil analysis (trend in results)	4	
Oil analysis	6	
Sum	**51**	
Weighted Average		

Brown et al. have explored a number of different mapping functions and have found that the exponential model is the most appropriate one for the relationship between the HI of the asset and the corresponding failure rate. This methodology is based on finding three pairs, namely (0, $\lambda(0)$), (0.5, $\lambda(0.5)$), and (1, $\lambda(1)$), which correspond to the best, average, and worst HIs, respectively; and then applying curve fitting in order to determine the A, B, and C model parameters. $\lambda(0.5)$ can be derived by employing average failure rates from the relevant literature or using the average failure rate from a large population of assets. $\lambda(0)$ and $\lambda(1)$ can be obtained via benchmarking, statistical analysis or heuristics; a detailed benchmarking can be found in [7].

Table 2.5: Failure rate model parameters for selected asset types (failure rate for OHLs/UGCs in f/yr·km)

Asset Type	$\lambda(0)$	$\lambda(0.5)$	$\lambda(1)$	A	B	C
Transformer	0.0075	0.040	0.140	0.01565	2.24786	-0.0081
CB	0.0005	0.010	0.060	0.00223	3.32146	-0.0017
UGC	0.0009	0.043	0.730	0.00282	5.55972	-0.0019
OHL	0.0062	0.062	0.373	0.01228	3.42960	-0.0061
Busbar	0.0005	0.010	0.076	0.00160	3.87673	-0.0011

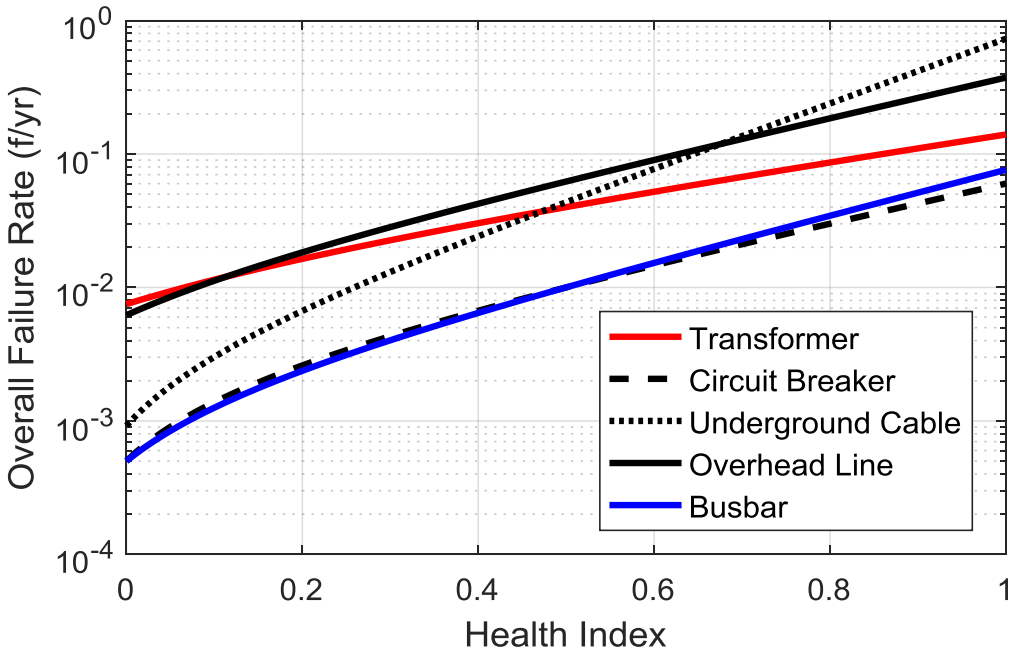

Figure 2.6: Specific asset failure rate functions (failure rate for lines/cables in f/yr·km). These are derived using (2.9) and coefficients from Table 2.5. The graph is semi-log (logarithmic scale on the y-axis, and linear scale on the x-axis). Note that this methodology employs an HI range from 0 to 1, in contrast to CNAIM.

2.4. Transformer Loading and Ageing

The condition parameters (and the associated HIs) that have been examined so far give an indication of the asset condition on a time scale of years. This section focuses on transformer loading, which is a critical parameter for this particular asset type, as it can significantly affect the condition of the asset on a time scale of hours, especially under overload conditions. In order to examine the effect of the loading of a transformer on its condition, a model developed in [44] is employed, which is presented in the following section.

2.4.1. TRANSFORMER AGEING MODEL

2.4.1.1. INTRODUCTION

This model concentrates on the ageing process of transformer insulation. Its inputs are: 1) the loading of the transformer, and 2) the ambient temperature; the model yields the hot-spot temperature, which in turn determines the relative ageing rate, and based on that finally the transformer loss of life can be derived. It should be noted that the term 'life' refers to the insulation life of a transformer. The process is illustrated in Figure 2.7.

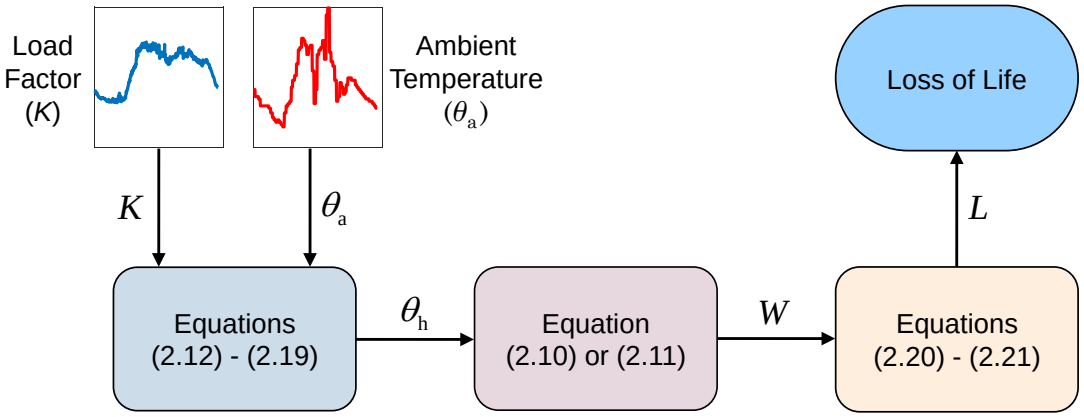

Figure 2.7: Overview of the transformer ageing model. The inputs (K, θ_a) are used to derive the hot-spot temperature (θ_h); θ_h defines the relative ageing rate (W), which in turn determines the loss of life (L).

2.4.1.2. RELATIVE AGEING RATE

The model considers that the deterioration of transformer insulation is influenced only by temperature, even though moisture, oxygen, and acid content have an impact on the ageing of the insulation as well. Winding hot-spot temperature is used to determine the deterioration of the insulation, since this is the highest temperature developed in the transformer, and hence this specific part of the asset experiences the greatest ageing. Equations (2.10) and (2.11) define the relative ageing rate W for non-thermally and thermally upgraded paper, respectively:

$$W = 2^{\left(\frac{\theta_h - 98}{6}\right)}, \tag{2.10}$$

$$W = e^{\left(\frac{15000}{110+273} - \frac{15000}{\theta_h+273}\right)}. \tag{2.11}$$

These equations denote that the relative ageing rate is very sensitive to the hot-spot temperature, as illustrated in Figure 2.8. It should be mentioned that there exists a degree of uncertainty in the effect of hot-spot temperature on the relative ageing rate; however, these relationships have been taken from an International Electrotechnical Commission (IEC) standard [44].

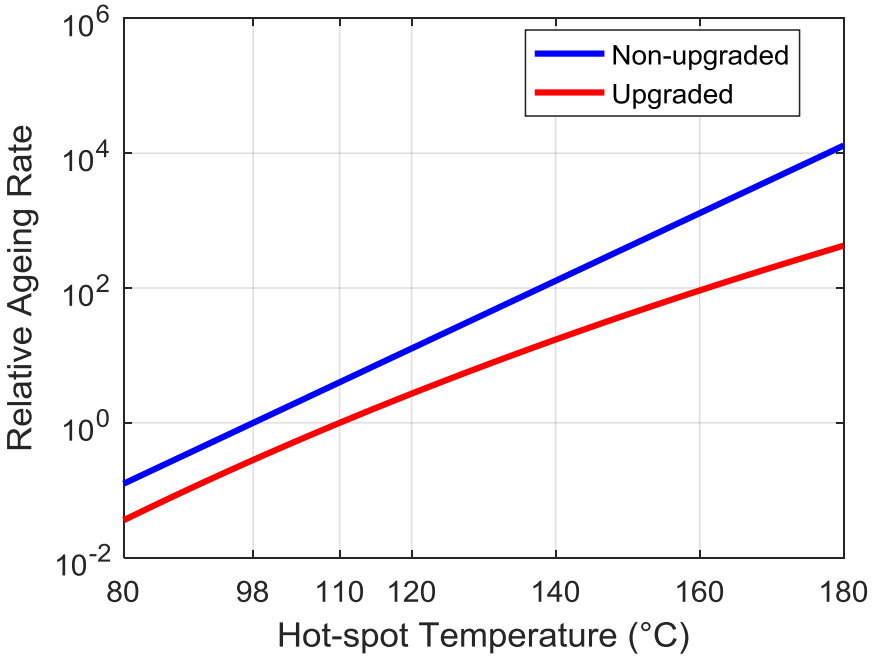

Figure 2.8: Relative ageing rates with respect to hot-spot temperature for both upgraded and non-upgraded paper insulation; relative ageing rate is equal to unity at 110 °C for upgraded paper, and at 98 °C for non-upgraded paper.

2.4.1.3. MODEL

The equations of the transformer ageing model are presented in this section. The inputs of the model are: 1) the loading of the transformer, expressed as the ratio of load current to rated current, which is the load factor K, and 2) the ambient temperature θ_a. Equations (2.12) and (2.13) take these inputs and yield the top-oil temperature θ_o:

$$D\theta_o = \frac{Dt}{k_{11}\tau_o}\left[\left(\frac{1+K^2R_L}{1+R_L}\right)^z \Delta\theta_{or} - \left(\theta_o - \theta_a\right)\right], \tag{2.12}$$

$$\theta_{o(n)} = \theta_{o(n-1)} + D\theta_{o(n)}. \tag{2.13}$$

Equations (2.14) – (2.18) give the hot-spot temperature rise ($\Delta\theta_h$) at the nth time step, which is determined by the load factor K. The equations are formulated in this manner ($\Delta\theta_h$ is solved as the sum of two difference equations), so as to consider that oil has (apart from thermal) mechanical inertia as well.

$$D\Delta\theta_{h1} = \frac{Dt}{k_{22}\tau_w}\left[k_{21}\Delta\theta_{hr}K^y - \Delta\theta_{h1}\right], \tag{2.14}$$

$$D\Delta\theta_{h2} = \frac{Dt}{\tau_o/k_{22}}\left[\left(k_{21}-1\right)\Delta\theta_{hr}K^y - \Delta\theta_{h2}\right], \tag{2.15}$$

$$\Delta\theta_{h1(n)} = \Delta\theta_{h1(n-1)} + D\Delta\theta_{h1(n)}, \tag{2.16}$$

$$\Delta\theta_{h2(n)} = \Delta\theta_{h2(n-1)} + D\Delta\theta_{h2(n)}, \tag{2.17}$$

$$\Delta\theta_{h(n)} = \Delta\theta_{h1(n)} - \Delta\theta_{h2(n)}. \tag{2.18}$$

Now, having computed both the top-oil temperature and the hot-spot temperature rise at the nth time step, the hot-spot temperature (θ_h) can be derived as the sum of these variables:

$$\theta_{h(n)} = \theta_{o(n)} + \Delta\theta_{h(n)}. \tag{2.19}$$

Note that the time step (Dt) must be less than one-half of the smallest time constant in order to have an accurate solution.

Finally, the relative ageing rate (at the nth time step) is determined by the hot-spot temperature, according to (2.10) or (2.11), and then the loss of life (L) is derived as follows:

$$DL_{(n)} = W_{(n)}Dt, \tag{2.20}$$

$$L_{(n)} = L_{(n-1)} + DL_{(n)}. \tag{2.21}$$

2.4.2. Simulation Results

The transformer ageing model (equations (2.10) – (2.21)) [44] described in section 2.4.1 is used in order to study an overload occurrence at a primary

S/S (in the north-east of England), which was studied as part of the Customer-Led Network Revolution (CLNR) project [45]. The transformer model parameter values for this simulation and the profiles of the input variables are shown in Table 2.6 and Figure 2.9, respectively. Note that: 1) the transformer loading data were scaled up so as to simulate the overload condition; 2) ambient temperature profile was unchanged; and 3) thermally upgraded paper was considered for this case study. The simulation results are illustrated in Figure 2.10.

Table 2.6: Transformer Model Parameters [44]

Parameter	Value
$\Delta\theta_{or}$	45
$\Delta\theta_{hr}$	35
τ_o	150
τ_w	7
R_L	8
z	0.8
y	1.3
k_{11}	0.5
k_{21}	2
k_{22}	2

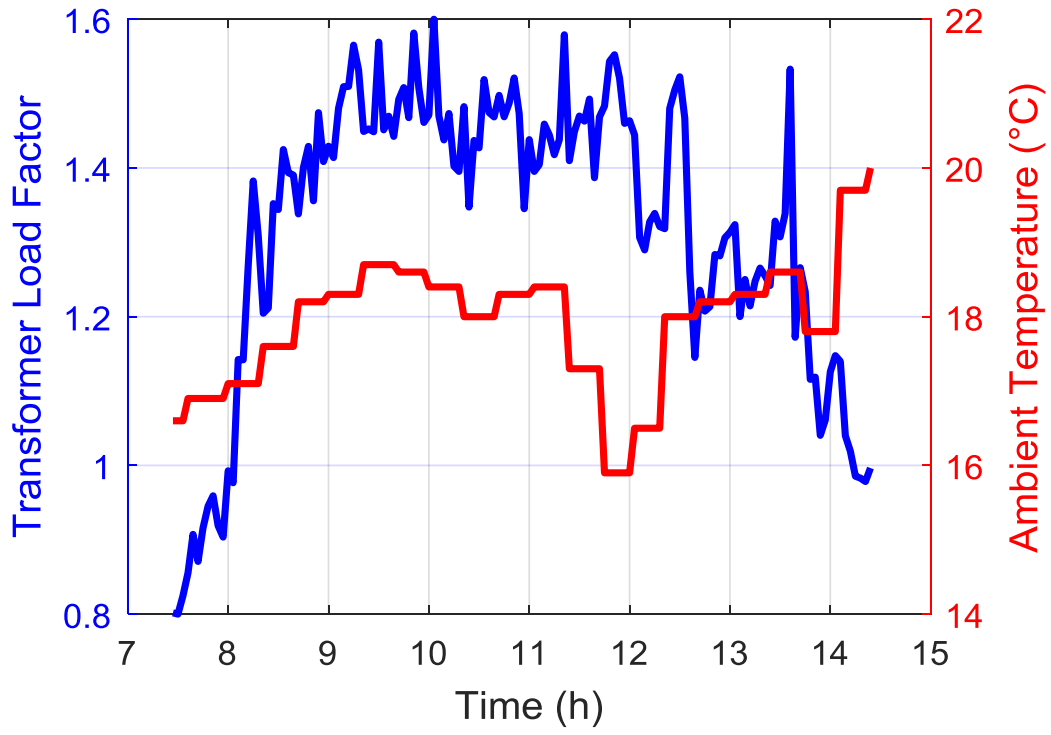

Figure 2.9: Input variable profiles; load factor (K) (scaled up), and ambient temperature (θ_a).

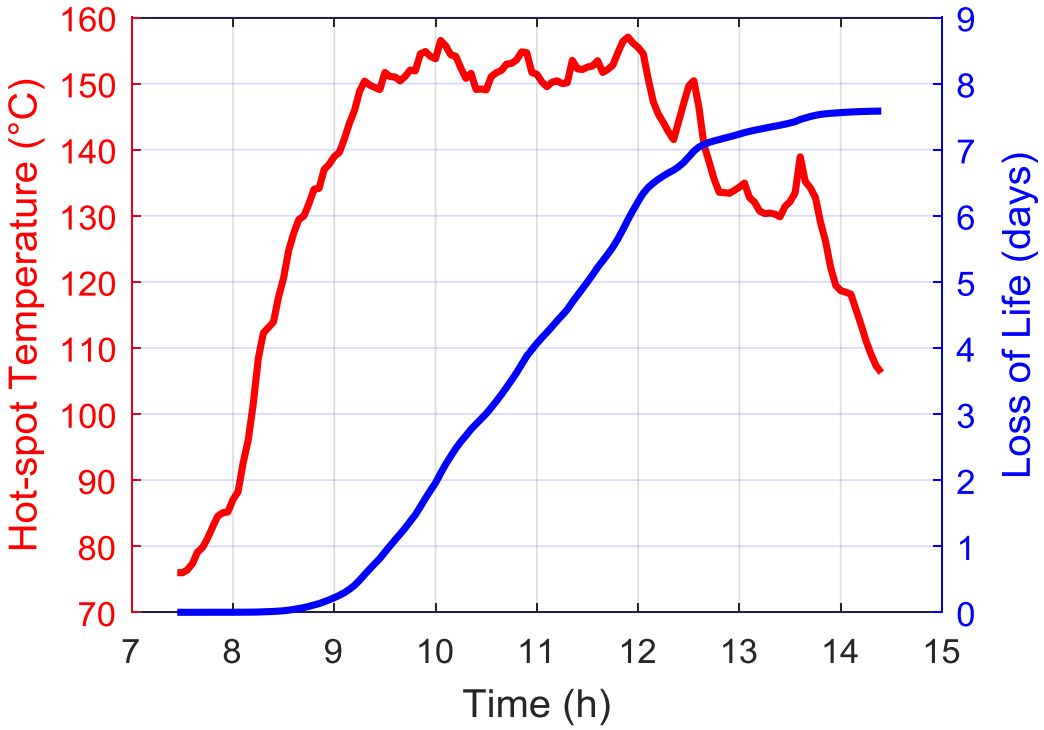

Figure 2.10: Simulation results; hot-spot temperature (θ_h) and loss of life (L).

As can be seen in Figure 2.10, an overload (even if it lasts only for several hours) can substantially accelerate the ageing of the transformer. For thermally upgraded paper, the unity relative ageing rate corresponds to 110 °C; this means that for one hour of transformer operation at this temperature, the loss of life is one hour as well. In this simulation, the hot-spot temperature is above 110 °C for about six hours; it almost reaches 160 °C, for which the relative ageing rate is equal to 100 (see Figure 2.8). This fact justifies the considerable amount of loss of life of the transformer in this case study.

The current situation is that (under normal operating conditions) transformers usually operate at temperatures, which correspond to relative ageing rates well below one. However, under the smart grid paradigm, network utilization is expected to significantly increase, e.g. through the use of RTTRs. In such a case, the relative ageing rate of transformers will exceed unity much more frequently, which is a fact that should be taken into account [46]. This can be achieved by optimally balancing asset utilization and ageing, which of course requires the incorporation of asset condition into network operation.

2.5. CONCLUSION

This chapter has described how asset condition can be translated into HIs and failure rates, which can allow an NMS (or an optimization algorithm) to make better informed decisions for a DN (see Figure 1.2). This can be realized through the use of appropriate asset condition assessment methodologies and failure rate models, which have been presented after having examined a number of relevant methods.

Finally, transformer loading was studied, as it is a significant operation variable, which has a considerable impact on the condition of transformers. It is also anticipated that transformers will be experiencing higher levels of loading, as mentioned above. Therefore, a balance needs to be sought between 'sweating the assets' and the associated loss of life, via condition-based operation of the network.

Chapter 3. Condition and Risk-Based DNR

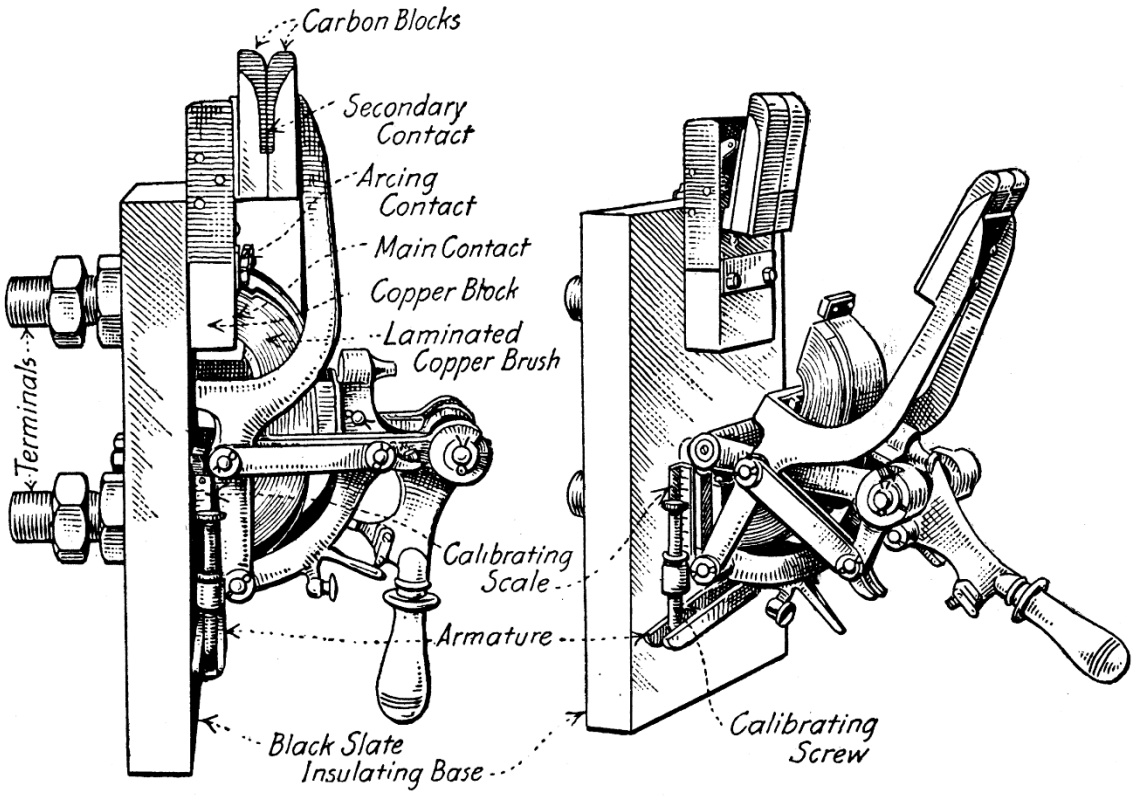

3.1. INTRODUCTION

One of the main research objectives of this thesis is to investigate the influence of asset condition on network reconfiguration. This chapter and Chapter 4 examine this impact on DNR, mainly focusing on S/S condition and reliability. The idea of load transfer from a feeder to another, which can be of a different S/S, is key in the proposed methodologies. This chapter presents the initial work completed by the author on this topic as part of his PhD, and Chapter 4 further develops (and improves) this methodology. The following section provides a literature review on DNR and identifies gaps in the present state of knowledge. It is then explained how these gaps are addressed; specifically section 3.3 incorporates condition-based risk in the DNR problem, and section 3.4 investigates the impact of transformer ageing on network reconfiguration.

3.2. LITERATURE REVIEW

DNR is usually structured as an optimization problem, with an objective to minimize power losses, voltage deviation, or load imbalance, or to maximize reliability. It is a combinatorial nonlinear optimization problem [14], which has often led to the use of heuristic solution algorithms, including: branch exchange method [47-51]; genetic algorithm (GA) [52-59]; particle swarm optimization (PSO) [60-64]; simulated annealing [65, 66]; artificial neural networks [67, 68]; ant colony search algorithm [69-71]; cuckoo search [72, 73]; invasive weed optimization [74]; and teaching-learning-based optimization [75]. Although heuristic optimization algorithms do not guarantee the optimal solution, they do identify high-quality solutions [59, 76].

In [47], the objective is to reduce losses and improve load balancing through DNR. In order to do so, a search over a number of radial configurations is involved; therefore, two approximate power flow methods were developed to reduce the computational burden. *Ch et al.* [51] investigate the impact of DNR on power quality (such as voltage harmonic distortion and unbalance), along with losses, in the presence of DG and reactive power sources.

Tahboub et al. [58] employ a clustering algorithm to acquire representative centroids from annual load and DG profiles in order to deal with their associated variability; loss minimization is the corresponding objective function. In [59], an adaptive fuzzy logic parallel GA is presented to solve the optimization problem. A paper by *Guan et al.* [62] considers different models of DG into the network reconfiguration problem; a decimal encoding of the decision variables is also proposed. In [73], a new methodology is developed to optimize the configuration of the network, as well as the location and size of DG. *Sudha Rani et al.* [74] present a multi-objective invasive weed optimization method in order to simultaneously minimize losses, maximum node voltage deviation, number of switching operations, and the load balancing index; they also implement a backward/forward sweep load flow for the power flow calculations. An advantage of the optimization methods in [72, 73, 75] – cuckoo search and teaching-learning-based optimization – is that they have few control parameters.

References [77, 78], investigate the impact of soft open points (SOPs) on DN operation. SOPs are power electronic devices installed between neighbouring feeders – instead of NOPs – in DNs, capable of controlling active and reactive power flow. *Cao et al.* [77] optimize the network for minimum loss and feeder load balancing, whereas *Qi* and *Wu* [78] maximize DG penetration. Both of these papers conclude that the optimal network operation is achieved when SOP control and DNR are used in combination. SOPs can be regarded as a very promising solution for DN operation; however, it is currently beyond the scope of this work.

As mentioned earlier, DNR involves a search over a number of network configurations; the size of the search space of the problem is related to the encoding of the state vector, i.e. what each decision variable represents [79]. The state vector in DNR represents a specific network topology. Two options are presented in [80]. The first option (binary encoding) assumes that each decision variable represents the status (open/closed) of the corresponding branch. The length of the state vector, in this case, is equal to the number of branches that are involved in the network reconfiguration. The second

option (integer encoding) considers that the network consists of a number of loops and each decision variable represents the integer index of the branch that breaks each loop; in this case, the length of the state vector is defined by the number of loops. These two options are compared in [80], and it is shown that the second alternative outperforms the first one in optimization time and number of objective function evaluations. The former approach is followed in [58] and [61], which use a binary GA and PSO, respectively; whereas the latter approach is followed in [62, 73-75], and it is stated that it can reduce the number of state variables, generate fewer infeasible solutions, and have better search efficiency.

From the perspective of reliability, *Brown et al.* [16] extended the use of DNR to improve network reliability. In [61], probabilistic reliability models are applied to assess the reliability at the LPs and the DNR problem is formulated in a multi-objective framework, considering power loss and reliability. *Paterakis et al.* [81] also propose a multi-objective optimization method, which minimizes active power losses and one of three commonly used system reliability indices. It is not uncommon to disregard customer interruption costs entirely [61, 81]. In [57, 82-84], an aggregate objective function is considered, which takes account of losses and reliability concurrently by expressing the objective in monetary terms via electricity price and customer interruption costs.

However, the aforementioned publications neglect asset condition when evaluating network reliability and use average failure rates that depend only on the type of the assets regardless of their condition. Furthermore, the available literature on DNR deals with networks that have only one S/S or, in cases where multiple S/Ss are present, the problem is formulated such that a single S/S is considered. Consequently, either the reliability of the S/Ss is not considered in network reconfiguration studies or they are assumed to be perfectly reliable.

Two of the main contributions of this thesis are to take asset condition and substation reliability into account within the DNR problem. Condition-based

failure rates are used to determine the reliability of the network compared to the standard approach using average failure rates. Networks with multiple S/Ss are considered and their reliability is determined by asset condition. In this chapter, the proposed objective function is an aggregate function, which considers losses and total network risk (TNR), and is expressed in monetary terms; it is also extended to include cost of transformer loss of life due to ageing.

Moreover, average customer interruption costs [57, 83] or composite customer damage functions [84] are considered, in order to convert customer interruptions to cost, for all LPs. In fact, the expected customer interruption cost (ECOST) depends on customer type and outage duration; two LPs can yield significantly different ECOSTs even if they have the same power demand and are interrupted for the same amount of time [6, 85].

In Chapter 4, S/S reliability is determined by asset condition, S/S configuration, and the network upstream of the S/Ss, which can lead to different reliability indices for the S/Ss supplying a given DN. The proposed objective function takes account of reliability and power losses, and is also expressed in monetary terms. Reliability is considered through the ECOST, which is calculated not only for interruptions that come from the primary DN (network between the distribution S/Ss and the distribution transformers), but also for outages that are caused by the S/Ss and the upstream network. Finally, each LP has a specific customer type and the associated customer damage function (CDF).

The models used in Chapters 3 and 4 consider constant loads (except section 3.4) and the reliability of the system is evaluated for a yearly period – but this does not preclude the application of the proposed methods to more discrete time periods. It should also be noted that this work does not focus on the optimization method; instead, it concentrates on demonstrating the value of including asset condition and S/S reliability into the DNR problem.

3.3. CONDITION–BASED RISK DNR

3.3.1. METHODOLOGY

In a representative DN, a number of network configurations are evaluated in terms of losses and TNR. Reconfigurations are implemented using the simple branch exchange method [47], i.e. closing one switch and opening another one at the same time. The minimum cost of annual energy losses and TNR determines the optimal configuration of the network. TNR consists of transformer (TX), CB, and OHL risks. The risk calculation models for these asset types are explained in sections 3.3.1.1 and 3.3.1.2.

3.3.1.1. OHL AND CB RISK CALCULATION MODELS

Risk calculation, according to CNAIM (see section 2.3.1), requires two key factors: 1) PoF and 2) CoF.

As far as CBs are concerned, PoF is derived using CNAIM. Regarding OHLs, PoF is here considered equal to the failure rate of MV lines (0.035 f/yr·km), which has been calculated using [8], and is assumed constant regardless the condition of the line.

The calculation of CoF for OHLs and CBs is based on CNAIM. As regards financial, safety, and environmental CoF, the corresponding reference values can be taken from CNAIM. However, this thesis deals only with Network CoF, as network reconfiguration can only have an impact on this CoF category. Network CoF is evaluated according to the CNAIM LV & MV Asset Consequences process, whose concept is illustrated in Figure 1.7, and is derived using (3.1).

$$\begin{aligned} OHL/CB\ Network\ CoF = [&(UCML \cdot 60 \cdot NC \cdot ST \cdot (1-R1)) \\ &+ (UCML \cdot 60 \cdot NC \cdot RT \cdot (1-R2)) \\ &+ (UCI \cdot NC \cdot (1-R1))] \cdot F, \end{aligned} \tag{3.1}$$

where ST and RT are the switching and restoration times (here in hours), respectively.

In the case of an OHL/CB active failure, the nearest CBs operate in order to clear the fault. Consequently, part of the healthy network is removed from service and more specifically the section that was supplied through the CBs. Following the operation of the breakers, the fault should be detected and isolated before the CBs can be reclosed. After the detection, isolation and switching (the total time interval required for these actions is called switching time), the power supply, between the switches around the failed component and the activated CBs, is restored. The rest of the customers are restored after the repair process has been completed, unless they can be supplied through an alternative route, e.g. by closing a NOP [6]. This process is illustrated in Figure 1.6.

3.3.1.2. TRANSFORMER RISK CALCULATION MODEL

The process begins with the evaluation of the appropriate condition parameters for the transformer (main transformer and tapchanger), according to CNAIM, as shown in Tables 2.2 and 3.1; then, separate HIs are derived for each subcomponent; finally, taking the maximum HI, the PoF can be computed using (2.1) and (2.8). As regards the data presented in these tables, the main transformer component has a greater HI than that of the tapchanger; therefore the HI of the former component should be used to calculate the transformer PoF.

Transformer Network CoF is calculated according to [86, 87], where Network Risk is composed of the expected annual cost of CIs and CMLs, as shown in (3.2) – (3.4). These equations can be used to assess the Network Risk, when two transformers (or, more generally, two circuits) are connected in parallel (see Figure 3.1), which is the case in the network of the case study that will be examined in the next section.

Table 3.1: Tapchanger condition assessment and HI calculation, according to CNAIM

Parameter	Value	Comments
Tapchanger HI	**5.84**	Initial HI × HI Factor
Age	45	
Initial HI	3.02	Related to Age
HI Factor	1.93	Related to Condition
Expected Life	60	
Initial Ageing Rate	0.04	
Observed Condition Factor	**1.87**	
External Condition	1.4	Some Deterioration
Internal Condition	1.2	Some Deterioration
Drive Mechanism Condition	1.4	Substantial Deterioration
Selector & Diverter Contacts	1.3	Substantial Deterioration
Selector & Diverter Braids	1.05	Some Deterioration
Measured Condition Factor	**1.1**	
Partial Discharge	1.1	Medium
Oil Test Factor	**1.1**	
Oil Condition Score	820	
Moisture Score	2	15 - 25 ppm
Acidity Score	4	0.15 - 0.20 mg KOH/g
Breakdown Strength Score	2	40 - 50 kV

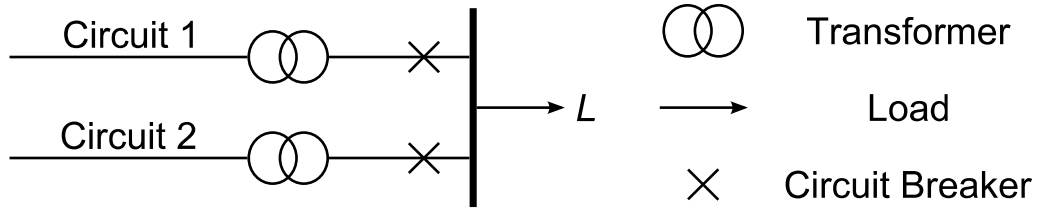

Figure 3.1: Two circuits connected in parallel.

$$CI = \left(PoF_1 + PoF_2\right) \cdot DF \cdot NC \cdot UCI, \tag{3.2}$$

$$CML = \left(PoF_1 + PoF_2\right) \cdot DF \cdot NC \cdot \left(R2 \cdot ST + \left(1 - R2\right) \cdot RT\right) \cdot UCML, \tag{3.3}$$

$$TX\ Network\ Risk = CI + CML, \tag{3.4}$$

where RT is the average time to restore at least one of the parallel branches (ST and RT, here, in minutes), and DF is the proportion of faults that result in a customer interruption, generally because two outages occur at the same time. This can happen for a number of reasons: common mode failure, second circuit tripping because of increased loading, or second circuit failing while the first is being maintained / repaired [87]. According to this

reference: '*the input parameter DF is a composite variable representing a number of distinct and different possible events. What they have in common is that they lead to an N-2 situation with consequent customer loss, in the case of a simple radial paired circuit. Estimating a value for DF can be done retrospectively using NaFIRS data on the proportion of extra high voltage faults which have led to loss of customer supply*.'

It should be noted that PoFs in these equations include the PoFs of the CBs associated with the transformers, i.e.:

$$PoF_i = PoF_{TX_i} + PoF_{CB_i}, \tag{3.5}$$

where i = 1, 2, represents the circuit number.

3.3.2. CASE STUDY

3.3.2.1. DESCRIPTION

The methodology explained in the previous section was applied to a representative MV network of four feeders, supplied by two primary substations, where each feeder is based on the standard IEEE 33-bus network [47]. This network allows the load transfer between feeders of different S/Ss, which is key in this work. Default values are considered for all input parameters, which are detailed in Appendix 1. In order to calculate the length of the branches of the network, a 6.05 MVA conductor with R = 0.579 Ω/km has been considered. Each feeder (F1 – F4) is assumed to supply 3715 customers. There are also six more feeders, not shown, connected to each common busbar at primary substations X and Y. It was considered that each one of them supplies 3000 customers. The network described above is illustrated in Figure 3.2, and the number of customers connected to each bus is given in Table 3.2.

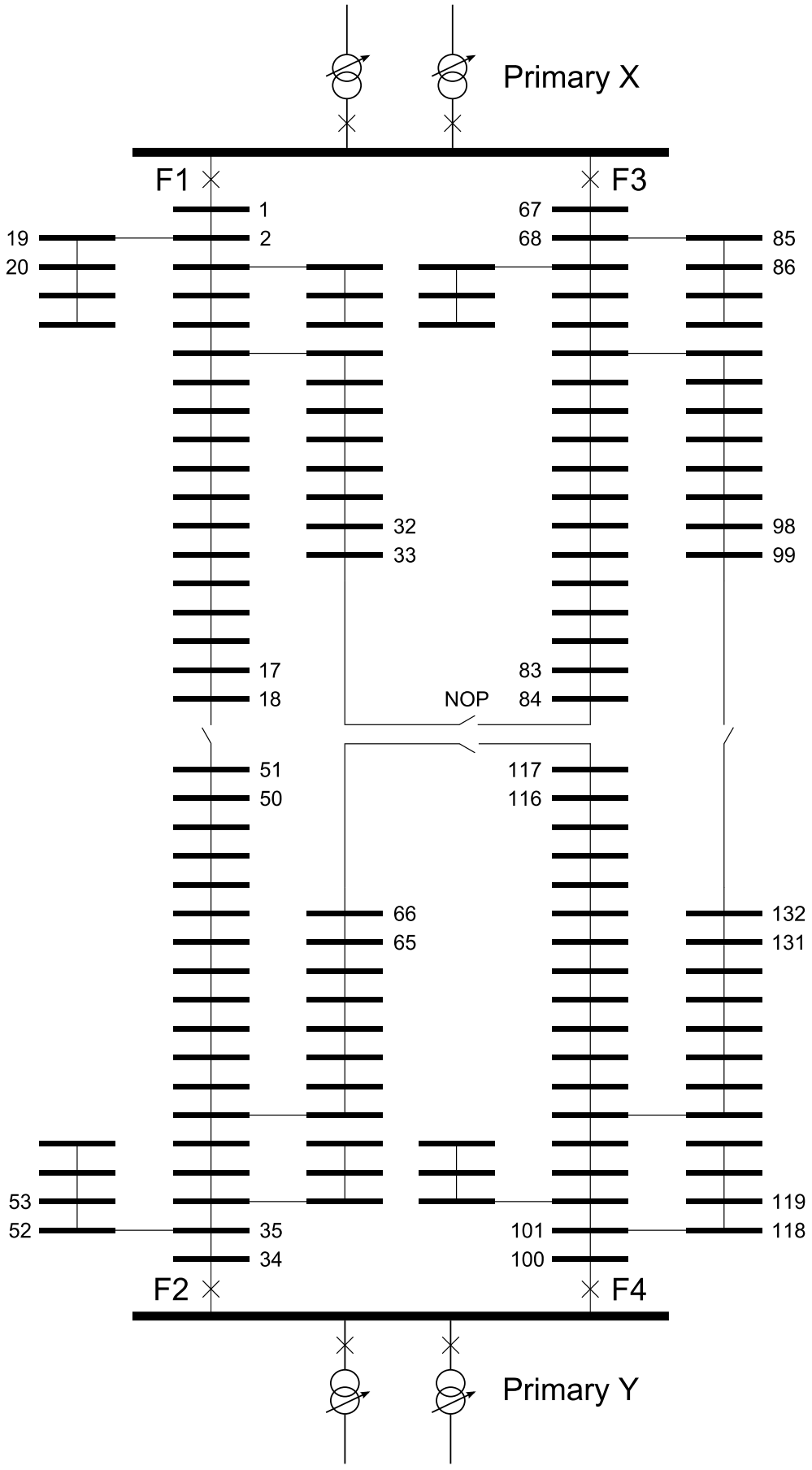

Figure 3.2: Case study network; it is composed of four standard IEEE 33-bus feeders.

Table 3.2: Number of customers connected to each bus of the case study network

Bus	*NC*	Bus	*NC*	Bus	*NC*
1	0	12	60	23	90
2	100	13	60	24	420
3	90	14	120	25	420
4	120	15	60	26	60
5	60	16	60	27	60
6	60	17	60	28	60
7	200	18	90	29	120
8	200	19	90	30	200
9	60	20	90	31	150
10	60	21	90	32	210
11	45	22	90	33	60

As mentioned in section 3.3.1, several network reconfigurations were performed via operating a pair of switches at the same time, and for each configuration, a number of variables were calculated. These include losses (computed using MATPOWER [88]) and their corresponding annual cost, asset risks, and minimum voltage magnitude.

The annual cost of active power losses [13] is given by:

$$Cost_{P_{\text{loss}}} = P_{\text{loss}} \cdot 8760 \cdot LLF \cdot EP, \tag{3.6}$$

where LLF is the Loss Load Factor, which is equal to $0.5LF + 0.5LF^2$ (according to [61]), and can be used to estimate total energy losses from power loss calculated at maximum load [89]; LF is the Load Factor, which was assumed to be 0.5; and the energy price was considered to be 64 \$/MWh (an exchange rate of 1.28 was used for the conversion from GBP to USD) [13].

Note that voltage was assumed to be 1.06 pu at S/S busbars, since IEEE 33-bus feeders experience significant voltage drop at their endpoints (see Appendix 1), and the statutory voltage limits in MV networks in the UK are ±6% of the nominal voltage [90].

Table 3.3 shows the HIs that have been considered for the transformers and the CBs in the case study network. As can be seen in this table, the

condition of the assets at primary S/S X was assumed much worse than that of Y. It should be mentioned that in this case study, HIs were allowed to take values up to 15, as future HIs in the CNAIM. All other parameter values that have been used in this case study are presented in Table 3.4.

Table 3.3: Asset Health Indices (the condition of S/S X is considered to be much worse than that of Y)

Primary S/S X		Primary S/S Y		Feeder CBs	
Asset	*HI*	Asset	*HI*	Asset	*HI*
TX 1	14.33	TX 1	5.66	F1 CB	4.00
TX 2	14.40	TX 2	6.52	F2 CB	4.00
CB 1	9.00	CB 1	4.00	F3 CB	4.00
CB 2	9.00	CB 2	4.00	F4 CB	4.00

Table 3.4: Case study parameter values (data taken from [11, 17, 86])

Parameter	Value	Parameter	Value	Parameter	Value
$K_{FR,TX}$	0.0454%	ST	1 h	F_{OHL}	100%
$K_{FR,CB}$	0.0052%	RT_{OHL}	5 h	F_{CB}	55%
$C_{TX/CB}$	1.087	RT_{CB}	4 h	$R2_{TX}$	50%
UCI	\$6.4	$R1$	0%	RT_{TX}	900 min
$UCML$	12.8 \$/h	$R2_{OHL/CB}$	100%	DF	0.2

3.3.2.2. RESULTS

The results of the present case study are shown in Table 3.5. In this table five criteria are shown, according to which the network can be reconfigured. It can be seen that different criteria result in different network configurations. Minimum losses lead to the initial network configuration (illustrated in Figure 3.2). OHL Risk becomes greater as the feeders become more asymmetrical, i.e. as load is transferred from one feeder to another. This is because, when a feeder becomes longer, the more likely it is for a failure to occur and when it does, more customers will be interrupted. In order to minimize TX Risk, load is transferred from primary X to Y, because of the deteriorated condition of the former S/S. The optimal network configuration is achieved when both cost of losses and TNR are considered. Figure 3.3 provides a graphical comparison of the results derived using the aforementioned criteria.

The first two criteria neglect asset condition, while the latter three take account of it. Comparing min Losses, and min (Overall Cost = Loss Cost + TNR) criteria, it can be derived that there is a difference of $7,350 in terms of overall cost. This saving is relatively small, as it accounts for the 0.75% of the overall cost; however, this saving corresponds to a single DN, which means that the overall saving for a DNO can be of substantial value. Therefore, it can be seen that the integration of asset condition in the decision-making process of network operation can lead to an improved overall outcome.

It should be noted that not all possible combinations of open switches have been examined, because as more load is transferred from one feeder to another, the more total OHL Risk and losses increase. This occurs because the feeders are interconnected at their endpoints, and by transferring load they become more unbalanced in terms of length and loading. Consequently, only five branches on either side of each NOP (referring to the initial network configuration) have been considered for this case study.

Table 3.5: Case study results; network reconfiguration using five different criteria: 1) min Losses (corresponds to the original configuration), 2) min OHL Risk, 3) min TX Risk, 4) min TNR, and 5) min (Overall Cost = Loss Cost + TNR)

Minimize:	Losses	OHL Risk	TX Risk	*TNR*	Overall Cost
Open Switches	18-51 33-84 66-117 99-132	16-17 82-83 63-64 129-130	13-14 28-29 61-62 94-95	16-17 30-31 115-116 94-95	16-17 82-83 115-116 96-97
Loss (kW)	709.34	766.22	1,438.20	898.93	744.39
V_{min} (pu)	0.979	0.937	0.800	0.893	0.954
OHL Risk	$354,999	$346,424	$371,430	$351,794	$348,340
S/S X Risk	$417,494	$421,926	$398,943	$402,883	$408,136
S/S Y Risk	$57,901	$57,285	$60,474	$59,927	$59,199
TX Risk	$475,395	$479,213	$459,415	$462,810	$467,334
CB Risk	$6,318	$6,318	$6,318	$6,318	$6,318
TNR	$836,712	$831,954	$837,165	$820,922	$821,993
Loss Cost	$149,132	$161,091	$302,367	$188,991	$156,502
Overall Cost	**$985,843**	$993,044	$1,139,532	$1,009,912	**$978,493**

In Table 3.5, Loss is the active power losses calculated at peak load; OHL Risk is the expected customer interruption cost (ECOST) from all OHL failures; S/S X Risk is the ECOST due to S/S X assets (i.e. TXs and CBs); likewise for S/S Y; TX Risk is the ECOST for all transformer failures; CB Risk is the ECOST for all feeder CB failures; *TNR* = OHL Risk + TX Risk + CB Risk; Loss Cost is the annual cost of active power losses; and Overall Cost = Loss Cost + *TNR*.

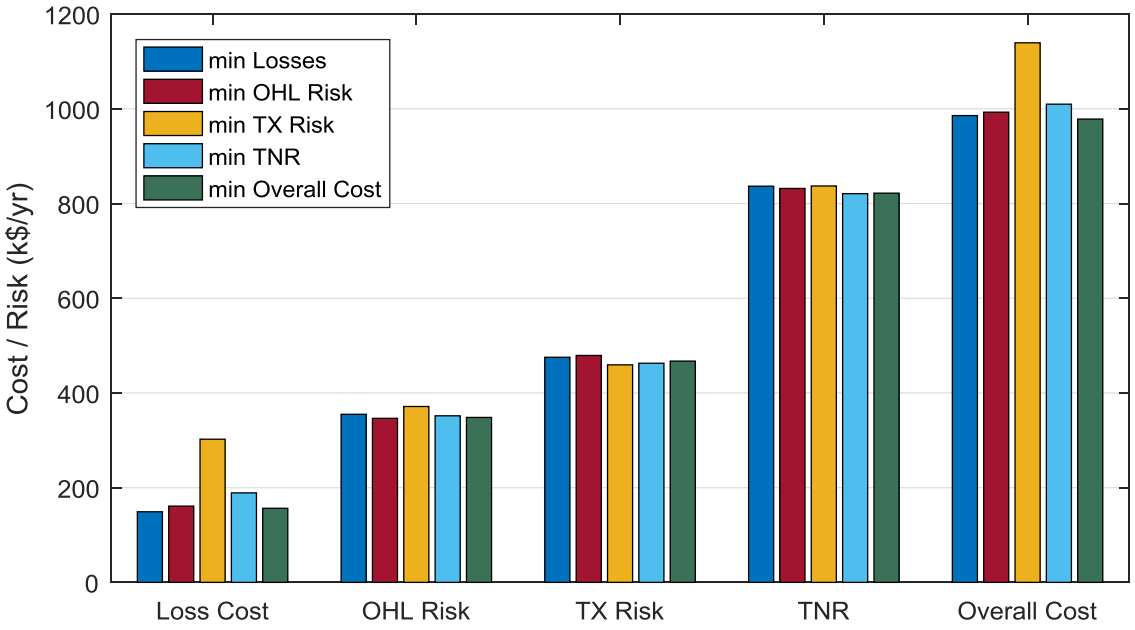

Figure 3.3: Graphical comparison of the results.

3.4. Incorporating Transformer Ageing into DNR

3.4.1. Methodology

This section extends the methodology presented earlier in this chapter, by incorporating the transformer ageing model analyzed in section 2.4. The ageing of the transformers is calculated and the corresponding loss of lives (expressed in monetary terms) are included in the objective function. To implement this methodology, a load profile is required, which is taken from [91]; and an overload condition needs to be simulated. For simplicity, all LPs are assumed to have the same load profile, which corresponds to residential customers. This load profile is illustrated in Figure 3.4.

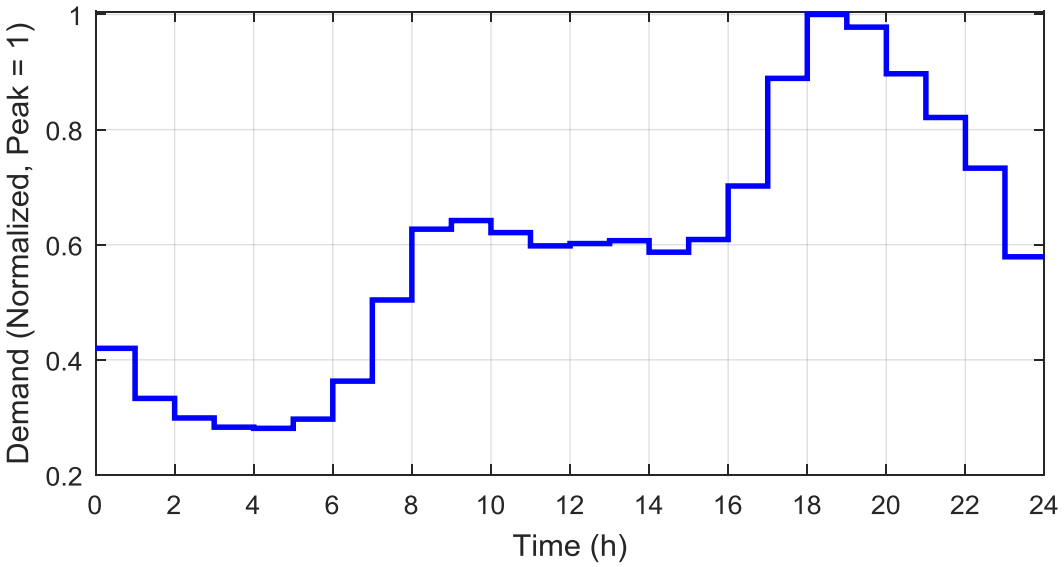

Figure 3.4: Load profile; 1) corresponds to residential customers, 2) hourly average values have been used, and 3) normalized so that peak is equal to one.

In order to simulate an overload to a transformer, it is assumed that one of the two S/S transformers is removed from service. This can occur either due to a planned or an unplanned outage. In this case, the equations ((3.2) and (3.3)) that yield *TX Network Risk* must be modified as follows:

$$CI = PoF \cdot NC \cdot UCI, \tag{3.7}$$

$$CML = PoF \cdot NC \cdot \left(R2 \cdot ST + \left(1 - R2\right) \cdot RT\right) \cdot UCML, \tag{3.8}$$

where *PoF* is the failure probability of the remaining S/S transformer (including the PoF of the associated CB). For a S/S that has both transformers in service, (3.2) and (3.3) should be used to calculate *TX Network Risk*, as presented in section 3.3.1.2.

It should also be stated that all risks and costs are derived for a one-day period. This means that all asset risk equations are modified appropriately in order to give the risk per day (i.e. dividing by 365); and the cost of losses becomes:

$$Cost_{P_{\text{loss,daily}}} = EP \cdot \sum_{h=1}^{24} P_{\text{loss},h} \cdot \Delta t, \tag{3.9}$$

where $P_{\text{loss},h}$ is the hourly active power loss during hour h, and Δt is the duration of each time interval, which is considered to be one hour.

The objective function can then be defined as:

$$\min f = Cost_{P_{\text{loss,daily}}} + TNR_{\text{daily}} + Cost_{\text{LoL}}, \tag{3.10}$$

where

$$Cost_{\text{LoL}} = \frac{\text{TX Replacement Cost}}{EL \cdot 365} \cdot L. \tag{3.11}$$

Taking data from [11], the asset replacement cost for a 33 kV transformer is \$424,724 and its expected life is 60 years (pre 1980). This yields

$$Cost_{\text{LoL}} = 19.39(\$/day) \cdot L(days) \tag{3.12}$$

for the following case study.

3.4.2. CASE STUDY

3.4.2.1. DESCRIPTION

The extended methodology described above was applied to the same network (see Figure 3.2) used in the previous case study. The modifications made in this case study (compared to the previous one) are the following:

1) load profiles were used for all LPs (see Figure 3.4);
2) one of S/S X transformers was removed from service (for one day), which caused an overload to the remaining transformer;
3) the duration of the study period was assumed to be one day;
4) the cost of loss of life of all S/S transformers was incorporated in the objective function;
5) no other feeders, except feeders F1 – F4 (which are shown in the network), were supplied through the S/Ss;
6) the rating of each S/S transformer was considered to be 5 MVA;
7) voltage limits were not taken into account, so as to be able to investigate the potential load transfer from the overloaded S/S to the other one, as this network has very high voltage drop;

8) seven branches on either side of each NOP (referring to the initial network configuration) were considered for network reconfiguration (the reasons for this have been explained in section 3.3.2.2).

The ambient temperature and the load factors (associated with the original network configuration) for the S/S transformers are illustrated in Figure 3.5. The transformers at S/S Y have the same load factor, as they share the S/S load. Hence, two lines are shown for transformer load factors in this figure; one for the remaining transformer at S/S X and one for each of the transformers at S/S Y.

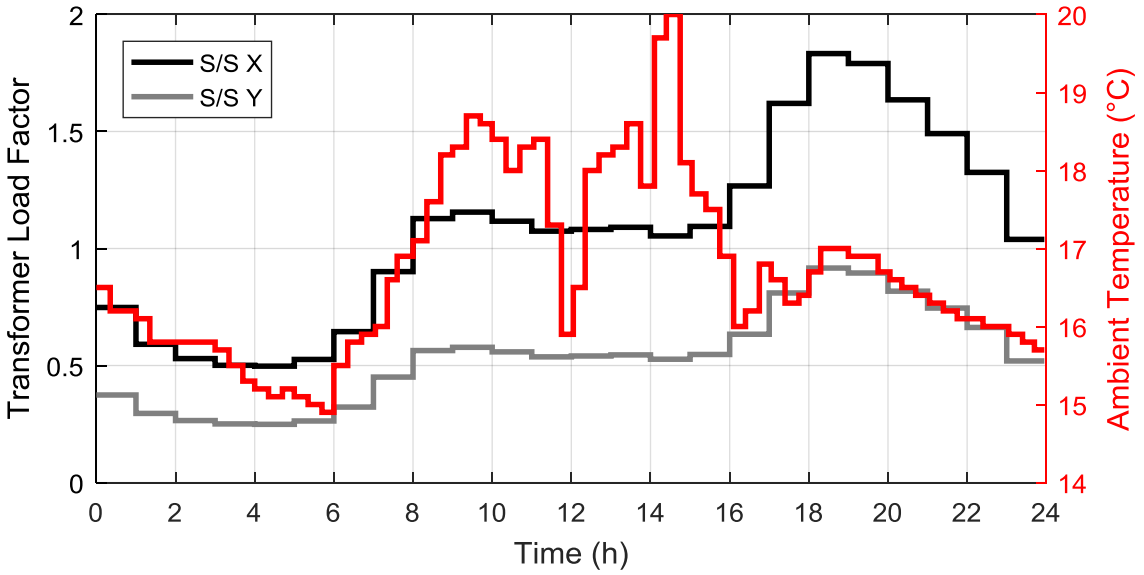

Figure 3.5: Ambient temperature and load factors for the remaining transformer at S/S X (black line), and each one of the transformers at S/S Y (grey line).

3.4.2.2. RESULTS

The results of this case study are presented in Table 3.6. The outage of the transformer at S/S X causes an overload at the transformer remaining in service. This can be clearly seen by its corresponding loss of life, which is 135 days for only one day of operation. This can be justified by Figure 3.5, according to which the load factor of the remaining transformer is above unity for 16 hours, and above 1.6 for four hours. Consequently, load transfer seems to be essential during this overload condition.

If loss of life of (all) transformers is included in the objective function (Overall Cost = Loss Cost + *TNR* + Cost of Loss of Life), then 12 LPs are transferred from S/S X to S/S Y (six from feeder F1 to F2, and another six from F3 to F4); this corresponds to a load of 1.25 MW (peak value). By performing this load transfer, S/S X is significantly relieved from the extremely heavy overload (in terms of ageing), whereas the impact of the additional load on the ageing of S/S Y transformers (both in service) is minimal. This is illustrated in Figures 3.6 and 3.7, where the transformer load factors and the corresponding relative ageing rates are shown for S/S X and S/S Y, respectively, for both network configurations (min Losses and min Overall Cost). Transferring a higher number of LPs would further improve the (total) cost of loss of life and S/S X risk, but it would also increase losses, OHL risk, and S/S Y risk (and that would result in a suboptimal overall cost).

For the original configuration, the maximum relative ageing rate for the transformer remaining at S/S X was above 1500, and the corresponding value for each of the transformers at S/S Y was below 0.1. These values for the second configuration were about 40 and 0.9, respectively. This means that the load transfer substantially reduced the highly accelerated ageing rate of the S/S X transformer, without leading to a significant loss of life for S/S Y transformers. This can be seen in Table 3.6, as well as in Figure 3.8, which illustrates the total loss of life (of all transformers), for both network configurations.

This balancing between the relative ageing rates of the transformers at S/Ss X and Y led to a reduction of $2,550 in terms of cost of loss of life (which is also equal to overall cost saving, as Loss Cost + *TNR* have the same values for both configurations). This saving is of significant value, as it corresponds to a single day (with an overload condition), and also accounts for five times the cost of energy losses for a day.

Table 3.6: Case study results; network reconfiguration according to the following objective functions: 1) min Losses, and 2) min (Overall Cost = Loss Cost + TNR + Cost of Loss of Life)

Minimize:	Losses	Overall Cost
Open Switches	18-51 33-84 66-117 99-132	12-13 33-84 115-116 93-94
Loss (MWh)	6.580	8.505
S/S X Risk	$841	$699
TNR	$1,865	$1,741
Loss Cost	$421	$544
Loss Cost + *TNR*	$2,286	$2,285
Loss of Life (S/S X TX)	**135.31 days**	**3.61 days**
Loss of Life (S/S Y TXs)	0.018 days	0.183 days
Cost of Loss of Life	**$2,624**	**$74**
Overall Cost	$4,910	$2,359

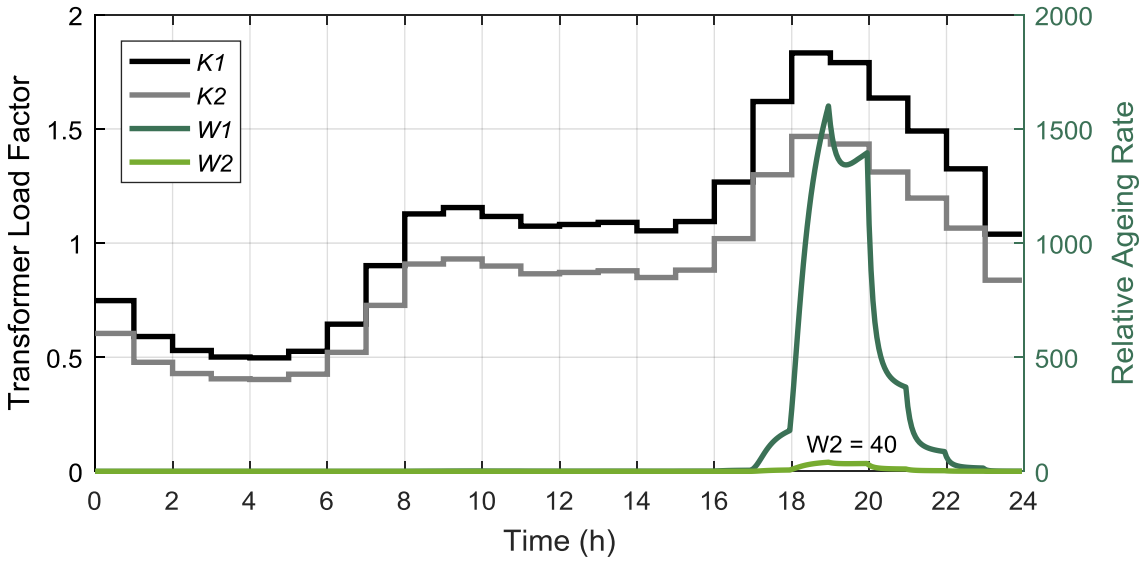

Figure 3.6: Transformer (S/S X) load factor (*K*) and relative ageing rate (*W*) for each of the two configurations: min Losses (1) and min Overall Cost (2).

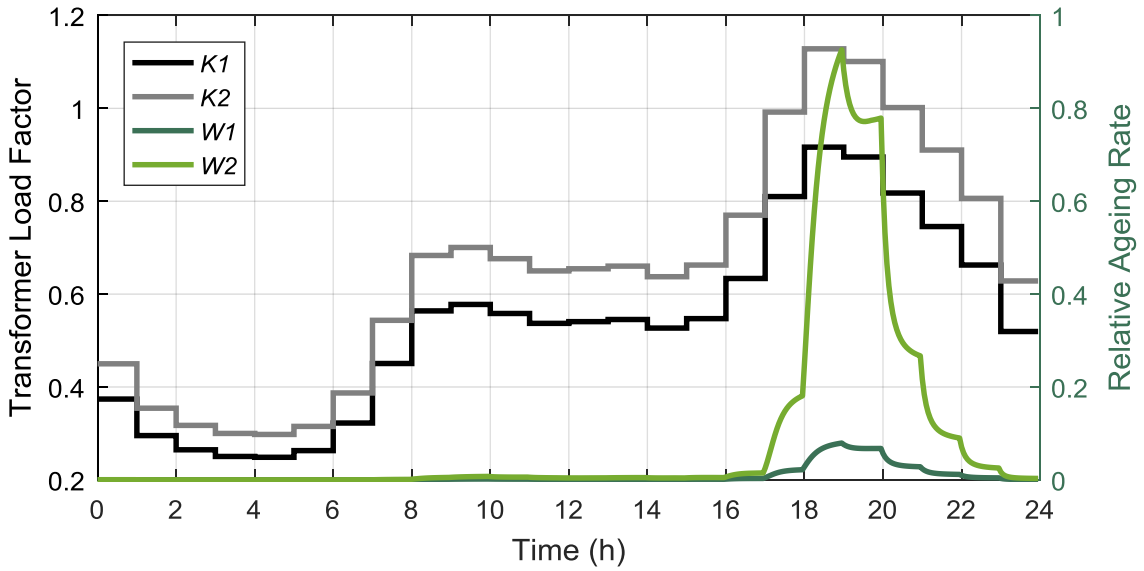

Figure 3.7: Load factor (*K*) and relative ageing rate (*W*) for each of the transformers at S/S Y, and for each of the two configurations: min Losses (1) and min Overall Cost (2).

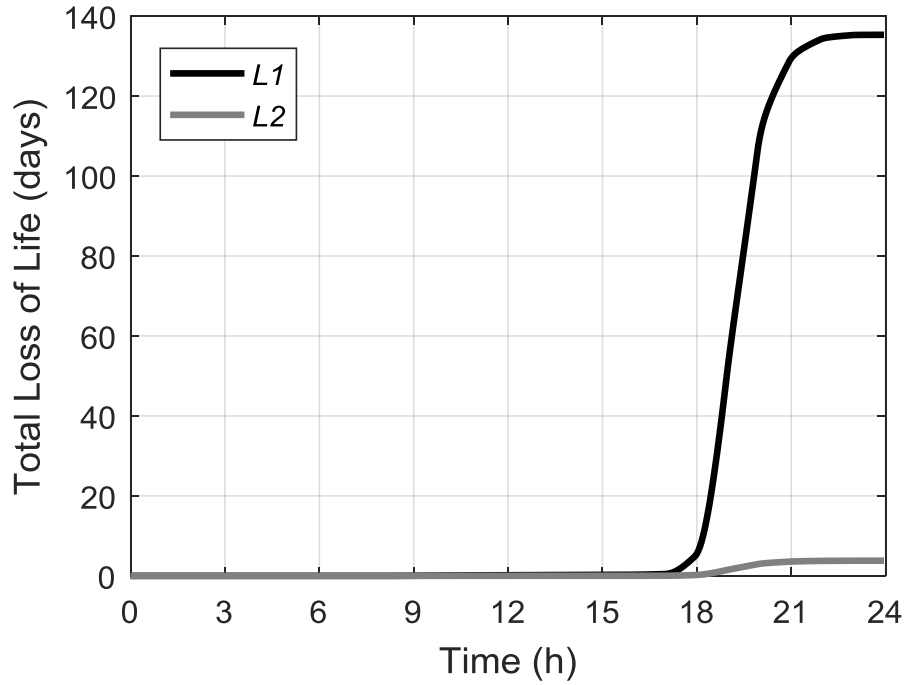

Figure 3.8: Total loss of life (*L*) of all transformers, for each network configuration: min Losses (black line) and min Overall Cost (grey line).

3.5. CONCLUSIONS

This chapter indicates that asset condition information can be used to have a positive impact on network operation. More specifically, the methodologies described in sections 3.3 and 3.4 have been applied to a representative MV DN and the results have shown that the incorporation of asset condition (through HIs, PoFs, risks, as well as transformer ageing and associated loss of lives) into DNR can result in reduced overall cost.

Particularly, the network configurations resulting from min Losses and min Overall Cost objective functions, had a difference (in terms of Overall Cost) of $7,350 per year in the first case study (section 3.3). This figure corresponds only to the four feeders of the case study network. However, a DNO typically has hundreds of feeders like those, and therefore, the overall savings can have a really significant value – potentially in the order of hundreds of thousands of U.S. dollars for one DNO.

The saving of $2,550 for a single day that an overload occurred – by taking transformer ageing into account, in section 3.4 – is of substantial value, as it corresponds to five times the cost of energy losses for a day. Moreover, despite the increase in losses, the load transfer is critical, as it balances – as much as possible – the relative ageing rates of the transformers at S/Ss X and Y, and hence their associated loss of lives.

Finally, by transferring load from a substation in deteriorated condition to another in a better state, it can be expected that the ageing rate of the former will be reduced, and accordingly its life is likely to be extended.

Chapter 4. Impact of Asset Condition and Substation Reliability on DNR

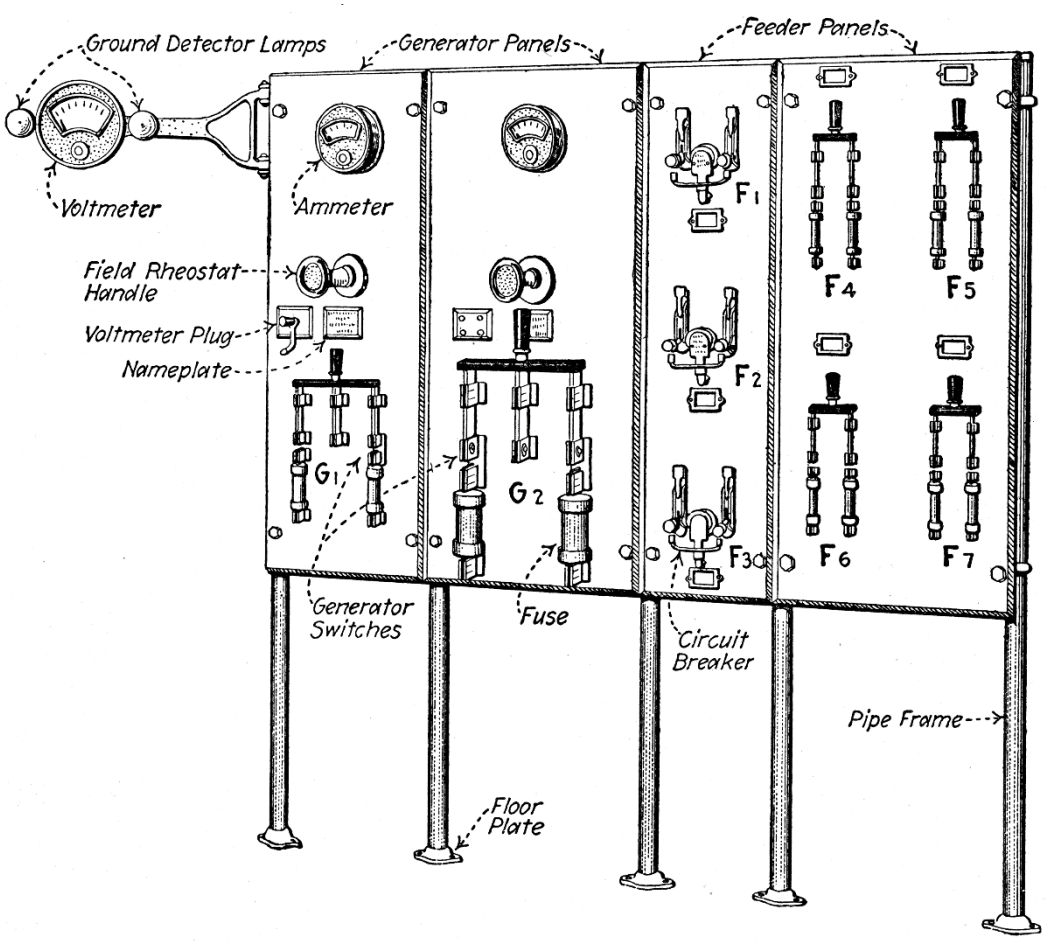

4.1. INTRODUCTION

This chapter further develops and improves the methodology presented in Chapter 3. Reliability analysis in this chapter includes: 1) the power of load points, instead of only number of customers; 2) various customer types and their corresponding CDFs; and 3) a number of different component failure modes. S/S reliability is evaluated in a more systematic way, according to three main factors: asset condition, S/S configuration, and the network upstream of the S/Ss. The first factor has already been analyzed; the other two are explained in this chapter. The reliability of the S/S then has an impact on the reliability indices of its LPs. All of these factors are combined to deliver a better informed algorithm for DNR, which is verified through its application on two DNs. The annual savings, compared to the formulation that neglects asset condition and S/S reliability, can be in the order of tens of thousands of U.S. dollars for a single DN.

4.2. RELIABILITY EVALUATION

As also mentioned in Chapter 3, the reliability model accounts for both the primary DN and S/Ss, which are analyzed in sections 4.2.1 and 4.2.2, respectively. The minimal cut set method is used to assess the network reliability [6, 92]. A minimal cut set is a set of components which, when all of them are out of service, an outage is caused to a specific LP. However, there is not an interruption of service, when at least one of these components remains operational. There are two failure modes for a component: passive and active. Passive events do not cause operation of the CBs and consequently do not affect any other healthy components, whereas active events cause the protection breakers to operate and a number of other healthy components are removed from service [6]. The following failure modes were considered in this chapter:

1) first-order permanent (total) failures (passive and active failures);
2) first-order active failures;
3) first-order active failures with stuck CBs;

4) second-order overlapping permanent failures (including maintenance).

The corresponding equations for the reliability indices of the above failure modes can be found in [6].

When all possible failure events and the LPs that are affected by each of them have been identified, the ECOST can be calculated. For each LP p and for each outage event j, the $ECOST_{jp}$ is calculated as follows [6, 85]:

$$ECOST_{jp} = C_{jp}(r_{jp})L_p\lambda_j. \tag{4.1}$$

The summation of $ECOST_{jp}$ for all LPs and all failure events yields the total ECOST of the network:

$$ECOST = \sum_{p=1}^{N_{\mathrm{LP}}} \sum_{j=1}^{N_{\mathrm{ev},p}} C_{jp}(r_{jp})L_p\lambda_j. \tag{4.2}$$

The interruption cost C_{jp} is a function of the interruption duration and is calculated using the CDF of each LP. Table 4.1 presents interruption cost estimates for various customer types and outage durations. These values are taken from [93] and are expressed in today's (2019) U.S. dollars. The CDFs are illustrated in Figure 4.1.

Table 4.1: Cost of interruption by customer type and outage duration (2019 $/kW)

User Sector	Interruption Duration				
	1 min	20 min	1 h	4 h	8 h
Industrial	2.853	6.791	15.950	44.176	97.976
Commercial	0.668	5.213	15.014	54.980	145.728
Residential	0.002	0.163	0.846	8.627	27.545
Office Buildings	8.389	17.342	36.982	120.837	209.197

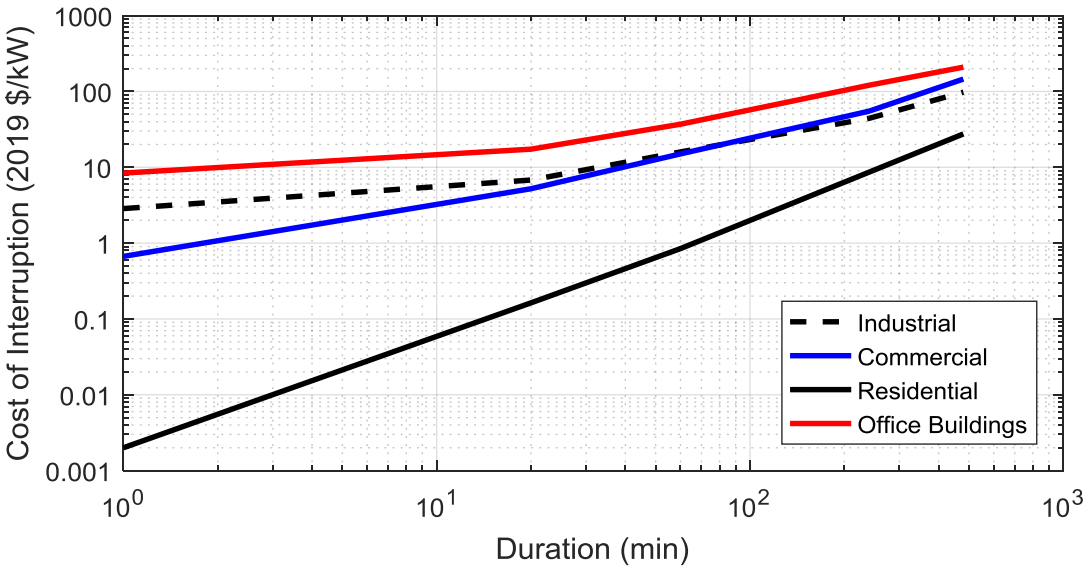

Figure 4.1: CDFs used to represent the cost of interruption for different customer types.

4.2.1. PRIMARY DISTRIBUTION NETWORK

A primary DN is the section of a network between the distribution S/Ss and the distribution transformers and comprises primary feeders which emanate from the low voltage buses of the distribution S/Ss [7]. These networks are operated in radial configuration; all of the minimal cut sets consist of a single component (line or CB) for each LP of the system. To demonstrate the reliability evaluation model for the primary DN, this was applied to one feeder (F2) of the RBTS Bus 4 DN [17], which is presented in Figure 4.2. In this network, there are disconnect switches at both ends of the main feeder sections and fuses in each lateral distributor. These components are not shown in Figure 4.2 and are considered perfectly reliable. Disconnect switches are generally not capable of breaking short-circuit currents and are used for isolation.

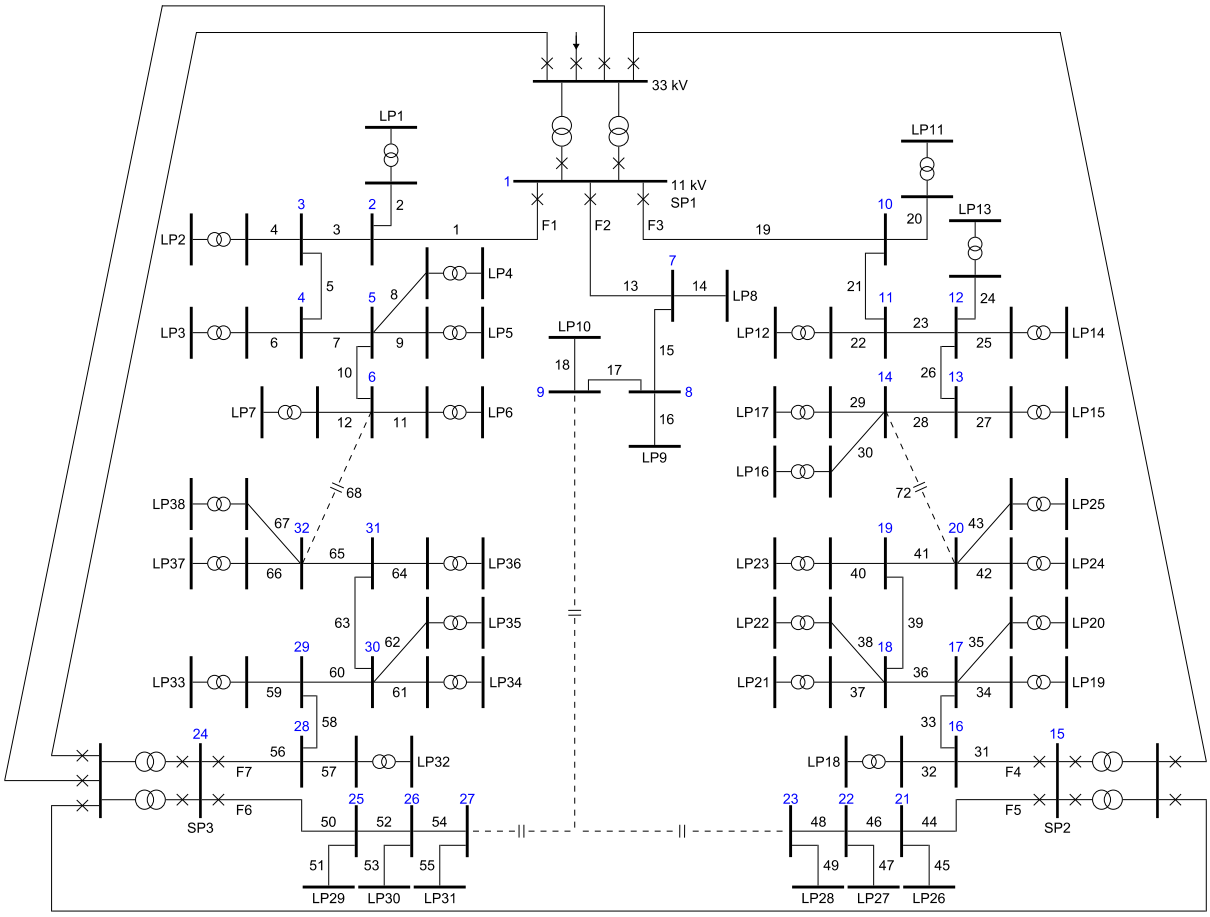

Figure 4.2: The RBTS Bus 4 DN (Branch numbers are shown in black; bus numbers are shown in blue).

An active failure along the main feeder causes the CB to operate to clear the fault, interrupting all LPs supplied by the feeder until the CB is reclosed. The time required to detect the fault and isolate is called switching time. After the CB has been reclosed, the power supply between the supply point (SP) and the point of isolation is restored. The LPs downstream of the faulted branch are restored following a repair, unless they can be transferred onto another feeder through a NOP.

If a fault occurs on a lateral distributor its fuse blows, causing the outage of the corresponding LP until the failed component is repaired. However, in this case, no other LPs are interrupted.

The failure of a feeder CB results in an outage of all LPs of the feeder. The failed CB must be repaired in order to restore the interrupted LPs unless an alternative supply is available.

To clarify the cases and processes above, Table 4.2 presents a reliability analysis for LP 9. Component reliability data were taken from [17] and LP 9 was considered to be an industrial customer with an average demand of 1.5 MW. The ECOST was calculated using (4.1) and the CDF for industrial customers.

Table 4.2: Results for Load Point 9 of the RBTS Bus 4 DN

Component Failure	λ (f/yr)	No Alt Supply r (h)	No Alt Supply *ECOST* (k$/yr)	Alternative Supply r (h)	Alternative Supply *ECOST* (k$/yr)
Main Feeder Section					
13	0.0520	5.00	4.453	1.00	1.244
15	0.0520	5.00	4.453	1.00	1.244
17	0.0390	1.00	0.933	1.00	0.933
Distributor					
16	0.0488	5.00	4.179	5.00	4.179
CB (total failure)	0.0060	4.00	0.398	1.00	0.144
Total	0.1978	4.18	14.416	1.99	7.744

In Table 4.2, r is the LP outage time, which is equal to the component repair time if the LP cannot be transferred, or equal to the switching time (assumed to be 1 hour) if the LP can be transferred.

4.2.2. SUBSTATIONS

S/Ss are the sources of the primary DN and are significant elements of power systems; their failure can lead to an outage at all LPs supplied by the failed S/S. To evaluate the reliability of S/Ss, three factors are considered in this chapter: asset condition, S/S configuration, and the network upstream of the S/Ss. The first factor was discussed in Chapter 2; sections 4.2.2.1 and 4.2.2.2 demonstrate the contribution of the other two factors to S/S reliability.

4.2.2.1. SUBSTATION CONFIGURATION

The arrangement of an S/S has an impact on its reliability indices. Two typical configurations [6] are shown in Figure 4.3. In configuration (a), the low voltage busbar, 7, is fed by two subtransmission lines, 1 and 4, through transformers 2 and 5. The low voltage side of each transformer is connected

to a CB (3 and 6). In configuration (b) the low voltage busbars, 7 and 8, are split by a normally open bus section CB.

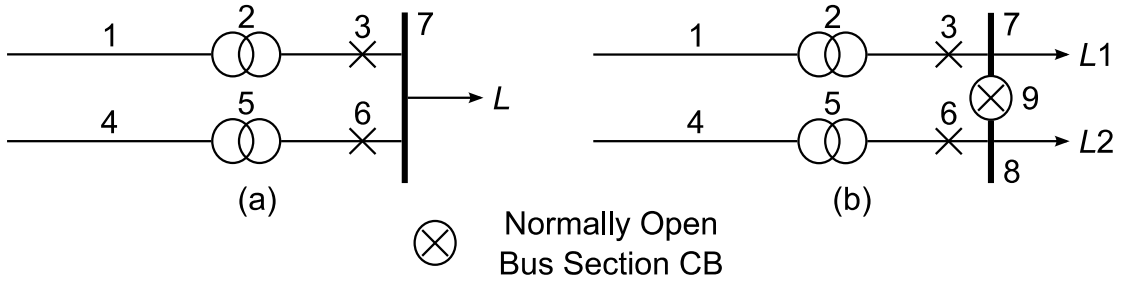

Figure 4.3: Typical S/S configurations: (a) shows a single low voltage busbar, while (b) shows two low voltage busbars separated by a normally open bus section CB.

These configurations were analyzed using component reliability data from [17], which are shown in Table 4.3. Every failure mode was included in the analysis for each configuration. The results of the reliability analysis are shown in Table 4.4 (the detailed reliability analysis can be found in Appendix 2). The results correspond to four cases:

1) non-automated S/S and no alternative supply;
2) automated S/S (with an S/S switching time of 10 min) and no alternative supply;
3) non-automated S/S and alternative supply;
4) automated S/S and alternative supply.

Table 4.3: Component Reliability Data

Component	λ_P	λ_A	λ''	r	r''	P_c
Transformers						
33/11 kV	0.0150	0.0150	1.0	15	120	–
11/0.4 kV	0.0150	0.0150	–	10*	–	–
CBs						
33 kV	0.0020	0.0015	0.5	4	96	0.05
11 kV	0.0060	0.0040	1.0	4	72	0.05
Busbars						
33 kV	0.0010	0.0010	0.5	2	8	–
11 kV	0.0010	0.0010	1.0	2	8	–
Lines**						
33 kV	0.0460	0.0460	0.5	8	8	–
11 kV	0.0650	0.0650	–	5	–	–

* Replacement time by a spare (h); ** Failure rates for lines in f/yr·km.

For each failure event, the failure rate, the outage time, and the ECOST were calculated. For the calculations, the S/S (each configuration) was assumed to be connected to SP2 of the RBTS Bus 4 DN, which supplies feeders F4 and F5, loaded at 4.01 MW and 3 MW, respectively. The sub-transmission line length was assumed to be 5 km.

Table 4.4: Substation Reliability Analysis Results; cases (1) – (4) correspond to the aforementioned four cases regarding the existence or not of S/S automation and alternative supply possibility

	Case	λ (f/yr)	r (h)	*ECOST* (k$/yr)
Config. (a)	(1)	0.0722	2.04	9.188
	(2)		1.47	6.957
	(3)		1.00	4.549
	(4)		0.43	2.318
Config. (b) Load L1 (Feeder F4)	(1)	0.2724	1.26	6.326
	(2)		0.47	3.009
	(3)		1.00	4.127
	(4)		0.17	0.794
Config. (b) Load L2 (Feeder F5)	(1)	0.2670	1.27	15.927
	(2)		0.47	7.633
	(3)		1.00	12.776
	(4)		0.17	4.482

Table 4.4 shows that different S/S configurations lead to different reliability indices and outage costs. S/S automation and alternative supply play an important role in determining the average outage duration of an S/S and the corresponding ECOST. The analysis also indicates: 1) the importance of considering active failures and stuck-breaker conditions, which depend on asset condition; 2) the impact of subtransmission lines on S/S reliability; and 3) the effect of asset maintenance.

If a CB fails to open, other CBs further from the failed component are activated; this might cause a greater part of the network, and more LPs, to be interrupted. Some of the failure events considered involve components that belong to the primary DN but cause the outage of the entire low voltage bus of the S/S; this is why it is critical to include these events in the analyses. These events are active failures of the feeder CBs (e.g. F4 CB) and

active failures on main feeder sections in combination with a stuck CB (e.g. (44, 46, 48)A + F5 CB S), which exhibit the interaction between S/Ss and the primary DN. The detailed S/S reliability analysis can be found in Appendix 2.

4.2.2.2. UPSTREAM NETWORK

Even if two S/Ss have the same configuration and the condition of their assets is identical, a difference in their upstream network can result in different reliability indices. To demonstrate this, the network upstream of the S/Ss of the RBTS Bus 4 DN (see Figure 4.4) was used as an example. Table 4.5 shows the results of the analysis.

Table 4.5: Impact of Upstream Network on Substation Reliability

Failure event	Number	λ (f/yr)	r (h)	*ECOST* (k$/yr)
Supply Point SP1				
First-order	2	2.00×10^{-3}	2.00	0.3099
Second-order	4	1.19×10^{-6}	5.93	0.0007
Second-order (m)	4	9.21×10^{-4}	10.37	0.9781
Active failure	10	5.45×10^{-2}	1.00	4.6458
Active + stuck	6	9.22×10^{-2}	1.00	7.8617
Total		1.50×10^{-1}	1.07	13.7961
Supply Point SP2				
First-order	3	3.00×10^{-3}	2.00	0.3362
Second-order	16	3.93×10^{-4}	3.99	0.0806
Second-order (m)	16	1.17×10^{-2}	7.40	5.3777
Active failure	15	9.15×10^{-2}	1.00	5.7647
Active + stuck	8	1.38×10^{-1}	1.00	8.7084
Total		2.45×10^{-1}	1.32	20.2676
Supply Point SP3				
First-order	3	3.00×10^{-3}	2.00	0.3403
Second-order	4	1.19×10^{-6}	5.93	0.0004
Second-order (m)	4	9.21×10^{-4}	10.37	0.6428
Active failure	16	9.30×10^{-2}	1.00	6.0214
Active + stuck	8	1.84×10^{-1}	1.00	11.9229
Total		2.81×10^{-1}	1.04	18.9278

(m) represents total outages overlapping a maintenance outage

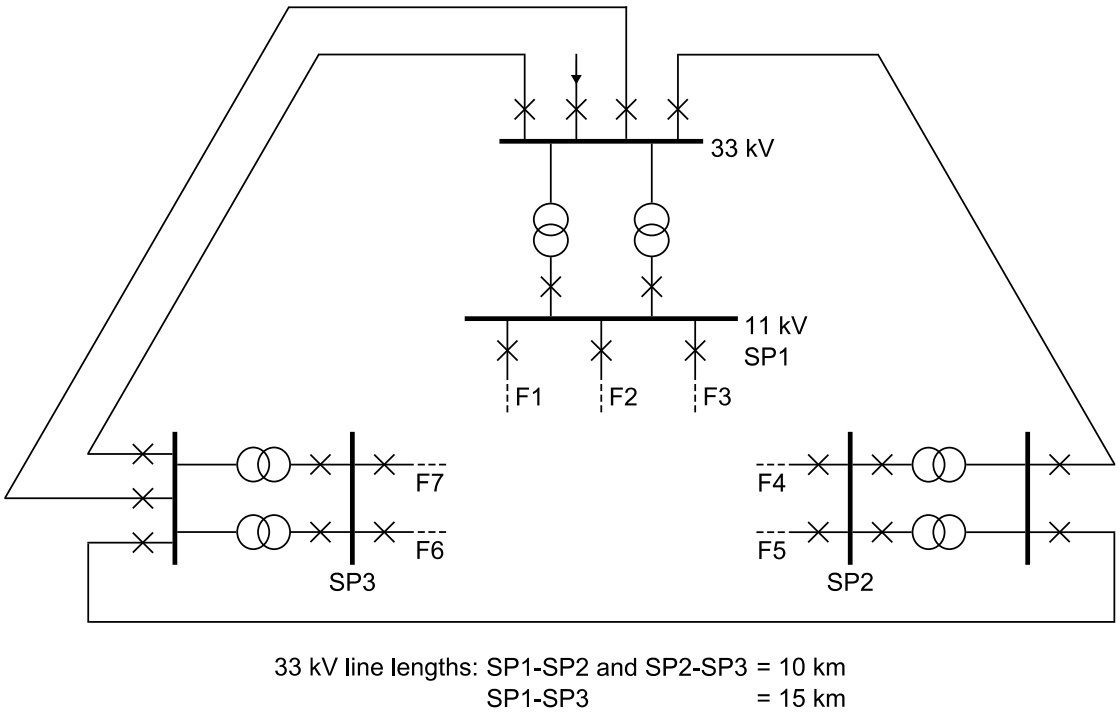

Figure 4.4: Upstream network of the RBTS Bus 4 DN.

Figure 4.4 shows that S/Ss 2 and 3 are fed through the 33 kV busbar of S/S 1. Therefore, it is expected that the failures rates of S/Ss 2 and 3 will be higher than the failure rate of S/S 1, as confirmed by Table 4.5. S/S 3 is supplied by three 33 kV lines, two of which are 15 km long. It can be deduced that their active failures, in combination with a stuck CB, are major contributors to the corresponding failure rate. This is why S/S 3 has the highest failure rate, illustrating the importance of the upstream network. S/S 2 is supplied by two 33 kV lines, which are 10 km long each, resulting in smaller contributions to the S/S failure rate by active + stuck failures compared to S/S 3. However, second-order outages (including maintenance) have a significantly higher contribution to the S/S failure rate, and an even larger impact on the ECOST.

Finally, the network downstream of the S/Ss has an impact on S/S reliability as well. This happens through main feeder section active failures in combination with a stuck feeder CB. This impact is small compared to the three aforementioned factors and this is why it is not analyzed separately, however it is considered in this study.

4.3. PROBLEM FORMULATION AND SOLUTION METHOD

4.3.1. PROBLEM FORMULATION

The goal of DNR is to find a radial configuration which optimizes a specific objective function whilst satisfying operational constraints. The proposed objective function and the relevant constraints are described in this section.

4.3.1.1. OBJECTIVE FUNCTION

This chapter proposes an aggregate cost function, comprising the annual cost of active power losses and the ECOST. The ECOST takes into account outages in the primary DN, and failures at S/Ss and the upstream network, while also considering the condition of network components through the use of condition-based failure rates within the reliability evaluation. The proposed cost objective function provides a balance between active power losses and network reliability, both of which are important issues to DNOs [84]. The objective function is as follows:

$$\min f = Cost_{P_{\text{loss}}} + ECOST + Pen. \tag{4.3}$$

The first term of (4.3) can be evaluated as follows [13]:

$$\begin{aligned} Cost_{P_{\text{loss}}} &= C_{P_{\text{loss}}} \cdot P_{\text{loss}} \\ &= 8760 \cdot LLF \cdot EP \cdot \sum_{k=1}^{N_{\text{br}}} \left|I_k\right|^2 R_k. \end{aligned} \tag{4.4}$$

The value of $C_{P_{\text{loss}}}$ has been considered here equal to 180 \$/kW, according to [84], and has been expressed in today's (2019) U.S. dollars.

4.3.1.2. TOPOLOGY CONSTRAINTS

The state vector (x) in DNR corresponds to a certain network configuration. The way decision variables are coded clearly affect the efficiency of the optimization algorithm [79]. In [80], a binary and a decimal encoding are presented. A binary encoding means that each decision variable represents the branch status – 0 for open, and 1 for closed; it is obvious that the

number of (reconfigurable) branches defines the length of the state vector in this case. A decimal encoding requires the identification of the fundamental loops of the network, and then each decision variable represents the open branch of each loop (in order to ensure a radial configuration); the length of the state vector in this case is equal to the number of loops. In the RBTS Bus 4 DN (see Figure 4.2), the size of the search space for binary encoding is 2^{34} = 1.718e+10, while the corresponding size for integer encoding is 11 × 7 × 7 × 7 × 11 = 41,503. Therefore, decimal encoding can substantially reduce the infeasible solution ratio, and thus improve the efficiency of the optimization algorithm (regardless of the method per se) [62].

In this study, integer encoding is adopted and it is applied to the RBTS Bus 4 DN in order to make it more comprehensible. In this network, only the main feeder sections are involved in the reconfiguration, since the disconnection of a lateral distributor would cause the isolation of an LP regardless of the wider network configuration. The loops of the network are shown below:

$$
\begin{aligned}
&L_1: \{1, 3, 5, 7, 10, 68, 65, 63, 60, 58, 56\},\\
&L_2: \{13, 15, 17, 69, 48, 46, 44\},\\
&L_3: \{13, 15, 17, 70, 54, 52, 50\},\\
&L_4: \{44, 46, 48, 71, 54, 52, 50\},\\
&L_5: \{19, 21, 23, 26, 28, 72, 41, 39, 36, 33, 31\},
\end{aligned}
$$

where branches 68-72 represent the NOPs between F1-F7, F2-F5, F2-F6, F5-F6, and F3-F4, respectively.

It has been assumed that F2, F5, and F6 are interconnected through single branches as shown in Figure 4.5.

The branches of each loop are renumbered sequentially and therefore the decision variables are constrained as follows:

$$
\begin{aligned}
&1 \le x_1, x_5 \le 11,\\
&1 \le x_2, x_3, x_4 \le 7,
\end{aligned}
\tag{4.5}
$$

where x_i, i = 1, 2,…, 5 represents the branch that is selected to break the loop i; generally, the state vector is $x = (x_1, x_2,\ldots, x_n)$, where n is the number of loops in the network under study, for example, if x = (5, 3, 4, 4, 5), the open branches of the network are the following: 10, 17, 70, 71, and 28.

The above constraints (4.5) are not sufficient to guarantee a feasible network configuration. Some non-smooth constraints are required to ensure connectivity of the network and that no loops are created. There can be multiple common branches between loops [64, 80] and this has to be taken into account. In this network, there are three loops (see Figure 4.5), that each two of them have branches in common. More specifically, branches {13, 15, 17}, {44, 46, 48}, and {50, 52, 54} are common between loops L_2 - L_3, L_2 - L_4, and L_3 - L_4, respectively. The first non-smooth constraint accounts for common branches between two loops. This means that from the above-mentioned sets of branches, not more than one branch from each set can be selected, e.g. if, branch 13 is open, then branches 15 and 17 should be closed. This topology (three loops, that each two of them have common branches) necessitates an additional non-smooth constraint, which is not mentioned in [64, 80]: not more than two branches of these sets can be selected, e.g. if branches 17 and 48 are open, then branches 50, 52, and 54 should be closed. Otherwise, a number of LPs would be isolated. These constraints can be written as:

$$Pen_1 = \begin{cases} \infty, & \text{loop constraints violation} \\ 0, & \text{otherwise} \end{cases} \tag{4.6}$$

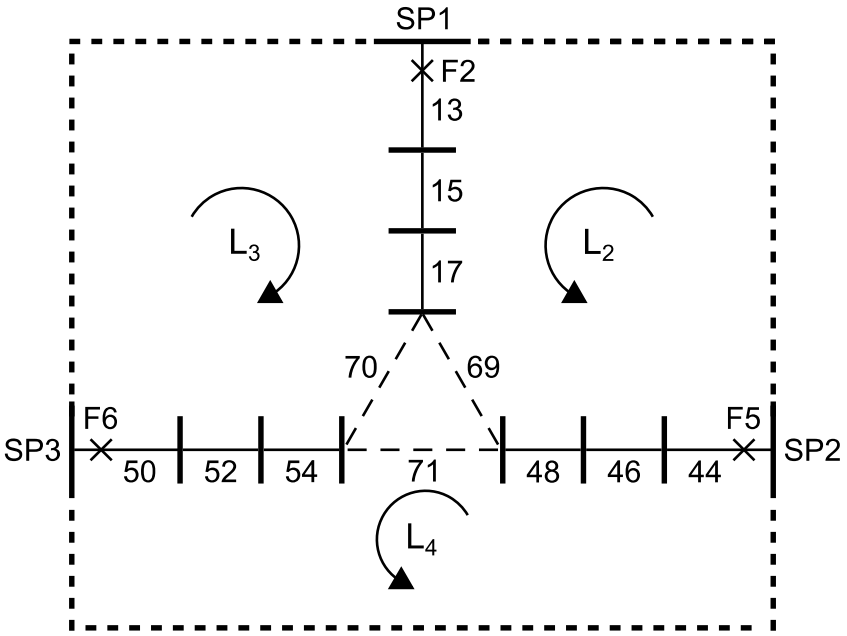

Figure 4.5: Part of the RBTS Bus 4 DN (loops 2-4, comprising F2, F5, and F6).

4.3.1.3. OPERATIONAL CONSTRAINTS

The network must respect operational voltage (4.7) and current (4.8) limits, which are enforced via a penalty constraint (4.9):

$$V_{\min} \le |V_i| \le V_{\max},\ i = 1,2,\ldots,N_{\text{bus}}, \tag{4.7}$$

$$|I_k| \le I_{k,\max},\ k = 1,2,\ldots,N_{\text{br}}, \tag{4.8}$$

$$Pen_2 = \begin{cases} \infty, & \text{operational constraints violation} \\ 0, & \text{otherwise} \end{cases} \tag{4.9}$$

The aforementioned penalty terms can thus be combined:

$$Pen = Pen_1 + Pen_2. \tag{4.10}$$

4.3.2. SOLUTION METHOD

Optimal DNR is a nonconvex mixed-integer nonlinear programming (MINLP) problem. Integer variables are introduced by the branch switches, through which the reconfiguration is implemented. Nonlinearity is introduced by the power-flow equations and the ECOST. These factors lead

to a heavy computational burden, especially when the network under consideration is large [58]; this has often led to the use of metaheuristics to solve the problem.

As far as the proposed solution approach is concerned, much weight is placed on the reduction of the size of the search space of the problem. A binary encoding of the decision variables (open/closed status) leads to a really high infeasible solution ratio; a decimal encoding can generate much fewer infeasible solutions, and therefore reduces the optimization time. Moreover, the formulation of extra (non-smooth) constraints, due to the existence of common branches between loops, reduces the number of power flow calculations – these of infeasible configurations – and in turn further decreases the computational time.

The problem formulation presented here can be used with any heuristic optimization algorithm. The GA has been selected in this work because it is an effective algorithm for large-scale combinatorial optimization problem and has been extensively used in the relevant literature [57-59]. It should also be noted that the *Integer ga* solver [94] used in this study is based on a modified and improved GA for solving integer and mixed integer optimization problems [79]. The performance of the optimization algorithm is presented in section 4.4.4 and is also compared to PSO.

The state vector, objective function, and constraints of the problem were explained in section 4.3.1. The problem has been formulated in MATLAB and is solved using the *Integer ga* solver [94]. The selected parameters for the GA are shown in Table 4.6. The stopping criterion for the algorithm is when the number of generations reaches *maximum generations*; however the GA will also stop if there is no change in the best objective function value in a sequence of generations equal to *maximum stall generations*. The power flow calculation for radial DNs are solved via a backward/forward sweep method, using MATPOWER [88]. The flowchart of the overall procedure is presented in Figure 4.6.

Table 4.6: GA Parameters

Parameter	Value
Population Size	50 (Case Study 1) / 100 (Case Study 2)
Maximum Generations	100
Maximum Stall Generations	30
Number of Runs	2

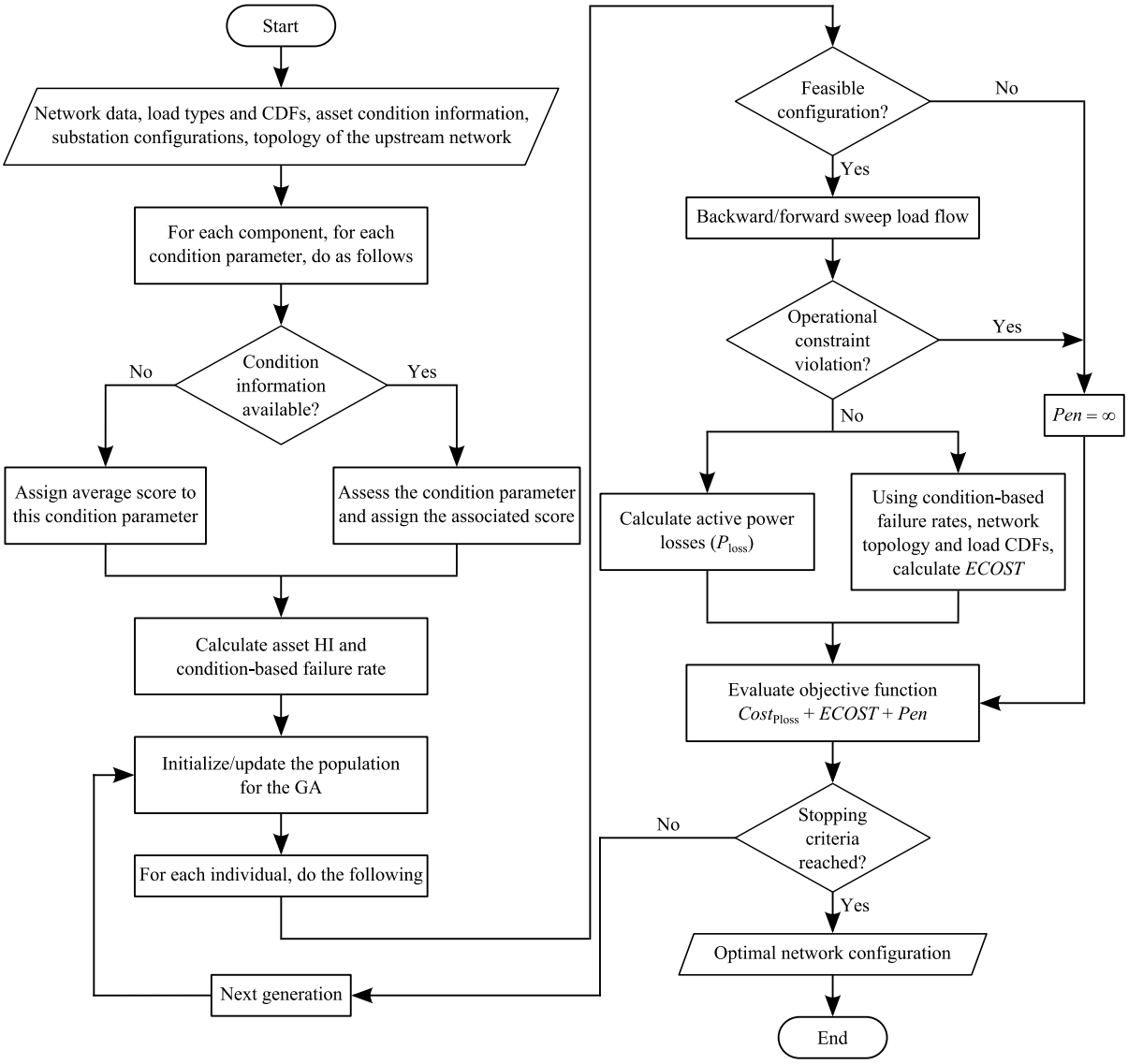

Figure 4.6: Flowchart of the proposed approach.

4.4. CASE STUDIES

The proposed DNR methodology was applied to two networks to demonstrate the value of incorporating asset condition and S/S reliability into the DNR formulation. The following assumptions were made for both case studies:

1) Condition-based failure rates are derived using Table 2.5;
2) CBs and OHLs in Table 2.5 are assumed to represent 11 kV assets;
3) Failure rates for 33 kV (the upstream network voltage) assets (CBs and OHLs) have been considered to be smaller than their 11 kV counterparts by the same proportion as in Table 4.3; the average failure rate for an 11 kV CB is assumed to be 0.01 f/yr, whereas the corresponding value for a 33 kV CB is 0.0033 f/yr. For OHLs, the average failure rate is considered to be 0.062 f/yr·km at 11 kV, and 0.044 f/yr·km at 33 kV;
4) CB failure rates illustrated in Table 2.5 are total failure rates and the associated active failure rates can be calculated using the ratio between these parameters in Table 4.3. Consequently, the average active failure rates for an 11 kV and a 33 kV CB are assumed to be 0.0067 f/yr and 0.0025 f/yr, respectively;
5) Component reliability data apart from failure rates are taken from Table 4.3;
6) All main feeder sections and laterals are considered as OHLs, unless otherwise stated;
7) OHL conductors are assumed to be ACSR 477 kcmil (R = 0.143 Ω/km).

4.4.1. RBTS BUS 4 DN

These case studies used the RBTS Bus 4 DN [17] (see Appendix 3), an 11 kV DN supplied by three 33/11 kV S/Ss, as shown in Figure 4.2. It has seven feeders, 29 normally closed branches (sectionalizing switches) and 5 normally open branches (tie switches).

The following modifications and assumptions have been made for the RBTS Bus 4 DN:

1) LPs 8-10 and 26-31 were industrial and LPs 24 and 25 were office buildings;
2) Alternative supply was available for all LPs (after switching), following a fault on a feeder or an S/S failure;

3) The failure rate for all distribution transformers was considered to be 0.015 f/yr;
4) Distribution transformers could be replaced by a spare following a failure;
5) The length of branches 68-72 was assumed to be 0.75 km;
6) Power factor for all LPs was 0.98 lagging.

The impact of the upstream network and the condition of S/S components on DNR is demonstrated through the following two test cases.

4.4.1.1. TEST CASE 1

This test case indicates that the network upstream of the S/Ss, if taken into account, can change the optimal configuration of the network, even if the S/Ss have the same configuration and their components are in identical condition. The upstream network can be seen in Figure 4.4. The HI of all network assets was assumed to be 0.5, which corresponds to average failure rates (taken from Table 2.5). Using these failure rates, the S/S failure rates were calculated using the methodology described in section 4.2, and are shown in Table 4.7. These S/S failure rates do not include the failure rates of active faults on main feeder sections in combination with a stuck feeder CB, because they change depending on network configuration. However, they are considered when determining the optimal DN configuration.

Table 4.7: Substation Failure Rates (Test Case 1); calculated according to the methodology described in section 4.2, using average failure rates from Table 2.5

Substation	S/S 1	S/S 2	S/S 3
Failure Rate (f/yr)	0.2313	0.3878	0.4012

The failure rates of S/Ss 2 and 3 are significantly higher than that of S/S 1. This is because S/Ss 2 and 3 are supplied by the high voltage busbar of S/S 1; therefore all failure events that cause the outage of this busbar also lead to the outage of S/Ss 2 and 3.

Optimal configurations were found using two objective functions: Total Cost 1 did not account for failures caused by components at S/Ss and the

upstream network. Total Cost 2 considered the total ECOST and resulted in a different optimal configuration. This was due to a load transfer from S/S 2, which had a higher failure rate and ECOST, to S/S 1, which had the lowest failure rate and ECOST. The results for this test case are shown in Table 4.8.

Table 4.8: Optimal Configuration for the RBTS Bus 4 DN (Test Case 1)

Configuration	Original	min Total Cost 1	min Total Cost 2
Open Branches	68-72	68-72	68-71, 41
$ECOST_1$ (\$/yr)	102,114	102,114	104,085
$ECOST_2$ (S/S 1) (\$/yr)	19,717	19,717	26,817
$ECOST_2$ (S/S 2) (\$/yr)	31,503	31,503	19,599
$ECOST_2$ (S/S 3) (\$/yr)	25,976	25,976	25,976
$ECOST_2$ (Total) (\$/yr)	77,196	77,196	72,392
ECOST (\$/yr)	179,310	179,310	176,477
Loss (kW)	730.86	730.86	742.14
Loss Cost (\$/yr)	131,555	131,555	133,585
Total Cost 1 (\$/yr)	233,669	233,669	237,670
Total Cost 2 (*f*) (\$/yr)	310,865	310,865	**310,062**

In Table 4.8, Open Branches are the inactive branches, which define a specific network configuration; $ECOST_1$ is the ECOST for failure events in the primary DN; $ECOST_2$ is the (total) ECOST for failure events at S/Ss and the upstream network; $ECOST_2$ (S/S 1), $ECOST_2$ (S/S 2), and $ECOST_2$ (S/S 3) are the $ECOST_2$ contributions from S/S 1, S/S 2, and S/S 3, respectively; *ECOST* is the total ECOST of the network ($ECOST_1$ + $ECOST_2$); Loss is the active power losses calculated at peak load; Loss Cost is the annual cost of active power losses; Total Cost 1 is the total cost considering the annual cost of active power losses and the ECOST for the primary DN only, i.e. Loss Cost + $ECOST_1$; and Total Cost 2 is the total cost considering the annual cost of active power losses and the total ECOST, i.e. Loss Cost + $ECOST_1$ + $ECOST_2$.

The optimal configuration of the network changed with the objective function. Specifically, LPs 24 and 25 (0.415 MW each, office buildings) were transferred from S/S 2 to S/S 1 by closing branch 72 and opening branch 41.

This change increased the cost of losses (+2,030 $/yr) and $ECOST_1$ (+1,971 $/yr), but reduced the $ECOST_2$ (-4,804 $/yr). This led to an overall cost reduction of 803 $/yr, which rose to 1,389 $/yr, if LPs 24 and 25 were increased to 1 MW.

4.4.1.2. TEST CASE 2

This test case examined the impact of S/S asset condition on optimal network configuration. The main assumption of this test case was that S/S 2 was in worse condition than the other S/Ss, as illustrated by the HIs (and associated failure rates) shown in Table 4.9. The HI of all other assets was considered to be 0.5. According to the condition-based failure rates of the S/S assets, the failure rate of each S/S was calculated; these are shown in Table 4.10. As in Test Case 1, the optimal configurations for minimum Total Cost 1 and Total Cost 2 were compared, and the results are presented in Table 4.11.

Table 4.9: Health Indices and Failure Rates of Substation Assets (Test Case 2)

Substation	S/S 1		S/S 2		S/S 3	
Asset	HI	λ (f/yr)	HI	λ (f/yr)	HI	λ (f/yr)
Transformers	0.26	0.020	0.86	0.100	0.26	0.020
33 kV Busbar	0.35	0.005	0.67	0.020	0.35	0.005
11 kV Busbar	0.35	0.005	0.67	0.020	0.35	0.005
33 kV CBs	0.37	0.002	0.74	0.008	0.37	0.002
11 kV CBs	0.44	0.008	0.75	0.025	0.44	0.008

Table 4.10: Substation Failure Rates (Test Case 2)

Substation	S/S 1	S/S 2	S/S 3
Failure Rate (f/yr)	0.1532	0.5319	0.2785

Table 4.11 shows that the minimization of Total Cost 2 resulted in a different optimal configuration, according to which LPs 24 and 25 (0.415 MW, office buildings) were transferred from S/S 2 to S/S 1. This load transfer reduced $ECOST_2$ (S/S 2) by 16,327 $/yr, and increased $ECOST_2$ (S/S 1) by only 4,703 $/yr. The difference in the overall cost (Loss Cost + *ECOST*) of the two aforementioned network configurations was 7,806 $/yr. This difference rose to 18,267 $/yr, when LPs 24 and 25 were increased to 1 MW

each. The process was repeated, with the S/Ss considered to be automated with a switching time of 10 minutes. The cost reductions became 1,929 $/yr and 4,106 $/yr for the initial and increased loads, respectively; these results are illustrated in Figure 4.7.

Table 4.11: Optimal Configuration for the RBTS Bus 4 DN (Test Case 2)

Configuration	min Total Cost 1	min Total Cost 2
Open Branches	68-72	68-71, 41
$ECOST_1$ ($/yr)	102,432	104,220
$ECOST_2$ (S/S 1) ($/yr)	13,059	17,762
$ECOST_2$ (S/S 2) ($/yr)	43,209	26,882
$ECOST_2$ (S/S 3) ($/yr)	18,032	18,032
$ECOST_2$ (Total) ($/yr)	74,300	62,676
$ECOST$ ($/yr)	176,732	166,896
Loss (kW)	730.86	742.14
Loss Cost ($/yr)	131,555	133,585
Total Cost 1 ($/yr)	233,987	237,805
Total Cost 2 (f) ($/yr)	308,287	**300,481**

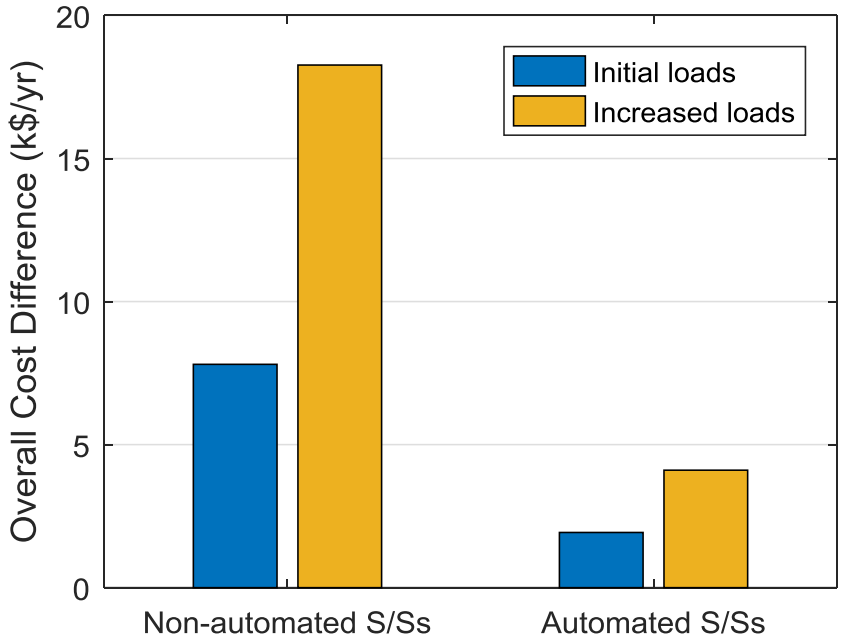

Figure 4.7: Overall cost difference for non-automated and automated substations, as well as initial and increased loads (Test Case 2).

4.4.2. TAIWAN POWER COMPANY (TPC) DN

In the second case study, the proposed methodology was applied on a real-world DN operated by Taiwan Power Company (TPC) [95] (see Appendix 4),

shown in Figure 4.8. This network is an 11.4 kV DN supplied by two S/Ss. It has 11 feeders, 83 normally closed branches and 13 normally open branches.

The following modifications and assumptions have been made for the TPC DN:

1) Customer types for all LPs were considered as shown in Table 4.12;
2) Subtransmission lines were assumed to be 10 km long;
3) The ratio between peak and average load was considered 1.63, as in [17];
4) LPs 55 and 72 were increased to 1 MW;
5) Alternative supply was available for all LPs (after switching) with the exception of LPs 8-10 and 21-24, for which there were a number of branch failures which led to an interruption until the failed component was repaired;
6) Branch failure rates were calculated using the considered conductor type and branch resistances.

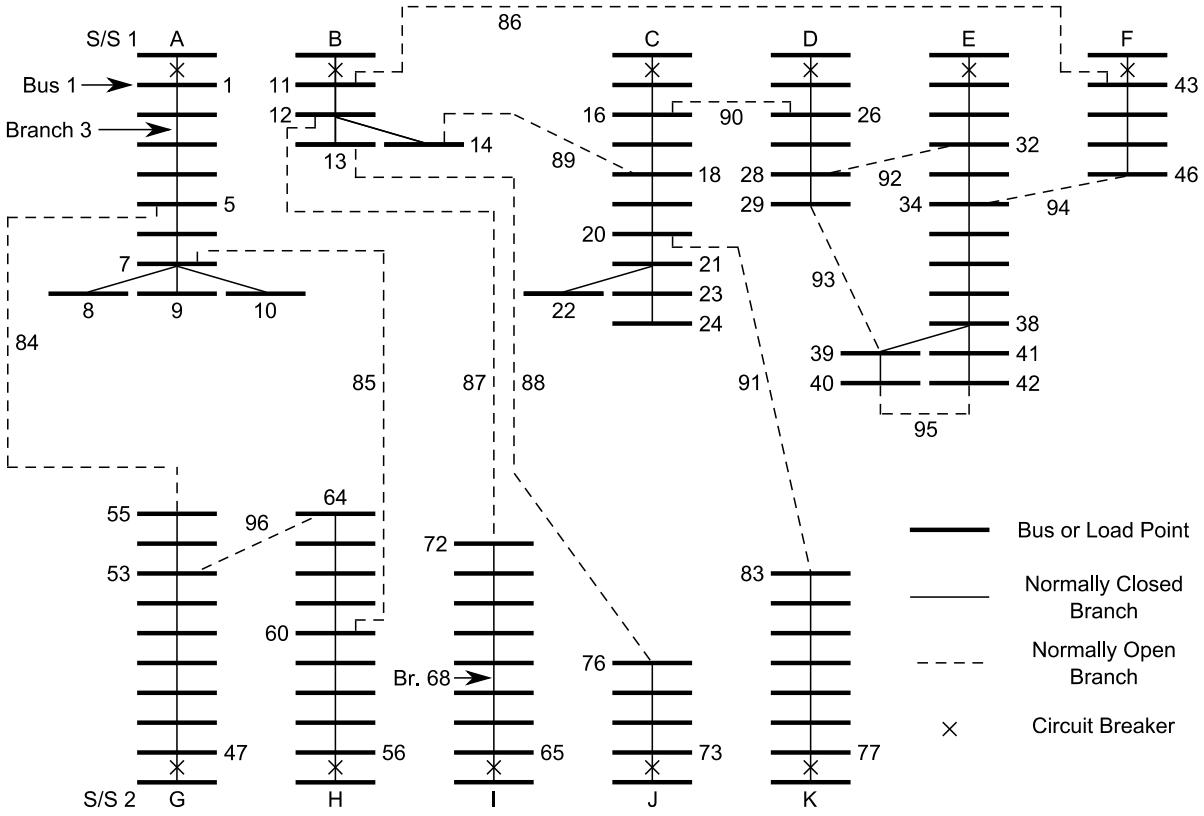

Figure 4.8: TPC DN.

Table 4.12: Load Types for the TPC DN

Load Type	Load Point (Bus)
Residential	2-4, 6, 8-10, 17-20, 22-28, 31, 34-42, 44, 45, 50, 51, 57, 59-62, 66, 71, 79, 80, 82
Commercial	5, 7, 16, 21, 29, 32, 33, 46, 52-54, 63, 64, 68, 78, 83
Industrial	12-14, 75, 76
Office Buildings	55, 58, 72, 81

4.4.2.1. TEST CASE 3

This test case demonstrated the effect of S/S configuration on DNR. The assumed S/S configurations (see Figure 4.3) were as follows: configuration (a) was used for S/S 1 and configuration (b) for S/S 2. The low voltage busbar of S/S 1 supplied feeders A-F, and the split low voltage busbar of S/S 2 supplied feeders G-I on one side (S/S 2a) and feeders J and K on the other side (S/S 2b).

Taking the S/S configurations into account, and assuming an HI of 0.5 for all network components, S/S failure rates were computed (see Table 4.13). S/S 2 had a higher failure rate than S/S 1 because of combination of the split low voltage busbar and the long subtransmission lines (10 km). The optimal network configurations for Test Case 3 are shown in Table 4.14.

Table 4.13: Substation Failure Rates (Test Case 3)

Substation	S/S 1	S/S 2a	S/S 2b
Failure Rate (f/yr)	0.1337	0.5270	0.5200

The higher failure rates of S/S 2 compared to S/S 1 led to a load transfer from the former to the latter; LPs 55 and 72 (1 MW each, office buildings) were transferred by closing branches 84 and 87, and opening branches 55 and 72. The $ECOST_2$ (S/S 2) reduction due to this load transfer was 23,913 \$/yr, and the $ECOST_2$ (S/S 1) increase was 6,067 \$/yr; considering S/S reliability within the DNR formulation led to a cost reduction of 11,025 \$/yr.

Table 4.14: Optimal Configuration for the TPC DN (Test Case 3)

Configuration	Original	min Total Cost 1	min Total Cost 2
Open Branches	84-96	7, 34, 36, 42, 63, 83, 84, 86-90, 92	7, 34, 36, 42, 55, 63, 72, 83, 86, 88-90, 92
$ECOST_1$ (\$/yr)	78,731	76,130	85,147
$ECOST_2$ (S/S 1) (\$/yr)	6,949	6,886	12,953
$ECOST_2$ (S/S 2a) (\$/yr)	44,131	46,319	22,406
$ECOST_2$ (S/S 2b) (\$/yr)	17,984	16,068	16,068
$ECOST_2$ (Total) (\$/yr)	69,064	69,273	51,427
$ECOST$ (\$/yr)	147,795	145,403	136,573
Loss (kW)	591.57	542.83	530.63
Loss Cost (\$/yr)	106,483	97,709	95,513
Total Cost 1 (\$/yr)	185,214	173,839	180,660
Total Cost 2 (f) (\$/yr)	254,278	243,112	**232,087**

4.4.2.2. TEST CASE 4

This test case considered the influence of primary DN asset condition on optimal DNR by comparing the optimal configuration from min Total Cost 1, which ignored asset condition, to its counterpart from min Total Cost 2, which took asset condition into account. In this test case, branch 68 (here considered as UGC) was considered to be in poor condition; specifically its HI was equal to 0.9, corresponding to a failure rate of 1.0635 f/yr (assuming a cable resistance of 0.086 Ω/km). The details for branch 68 are presented in Table 4.15. The HI of all other primary DN assets was considered to be 0.5. It should be noted that if condition data are available for a number of assets, then all of them can be used in order to inform the optimization algorithm. In this test case, only one branch was assumed to be in a condition other than average. This is because one is enough to indicate the impact of the condition of primary DN assets on DNR. The optimization results for the present test case are shown in Table 4.16.

The high condition-based failure rate of branch 68 led to the transfer of LP 72 (1 MW, office buildings) from feeder I to feeder B. This transfer can be justified through the failure rate and the ECOST of LP 72 for the two configurations. In the first case, LP 72 was connected to feeder I, and its

failure rate was 1.3031 f/yr; in the second case, it was connected to feeder B and the failure rate fell to 0.3783 f/yr, reducing the ECOST of this LP by 20,982 $/yr. Table 4.16 shows that the overall cost reduction through taking asset condition into account, was 18,877 $/yr.

Table 4.15: Branch 68 Parameters

Parameter	Value
Section Resistance (Ω)	0.2187
Conductor Resistance (Ω/km)	0.0860
Length (km)	2.5430
Health Index	0.9000
Failure Rate (f/yr)	1.0635

Table 4.16: Optimal Configuration for the TPC DN (Test Case 4)

Configuration	min Total Cost 1	min Total Cost 2
Open Branches	7, 34, 36, 42, 63, 83, 84, 86-90, 92	7, 34, 36, 42, 63, 72, 83, 84, 86, 88-90, 92
$ECOST_1$ ($/yr)	111,708	95,256
$ECOST_2$ ($/yr)	21,985	22,135
$ECOST$ ($/yr)	133,693	117,391
Loss (kW)	542.83	528.52
Loss Cost ($/yr)	97,709	95,134
Total Cost 1 ($/yr)	209,417	190,390
Total Cost 2 (f) ($/yr)	231,402	**212,525**

The annual savings (for both case studies) – compared to the formulation that neglects asset condition and S/S reliability – can be in the order of tens of thousands of U.S. dollars for a single DN. This corresponds approximately to 10% of the annual cost of active power losses, which is a considerable amount of saving. It should also be noted that this can mean hundreds of thousands – or even millions – of U.S. dollars for a single DNO (as it typically has hundreds of primary S/Ss).

4.4.3. Sensitivity Analysis

A sensitivity analysis was conducted to investigate how overall cost difference (difference in Total Cost 2 for min Total Cost 1 and min Total Cost 2 configurations) is influenced by three parameters:

1) S/S 2 failure rate;
2) power demand of LPs 24 and 25;
3) S/S switching time (which is related to S/S automation).

The sensitivity analysis was carried out using Test Case 2, with increased loading on LPs 24 and 25. The corresponding results are illustrated in Figures 4.9-4.11.

Increasing S/S 2 failure rate also increased the difference between the failure rates of S/Ss 1 and 2 (given that S/S 1 failure rate was kept constant), which caused the increase in the overall cost difference. Moreover, as the failure rate of S/S 2 increased, the optimal configuration of the network changed. Consequently, Figure 4.9 is divided into five segments, which represent five different network configurations; when the failure rate reached given thresholds, LPs were transferred from S/S2 to S/S1, as illustrated in the figure.

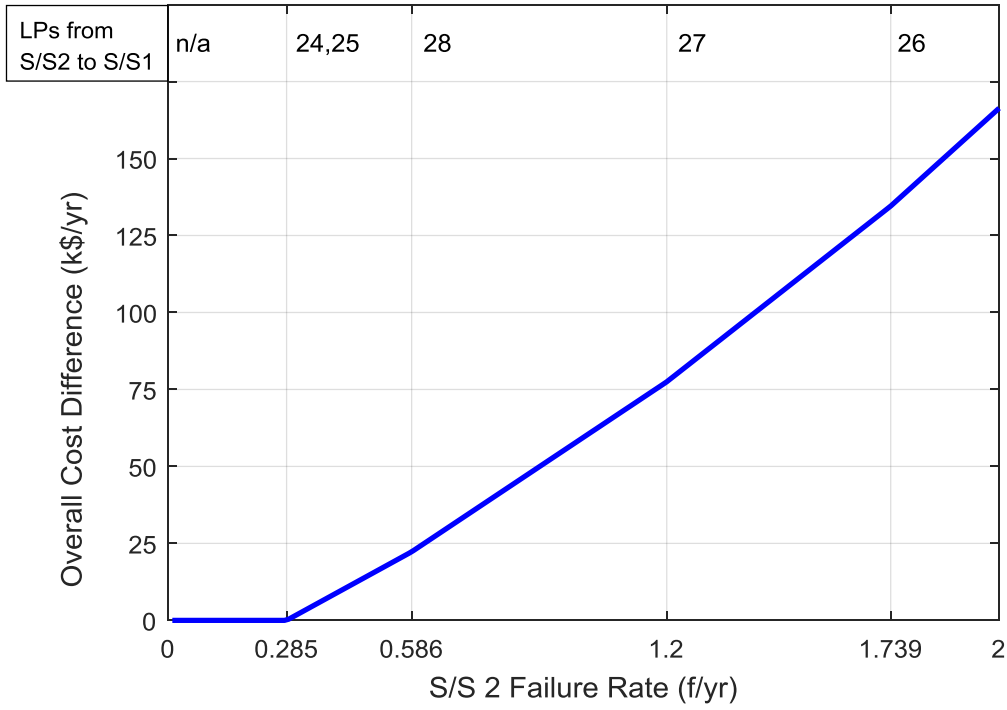

Figure 4.9: Sensitivity analysis of S/S 2 failure rate on the overall cost difference and thresholds at which LPs are transferred from S/S 2 to S/S 1.

As the demand of LPs 24 and 25 was increased up to 2 MW each, the overall cost difference became greater as well, as illustrated in Figure 4.10. This was due to the difference in the S/S failure rates; more load was transferred, leading to higher reduction in ECOST. However, for demands greater than 2 MW, the overall cost difference started to decline, because the increase in loss cost was greater than the corresponding decrease in ECOST. It should also be mentioned that the load transfer is no longer worthwhile for demands greater than 2.9 MW; in this case the optimal configuration is the original one.

The variation of S/S switching time did not lead to a change in the optimal configuration of the network. However, the greater the S/S switching time, the greater the overall cost difference, as can be seen in Figure 4.11. The change in the slope at 20 min occurs because the ECOST calculation is different for outage durations between 1-20 min and 20-60 min.

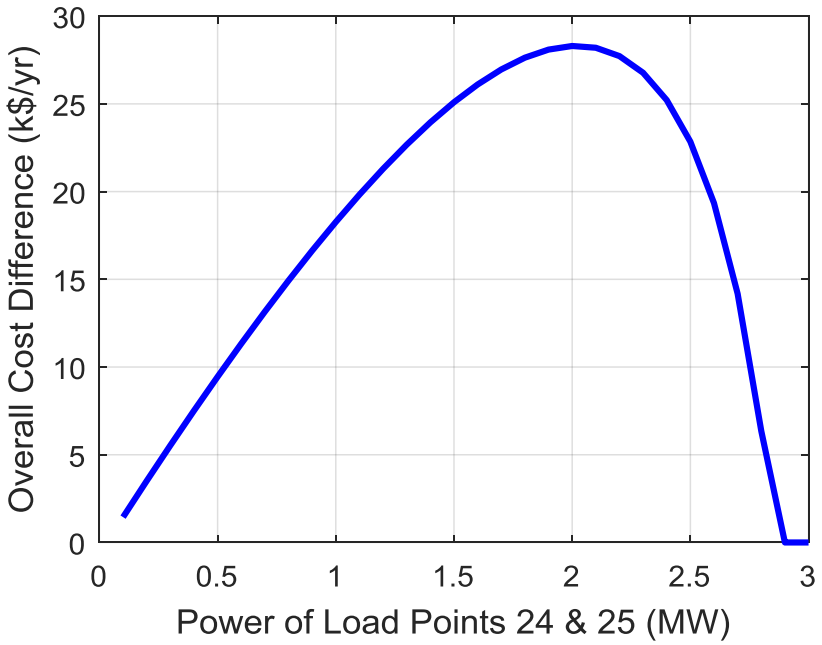

Figure 4.10: Sensitivity analysis of power of load points 24 and 25 on the overall cost difference.

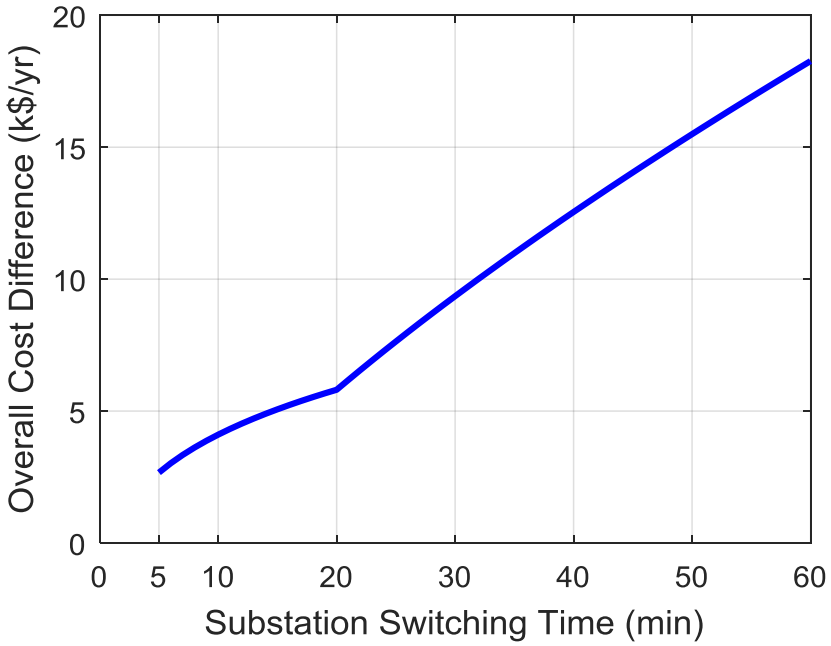

Figure 4.11: Sensitivity analysis of substation switching time on the overall cost difference.

4.4.4. Performance of Integer GA and Comparison with DPSO

This section describes the performance of the optimization algorithm used in this work; and also provides a comparison with a discrete PSO (DPSO) [64] using the same values for the population size (swarm size), maximum iterations, maximum stall iterations, and number of runs (see Table 4.6). The results are presented in Table 4.17 for Test Cases 2 and 3; the associated convergence graphs are illustrated in Figures 4.12 and 4.13. The simulations were performed using an Intel Core i5 quad-core processor at 3.2 GHz and 8 GB of RAM.

Table 4.17: Comparison of Integer GA and DPSO for Test Cases 2 and 3

Test Case Number	Optimization Method	Best Total Cost 2 (k$/yr)	Iteration (finding opt.)	Comp. Time (s)
2	Integer GA	300.48	6	64
	DPSO	300.48	13	76
3	Integer GA	232.09	42	166
	DPSO	232.95	34	152

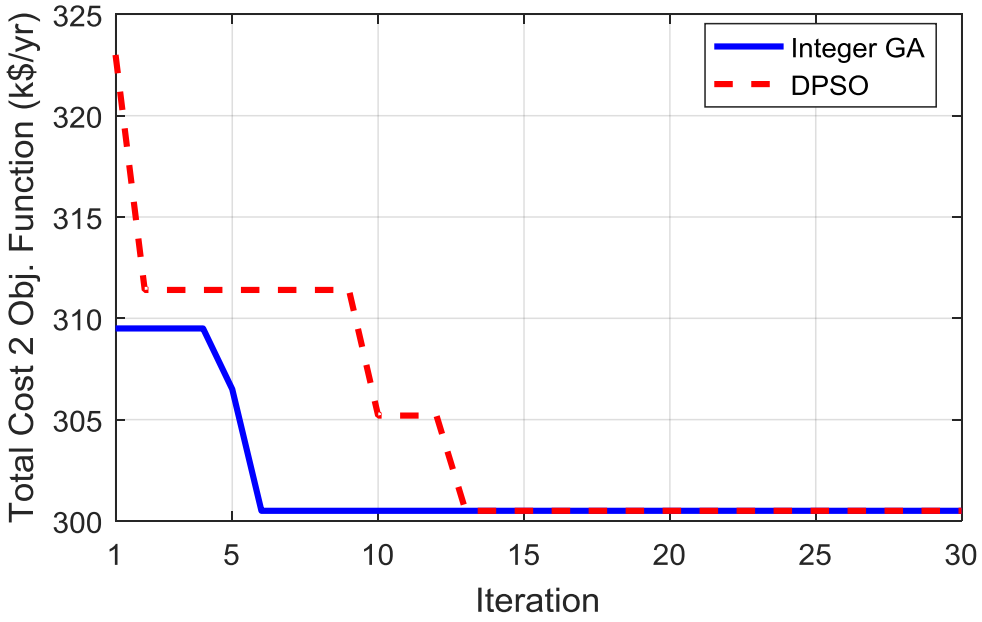

Figure 4.12: Convergence graph of Total Cost 2 objective function using Integer GA and DPSO (Test Case 2).

In Test Case 2, the same optimal solution was obtained, and Integer GA required less generations to find the optimal configuration. In Test Case 3 (which used a practical DN), DPSO was quicker; however, it produced a worse solution than Integer GA. This can be justified by the fact that an improved GA and modified for integer and mixed integer optimization has been used in this study (see section 4.3.2).

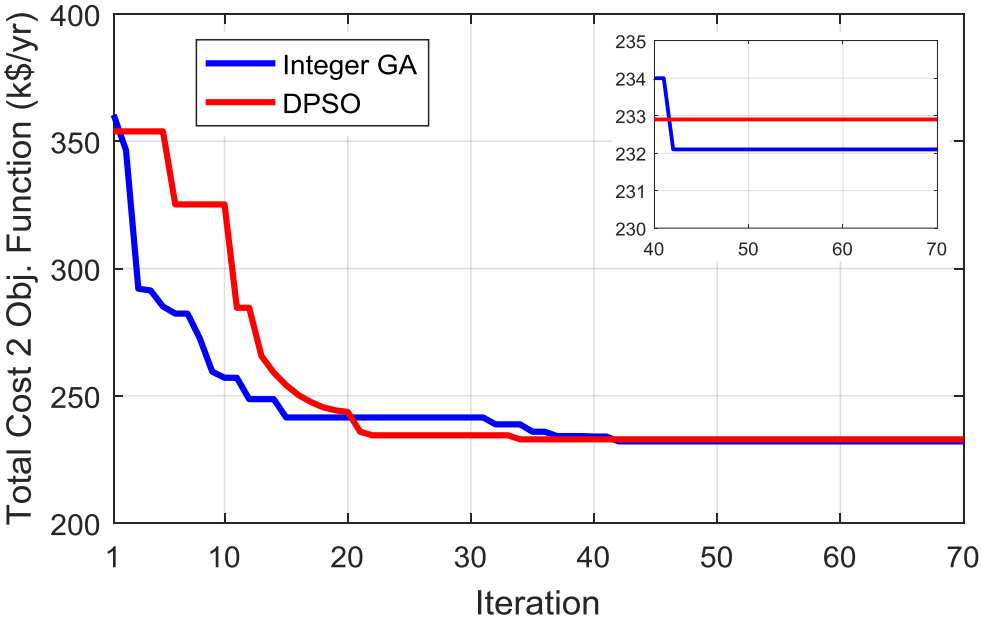

Figure 4.13: Convergence graph of Total Cost 2 objective function using Integer GA and DPSO (Test Case 3).

4.4.5. VOLTAGE PROFILES AND FEEDER LOADING

This section analyzes the impact of network reconfiguration on voltage and feeder loading with and without considering asset condition and S/S reliability; the analyses are carried out using Test Cases 2 and 3, and are presented in sections 4.4.5.1 and 4.4.5.2, respectively. It should be noted that min Total Cost 2 corresponds to DNR, which considers asset condition and S/S reliability, whereas the min Total Cost 1 objective function does not account for these factors.

4.4.5.1. TEST CASE 2 (RBTS BUS 4 DN)

The results for Test Case 2 are illustrated in Figures 4.14-4.15, and Table 4.18. In this test case, LPs 24 and 25 were transferred from feeder F4 (of S/S 2, which had a high failure rate) to feeder F3 (of S/S 1, which was more reliable). This load transfer reduced the loading on feeder F4, and improved its voltage profile; however, it increased the loading on feeder F3, as well as its voltage profile deteriorated. After the load transfer, feeder F3 became longer (six main feeder sections – 19, 21, 23, 26, 28, and 72) and supplied two more LPs; therefore, network losses increased and this is why minimum voltage was lower and network loading was (slightly) higher. This happened because the feeders of this network were connected to each other only at their endpoints; more normally open branches could provide better reconfiguration options (as in Test Case 3). Nevertheless, if the minimum voltage reached an unacceptable value after the load transfer, the transformer tap changer at the S/S would be able to resolve this issue. Note that as far as the network loading is concerned, only the first branch of each feeder has been considered, i.e. branches 1, 13, 19, 31, 44, 50, and 56. This is because the first branch of each feeder experiences the heaviest loading (between all feeder sections).

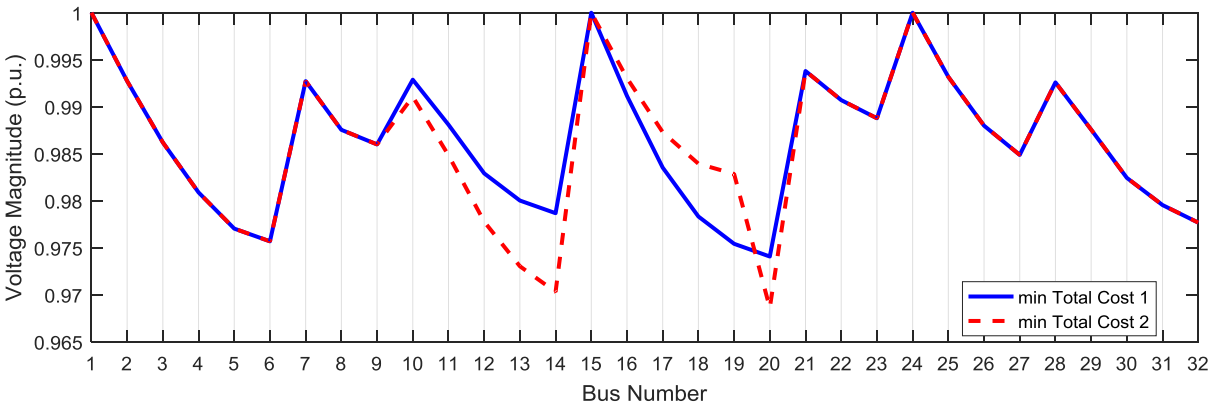

Figure 4.14: Voltage profiles for Test Case 2.

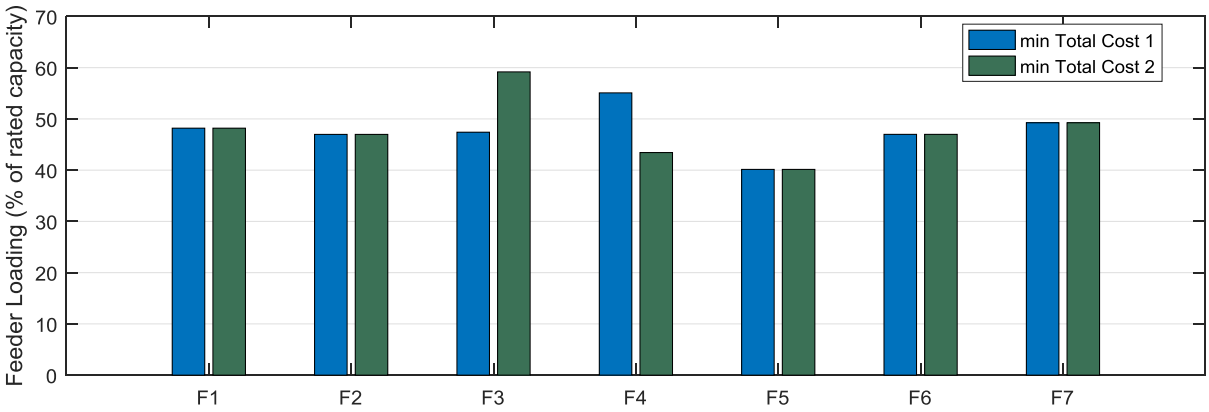

Figure 4.15: Feeder loading for Test Case 2.

Table 4.18: System indices for bus voltages and feeder loading (Test Case 2)

Objective Function	Min. Voltage Magnitude (p.u.)	Mean Voltage Magnitude (p.u.)	Mean Feeder Loading (% of rated capacity)	Load Balance Index [47]
Total Cost 1	0.9741	0.9863	47.72	1.6057
Total Cost 2	0.9686	0.9860	47.74	1.6164

4.4.5.2. TEST CASE 3 (TPC DN)

The network used in Test Case 3 offered many more reconfiguration options (compared to Test Case 2), as it had more normally open branches, which connected several points of a feeder to other feeders of both S/Ss. In this test case, LPs 55 and 72 were transferred from feeders G and I (of S/S 2a, which had a high failure rate) to feeders A and B (of S/S 1, which was more reliable), respectively. The results for this test case are illustrated in Figures 4.16-4.17, and Table 4.19. LPs 55 and 72 were connected at the ends of the (relatively) highly loaded feeders G and I; this also caused high

voltage drops along these feeders – bus 72 had the minimum voltage magnitude (0.942 p.u.) for min Total Cost 1 configuration. The transfer of these LPs substantially improved the voltage magnitude (0.97 p.u.) at bus 72, as well as balanced the loading between feeders G and A; network losses were also reduced.

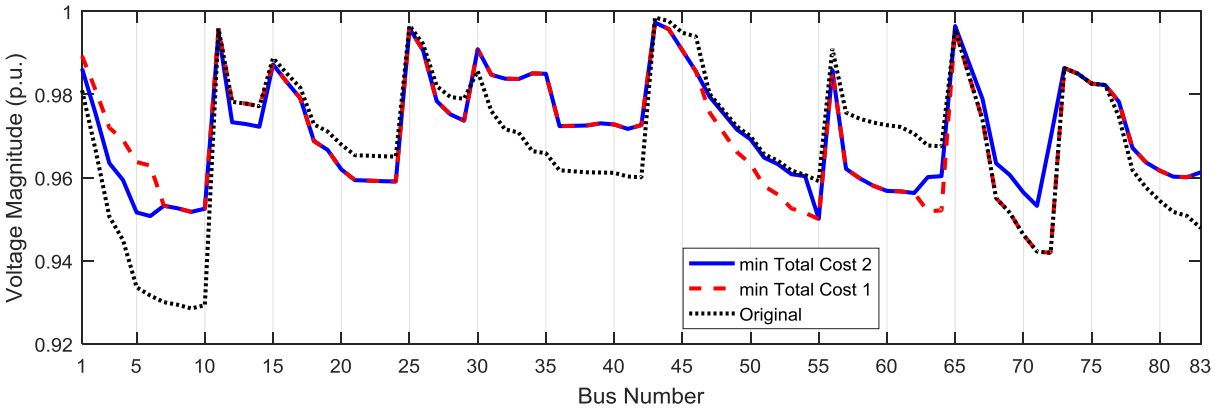

Figure 4.16: Voltage profiles for Test Case 3.

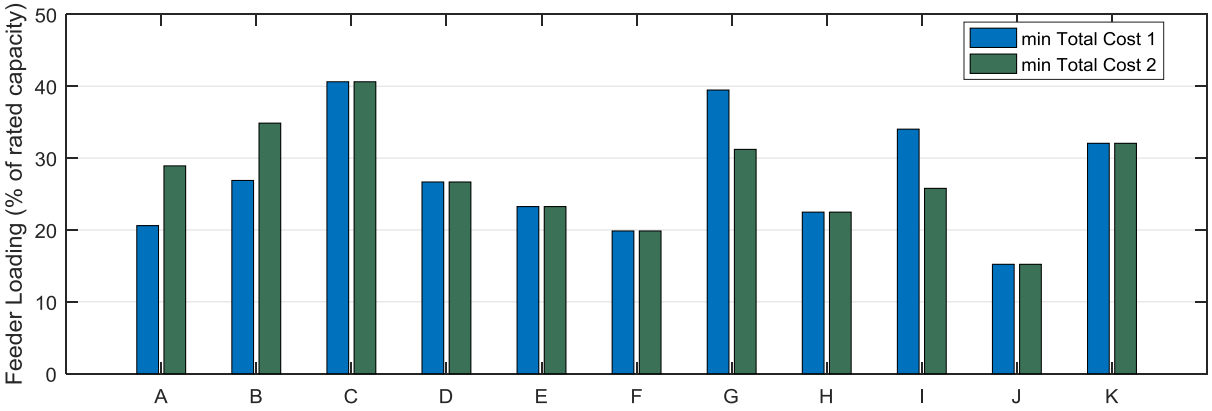

Figure 4.17: Feeder loading for Test Case 3.

Table 4.19: System indices for bus voltages and feeder loading (Test Case 3)

Network Configuration	Min. Voltage Magnitude (p.u.)	Mean Voltage Magnitude (p.u.)	Mean Feeder Loading (% of rated capacity)	Load Balance Index
Original	0.9285	0.9682	27.46	0.9295
min Tot. Cost 1	0.9419	0.9702	27.38	0.8926
min Tot. Cost 2	0.9501	0.9711	27.36	0.8754

Overall, the inclusion of asset condition and S/S reliability into DNR may lead to better or worse voltage profile and load balance of the network; however, a greater number of reconfiguration options – in terms of feeder

interconnections between each other – can help finding an optimal solution with improved bus voltages and feeder loadings.

4.5. CONCLUSION

This chapter proposes a new, better informed, methodology for DNR, which minimizes the total cost of active power losses and ECOST by making use of asset condition data and considering S/S reliability. Typically in network reconfiguration studies, average failure rates based on asset type are used and S/S reliability is ignored. In this study, condition-based failure rates are employed and the reliability of each S/S is taken into account. S/S reliability is determined by three factors: asset condition, S/S configuration, and the upstream network. Moreover, each LP of the DN is assumed to have its own CDF, which depends on its type. The major conclusion of this work is that there is significant value in incorporating asset condition and S/S reliability into the DNR problem. Particularly, the inclusion of these factors in the optimization process leads to a better informed optimal network configuration. This is shown by the successful application of the proposed methodology to the RBTS Bus 4 DN and on a practical DN of Taiwan Power Company. The annual savings, compared to the formulation that neglects asset condition and S/S reliability, can be in the order of tens of thousands of U.S. dollars for a single DN.

In general, the proposed methodologies in Chapters 3 and 4 can be used in order to examine if there is value in changing the configuration of a DN. This can be done, for example, if new condition data become available to the DNO, or in the case of an outage – planned or unplanned – of an S/S transformer. It is expected that it will be more beneficial if there is a difference in the reliability of the S/Ss. If all S/Ss are considered identical, then the inclusion of the aforementioned factors will not change the optimal network configuration. However, if there are differences because of asset condition, S/S configuration, and/or upstream network, then the optimal configuration of the network might be different, especially if there are LPs

with high interruption costs that can potentially be transferred to other S/Ss.

It is also not necessary to have information for all condition parameters; the ones, for which there is information can be evaluated and a default score can be assigned to the rest of the parameters. However, as has already been mentioned, Ofgem has recently approved a common methodology [11] across all UK DNOs for the assessment of asset HIs and risks. This will encourage DNOs to collect and utilize condition data in a more organized way; therefore they will obtain a better knowledge of the condition of their assets, which could clearly facilitate the application of the proposed methodologies to a DN.

Chapter 5. Distribution Switch Automation

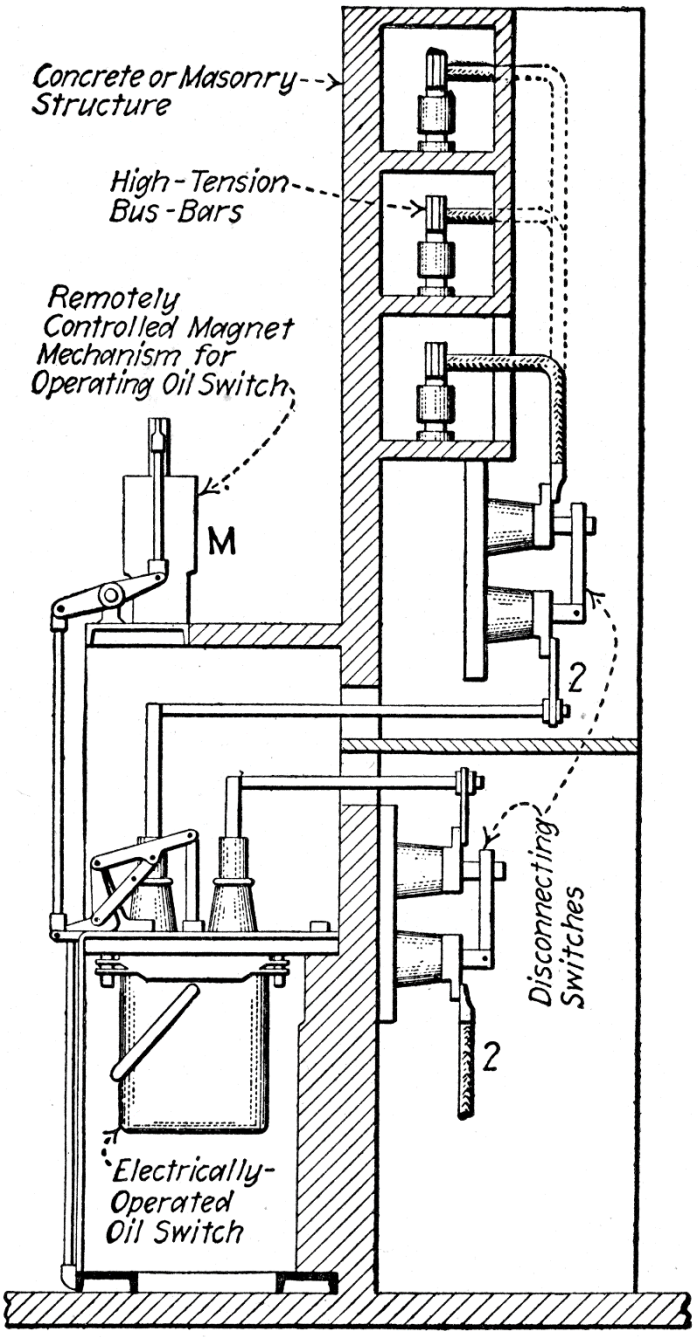

5.1. INTRODUCTION AND LITERATURE REVIEW

DNs are the highest contributors to customer service interruptions in power systems. Concurrently, DNOs are reducing – as a result of the deregulation of the electrical power industry – capital expenditure by deferring investments; in-house expertise; and maintenance frequency. Therefore, it is likely that DN reliability will start to deteriorate in the coming years [6, 7]. This justifies that a significant amount of research has been undertaken to minimize the effects of failures in DNs by making use of automation. In particular, remote controlled switches (RCSs) mitigate the impact of a fault in the following way: 1) if the RCS is installed in a normally closed branch, it drastically reduces the isolation time; and 2) if the RCS is placed in a normally open branch, it allows a much quicker (post-fault) reconfiguration of the network [18].

However, the installation of RCSs comes at a considerable cost and given the size of DNs, the determination of the number and location of these switches becomes critical. This decision is a combinatorial nonlinear optimization problem with a non-differentiable objective function [96]. This has often led to the use of heuristic optimization algorithms, such as GA [97-99]; PSO [100]; simulated annealing [96]; ant colony optimization [101-103]; the immune algorithm [104]; and the alliance algorithm [105].

DNOs have traditionally made decisions about this problem based on their past experience and specific rules [106]. *Luth* [107] provides four rules to specify the location of protective devices to enhance the reliability of the network; system average interruption duration index (SAIDI) is used as the reliability metric. In [108] a direct search technique and a bisection approach is proposed in order to optimally select the switching devices. *Celli et al.* [109] propose a method based on Bellman's optimality principle, along with specific logic rules. A paper by *Carvalho et al.* [18] present a two-stage decomposition approach to optimize the investment in RCS devices, where: 1) the solution space is partitioned into independent subsets; and 2) each optimization problem is solved separately. In [57] the switch upgrade is

decided not only for reliability improvement, but also for loss reduction of the network; this is based on the results of optimal reconfiguration. *Heidari et al.* [110] formulate the problem in an MINLP framework in presence of DG units, considering RCSs and other protective devices.

The majority of the aforementioned papers consider ECOST as the reliability metric in their objective functions, while also taking into account the RCS investment and maintenance cost; this is the case in the problem formulated in this chapter as well.

The existing literature does not address asset condition and ageing, and therefore constant (average) failure rates are assumed for all network components over the study period. Ageing also depends on the type of the asset as indicated by Figure 2.5. Consequently, this chapter investigates the impact of asset condition and ageing (which depends on the type) on the optimal selection of number and location of RCSs.

5.2. METHODOLOGY

This section describes: 1) the impact of automated feeder switches in DNs; 2) the modelling assumptions; 3) the problem formulation; and 4) the solution algorithm. Asset condition assessment and ageing have been analyzed in section 2.3.1 and network reliability evaluation has been presented in section 4.2.

5.2.1. AUTOMATED FEEDER SWITCHES IN DNS

The main benefit of automated switches (or RCSs) is that they can operate (open/close) much more quickly than manual switches; this impact can be incorporated in the model by modifying the switching time of the RCSs [7]. The steps followed after a failure on a main feeder section are shown in Figure 1.6, considering a feeder without automation. This subsection explains the same process, but assuming a number of RCSs have been installed along the feeder; this is illustrated in Figure 5.1. It is considered that there are (manual) disconnect switches at both ends of the main feeder sections.

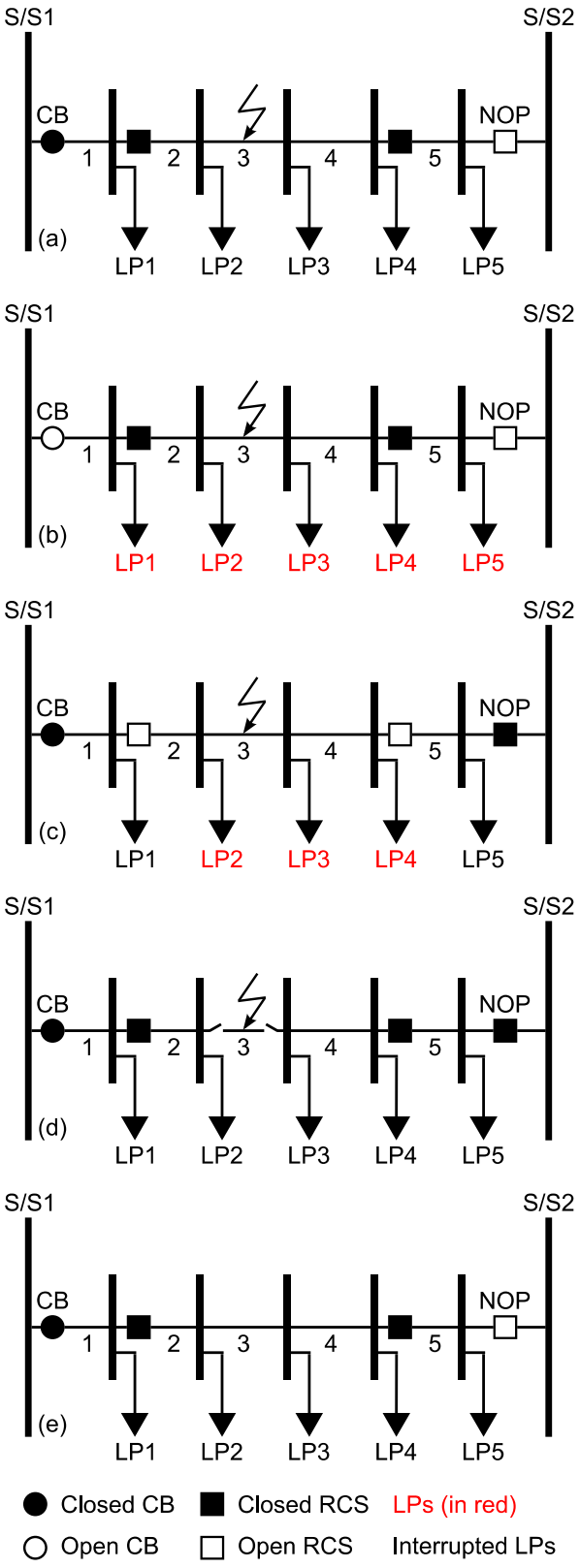

Figure 5.1: Radial distribution feeder with three RCSs and restoration steps followed after a failure on a main feeder section. (a) Fault occurred in branch 3 (t=0); (b) CB was activated to clear the fault (immediately), all LPs are interrupted; (c) the nearest RCSs open to isolate the fault (RCS switching time), CB and automated NOP close to restore supply to LPs 1 and 5; (d) the nearest manual switches open to further isolate the fault (manual switching time) in order to minimize the number of LPs that are out of service; and (e) the failed section has been repaired (repair time) and the feeder operates in its initial state.

After a fault has occurred in branch 3 (t = 0), the following restoration steps should be implemented:

1) Fault clearance (immediately after the fault): The short-circuit current trips the CB and as a result, all LPs are disconnected.
2) Fault isolation by RCSs (RCS switching time): The nearest RCSs open to isolate the fault quickly in order to minimize the outage duration for the LPs than can be restored via closing the CB and the automated NOP at the end of the feeder. After these actions have been performed, LP1 is supplied from S/S1 and LP5 through S/S2. This means that the interruption duration of LPs 1 and 5 is equal to the RCS switching time.
3) Fault isolation by manual disconnect switches (manual switching time): The nearest manual switches open in order to further isolate the fault and, in turn, reduce the number of interrupted LPs. When manual switching has been completed, LP 2 is restored via S/S1 and LPs 3 and 4 are restored through the alternative supply of S/S2. The outage duration of LPs 2-4 is equal to the manual switching time.
4) Repair of the faulted section (repair time): In this case, because of the availability of alternative supply, the LPs located downstream of the fault can be restored after manual switching has been performed. After the repair has been completed, the feeder is set back to its initial state.

If it is considered that each LP of Figure 5.1 corresponds to 200 customers and the RCS switching time is 1 minute, then the customer minutes lost is equal to 1,000×1 + 600×59 = 36,400. In the case of no automation, there would only be fault isolation by the manual switches around the failed branch, and the customer minutes lost would be 1,000×60 = 60,000.

5.2.2. MODELLING ASSUMPTIONS

Before the problem can be described, a number of modifications and assumptions should be made:

1) The network used in this chapter (see Figure 5.2) is the RBTS Bus 4 DN, which has been modified as follows: a) only main feeder sections are considered; and b) feeders F2, F5, and F6 are connected via single branches, as in Figure 4.5.
2) There are manual disconnect switches at both ends of the main feeder sections and fuses in each lateral distributor. These components are not shown in Figure 5.2 and are considered perfectly reliable.
3) There are CBs at the sending end of each feeder, as shown in Figure 5.2 (branches 1, 6, 9, 14, 19, 22, and 25), which are also considered fully reliable.
4) Possible locations for a switch upgrade (manual to RCS) are assumed to be only the sending ends of each branch.

5.2.3. PROBLEM FORMULATION

The state vector (x) in this problem represents the set of switches to be automated (replaced by RCSs). Each decision variable corresponds to a specific location and can be equal to one or zero, if the switch is to be automated or not, respectively. This is illustrated in Table 5.1; if a network has 10 branches, then this specific solution indicates that RCSs should be placed in branches 2, 5, 7, and 8. The sum of x expresses the number of RCSs to be installed (N_S). The case study network has 34 main feeder sections (including the NOPs); however, there are seven CBs installed (sending end of each feeder). Thus, there are 27 possible RCS locations.

Table 5.1: Illustration of the decision variable representation

Branches	1	2	3	4	5	6	7	8	9	10
x	0	1	0	0	1	0	1	1	0	0

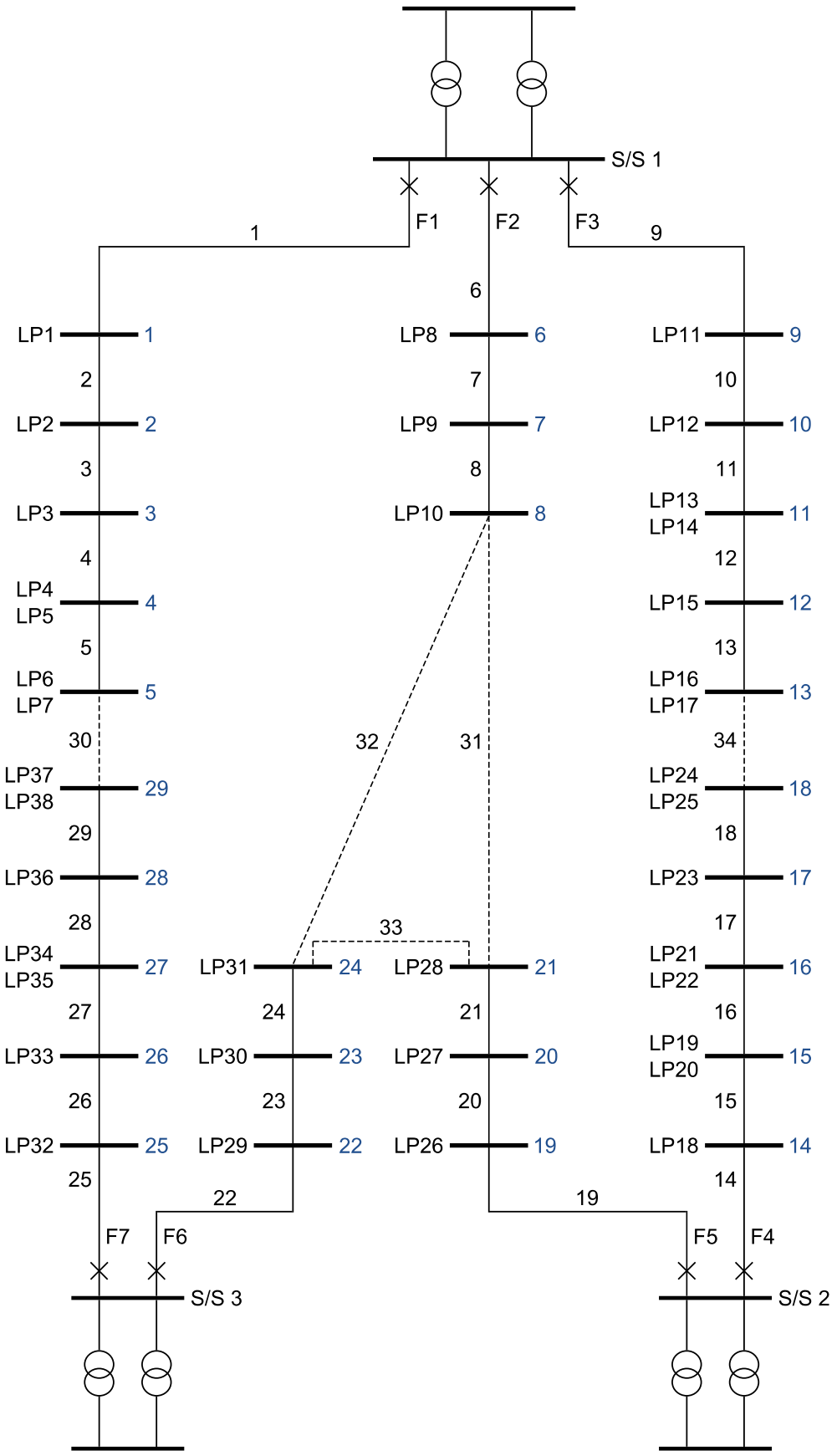

Figure 5.2: The RBTS Bus 4 DN, which has been modified for this chapter: 1) only main feeder sections are considered; and 2) feeders F2, F5, and F6 are connected through single branches. Branch numbers are shown in black; bus numbers are shown in blue.

The objective function consists of three terms: 1) the ECOST; 2) the installation cost (IC); and 3) the maintenance cost (MC). The first term has been thoroughly explained in section 4.2; it is slightly modified here in order to account for the load growth and asset ageing.

$$ECOST = \sum_{year=1}^{N_{\text{years}}} \sum_{p=1}^{N_{\text{LP}}} \sum_{j=1}^{N_{\text{ev},p}} C_{jp}(r_{jp}) \cdot [(1+(year-1)LG)L_p] \cdot \lambda_j(year) \cdot (1+IR)^{-year} \quad (5.1)$$

The average load of each LP is multiplied by $(1+(year-1)LG)$ to incorporate the effect of load growth. Also, the branch failure rates are updated each year – according to the methodology presented in section 2.3.1 – in order to take asset ageing into account; this will be further described in section 5.3.

The second term represents the total capital investment and installation cost; this given by (5.2).

$$IC = N_S \cdot SC. \quad (5.2)$$

The third term expresses the operation and maintenance cost and is derived using (5.3).

$$MC = N_{\text{S}} \cdot \sum_{year=1}^{N_{\text{years}}} MC_{\text{unit}} \cdot (1+IR)^{-year}. \quad (5.3)$$

The factor $(1+IR)^{-year}$ is used in (5.1) and (5.3) in order to discount annual costs to the present value.

The objective function is given by (5.4).

$$\min f = ECOST + IC + MC. \quad (5.4)$$

5.2.4. SOLUTION METHOD

The optimal decision for the number and location of RCSs in a DN is a combinatorial nonlinear optimization problem with a non-differentiable objective function [96]; this has often resulted in the use of heuristic optimization algorithms. It should be mentioned that this study does not focus on the optimization method; instead, it concentrates on demonstrating the value of considering asset condition and ageing into the optimal RCS placement problem. Therefore, the GA is used to determine the optimal RCS locations, which has been widely applied in the relevant literature [97-99].

The problem has been formulated in MATLAB and is solved using the *Integer ga* solver [94]. The selected parameters for the GA are shown in Table 5.2. The stopping criterion for the algorithm is when the number of generations reaches *maximum generations*; however the GA will also stop if there is no change in the best objective function value in a sequence of generations equal to *maximum stall generations*. The flowchart of the overall procedure is presented in Figure 5.3.

Table 5.2: GA Parameters

Parameter	Value
Number of Variables	27
Population Size	100
Maximum Generations	50
Maximum Stall Generations	10
Number of Runs	5

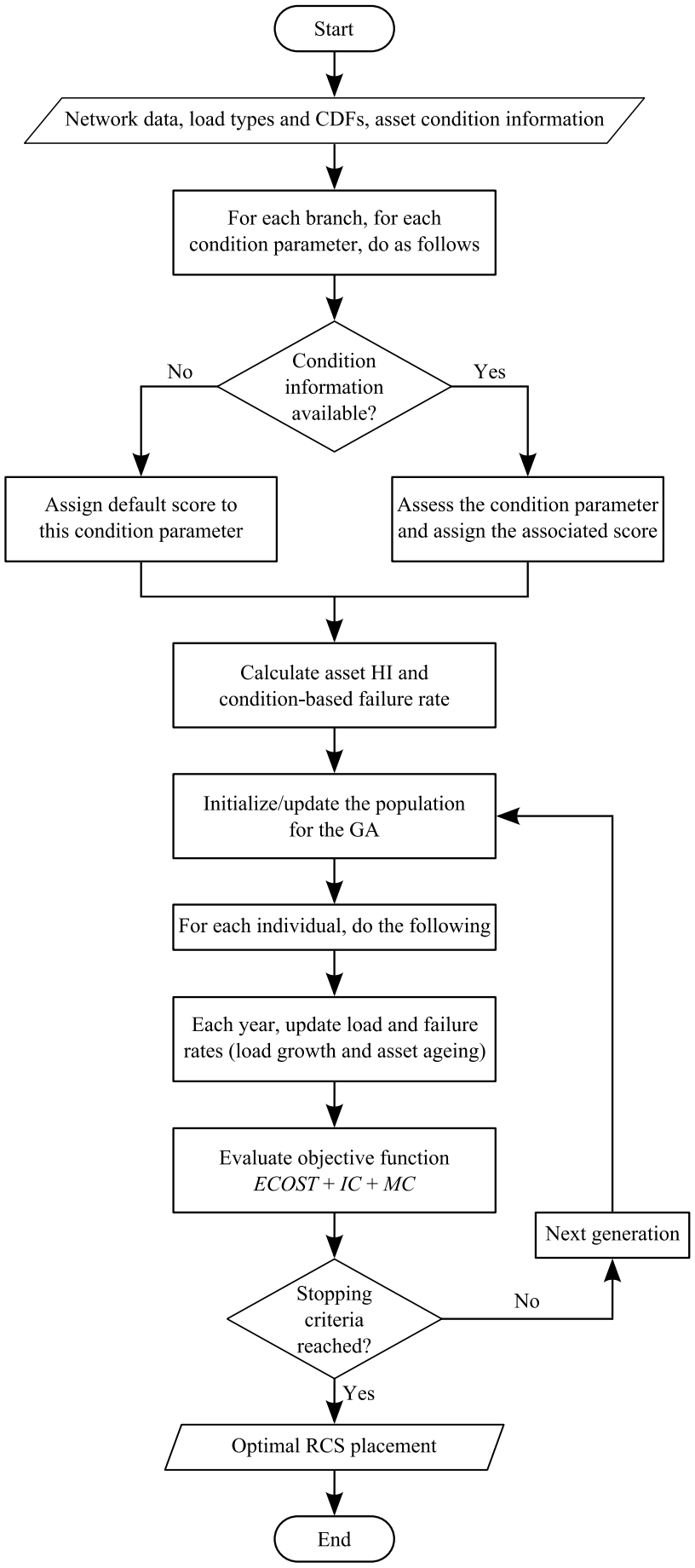

Figure 5.3: Flowchart of the proposed method.

5.3. CASE STUDY

The proposed methodology is applied to the case study network (see Figure 5.2), considering the branches (main feeder sections) as OHLs in Test Case 1, and as UGCs in Test Case 2. Asset condition data and other parameter values required for the simulations are given in sections 5.3.1 and 5.3.2, respectively.

5.3.1. ASSET CONDITION

The condition data for the OHLs and the UGCs are presented in Tables 5.3 and 5.4, respectively. The future HIs and the corresponding overall failure rates (according to section 2.3.1) for the next 20 years are illustrated in Figure 5.4. The future HI of the OHLs can be calculated as follows:

$$HI_{\mathrm{f}} = 3.14 \cdot e^{0.045144 \cdot year}, \tag{5.5}$$

and for the UCGs as:

$$HI_{\mathrm{f}} = 5.5 \cdot e^{0.032 \cdot year}. \tag{5.6}$$

As can be seen in Figure 5.4, the UGC failure rate increases much more rapidly compared to the OHL failure rate; this fact can have an impact on the optimal RCS placement, which is shown in section 5.4.

Table 5.3: Condition assessment for the OHLs

Parameter	Value	Comments
Asset HI	**3.14**	Initial HI × HI Factor
Condition-Based Failure Rate	**0.0023**	Equation (2.1)
Overall Failure Rate	**0.0565**	Equation (2.8)
Age	35	
Initial HI	2.3	Related to Age
HI Factor	1.37	Related to Condition
Expected Life	55	
Observed Condition Factor	**1.3**	
Visual Condition	1.3	Some Deterioration
Midspan Joints	1.05	1 joint in the span
Measured Condition Factor	**1.1**	
Conductor Sampling	1.1	Medium/Normal
Corrosion Monitoring Survey	1.1	Medium/Normal

Table 5.4 Condition assessment for the UGCs

Parameter	Value	Comments
Asset HI	**5.50**	(min HI limit applied)
Condition-Based Failure Rate	**0.0398**	Equation (2.1)
Overall Failure Rate	**0.0582**	Equation (2.8)
Age	40	
Initial HI	1.3	Related to Age
HI Factor	1.7	Related to Condition
Expected Life	100	
Observed Condition Factor	**1.0**	
None		
Measured Condition Factor	**1.7**	
Sheath Test Result	1.0	Pass
Partial Discharge Test Result	1.15	Medium
Fault Rate (faults per annum)*	1.6	(> 0.01/km) and (< 0.1/km)

* The score of this condition parameter introduces a minimum HI limit of 5.5.

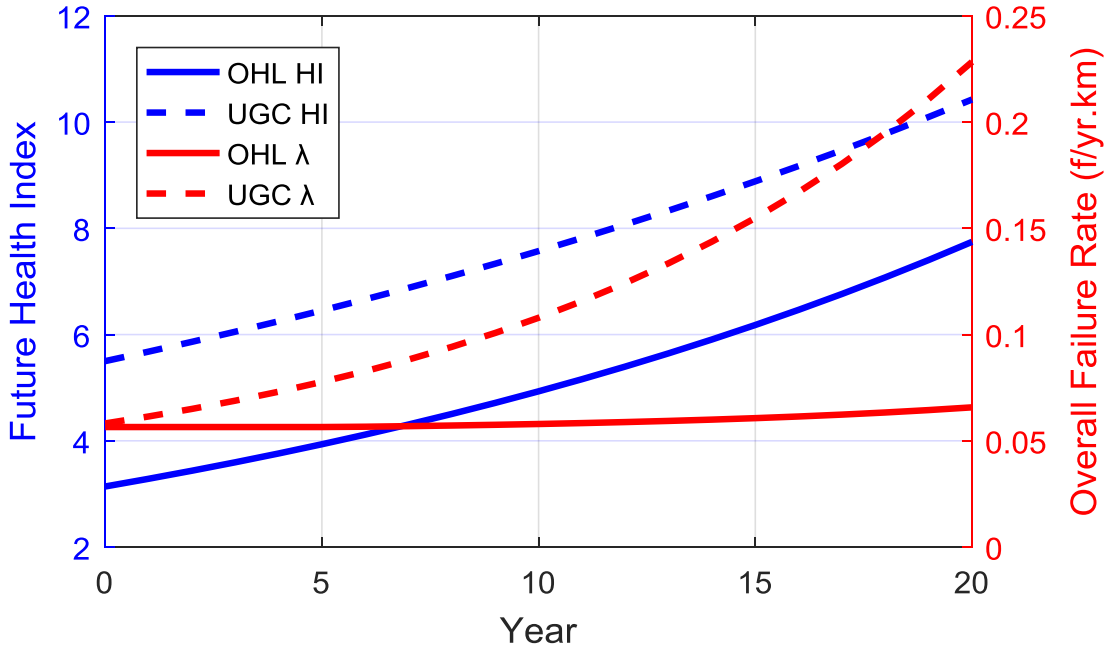

Figure 5.4: Future HIs and overall failure rates for OHLs and UGCs for the next 20 years.

5.3.2. Parameter Values

The capital investment cost of an RCS (SC) has been considered as the average value of the corresponding costs in [57, 64, 111], i.e. $16,000. The annual maintenance cost (MC_{unit}) is 2% of the capital investment cost. The RCS life period, which is also the simulation period (N_{years}) is assumed to be

20 years and the interest rate (*IR*) is equal to 8%. The RCS switching time is 1 minute and the load growth rate (*LG*) is 1% per year without compounding.

5.4. RESULTS

5.4.1. TEST CASE 1

This test case considered the branches of the case study network as OHLs. Table 5.5 shows the optimal number of RCSs and their locations with and without having considered ageing in the optimization problem. The case without ageing assumed a constant OHL failure rate of 0.0565 f/yr throughout the whole simulation period. In the case that ageing was taken into account, the OHL failure rate presented only a slight increase over a period of 20 years (0.0565 f/yr → 0.0657 f/yr), as can be seen in Figure 5.4. Therefore, asset ageing did not have a material impact on the optimal RCS placement; the number of RCSs and their locations was the same for both cases. However, there was a small difference in the ECOST with and without considering ageing (because of the different failure rate model). It should be noted that the values of the ECOST (for a period of 20 years) were relatively low due to: 1) the interest rate; and 2) the availability of alternative supply.

Table 5.5: Optimization results for Test Case 1 (OHLs) with and without considering asset ageing

Parameter	Opt. without ageing	Opt. with ageing
RCS Locations	7, 24, 32	7, 24, 32
ECOST (without ageing) ($)	309,689	–
ECOST (with ageing) ($)	317,230	317,230
IC ($)	48,000	48,000
MC ($)	10,179	10,179
Obj. Function Value ($)	367,868	375,409
Total Cost (with ageing) ($)	375,409	375,409

5.4.2. TEST CASE 2

Test case 2 assumed the main feeder sections of the network to be UGCs; Table 5.6 presents the optimal RCS placement for this case. Without accounting for ageing, the UGC failure rate remained constant at a value of 0.0582 f/yr over the 20-year simulation period. When ageing was considered, the UGC failure rate rose from 0.0582 f/yr to 0.2283 f/yr; this was a significant increase, which had a substantial effect on the optimal solution. This can be seen in Table 5.6, where the number of RCSs increased from 3 to 14, when ageing was considered; the associated reliability benefit was \$70,000. In this case also, the inclusion or not of ageing leads to a major difference in the ECOST, namely \$223,000, which manifests the importance of incorporating ageing in the given problem. This is illustrated in Figure 5.5(a); this figure compares the objective function value and the total cost (with ageing) in the case of optimization without considering ageing. Figure 5.5(b) compares the total cost (with ageing) for optimization with and without ageing; these differences express the reliability benefit for each case.

Table 5.6: Optimization results for Test Case 2 (UGCs) with and without considering asset ageing

Parameter	Opt. without ageing	Opt. with ageing
RCS Locations	7, 24, 32	5, 7, 8, 13, 18, 20, 21, 23, 24, 29, 30, 32-34
ECOST (without ageing) (\$)	319,007	–
ECOST (with ageing) (\$)	542,156	258,750
IC (\$)	48,000	224,000
MC (\$)	10,179	47,504
Obj. Function Value (\$)	**377,186**	**530,254**
Total Cost (with ageing) (\$)	**600,335**	530,254

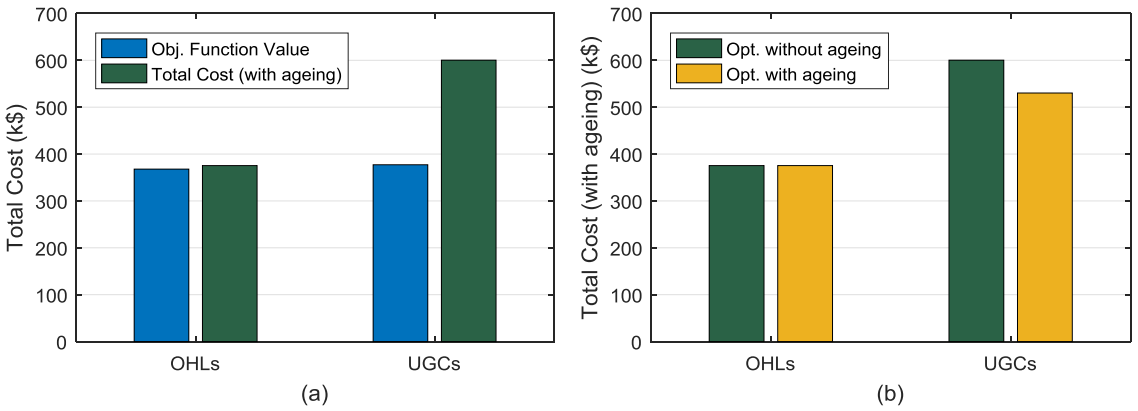

Figure 5.5: (a) shows the comparison between the objective function value and the total cost (with ageing) in the case of optimization without considering ageing; (b) compares the total cost (with ageing) for optimization with and without ageing.

5.4.3. Sensitivity Analysis

A sensitivity analysis was performed to investigate the impact of RCS capital investment cost on the optimal RCS placement. The base case was assumed to be Test Case 1 (OHLs), considering optimization with ageing. The sensitivity analysis was carried out by reducing the RCS capital cost, starting from \$18,000 down to \$1,000; the corresponding results are presented in Table 5.7. Figure 5.6 illustrates these results on the case study network, considering that the order of the additional RCSs – as the investment cost was reduced – expresses a priority (or significance) of each RCS group placement; this is explained below.

Table 5.7: Sensitivity analysis of RCS capital investment cost on the optimal RCS placement

RCS Capital Cost	RCS Locations
\$18,000	None
\$16,000	7, 24, 32
\$14,000	7, 13, 18, 24, 32, 34
\$12,000	5, 7, 8, 13, 18, 24, 29, 30, 32, 34
\$8,000	5, 7, 8, 13, 18, 20, 21, 23, 24, 29, 30, 32-34
\$1,000	3, 5, 7, 8, 11, 13, 16, 18, 20, 21, 23, 24, 27, 29, 30, 32-34

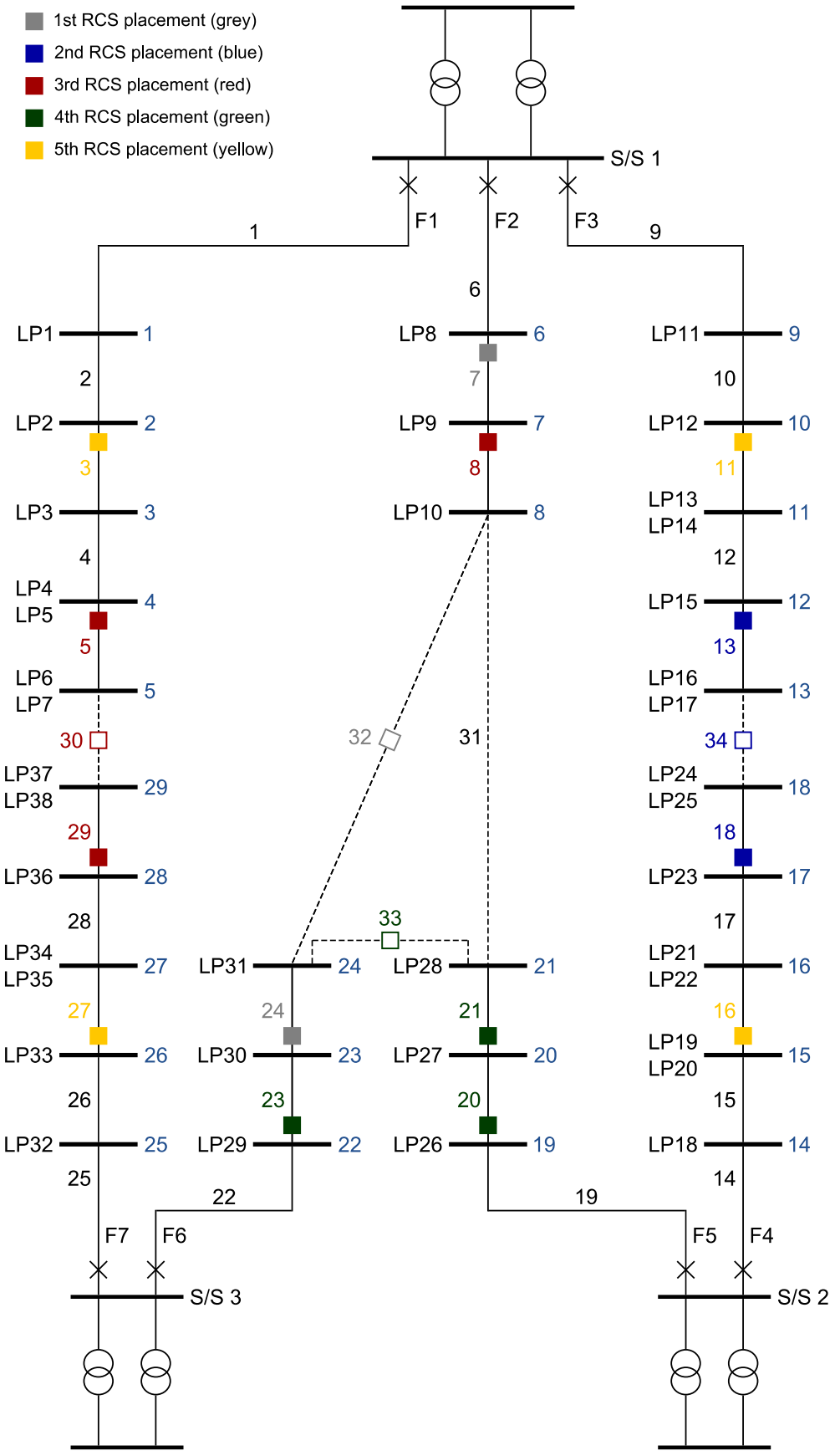

Figure 5.6: Placement of RCSs as the investment cost was reduced in the sensitivity analysis; different colours represent a priority in the RCS placement.

An RCS capital cost higher than \$18,000 led to no automation of the network. A cost of \$16,000 had as a result the placement of RCSs in branches 7, 24, and 32; these RCSs protect the most expensive LPs (LPs 9 and 31 are the ones with the highest interruption cost – 1.5 MW, industrial). The additional RCSs that would be installed – if the RCS cost was \$14,000 – are 13, 18, and 32; these switches automate the second NOP (branch 34) in the network and protect the commercial LPs 16, 17, 24, and 25 (0.415 MW each) which also have a high outage cost. A further reduction of the RCS investment cost (\$12,000) would automate the third NOP (branch 30) and would protect the commercial LPs 6, 7, 37, and 38. At a price of \$8,000, RCSs were placed in all remaining feeder sections supplying industrial loads, i.e. branches 20, 21, 23, and 33. The last addition was the installation of RCS in all (remaining) middle feeder sections, i.e. branches 3, 11, 16, and 27. From the above analysis, it is obvious that the prioritization of RCS placement is heavily influenced by customer interruption cost, which in turn is determined by the load type and power of each LP.

5.5. CONCLUSIONS

This chapter presents a new methodology for optimal RCS placement, which incorporates asset condition assessment and ageing; normally these factors are not considered within problem formulations in the relevant literature. Moreover, the feeder type (OHLs/UGCs) plays an important role in the reliability evaluation of the network, when ageing is considered; the UGC failure rate rises much more rapidly than the failure rate of OHLs, as HI increases. The inclusion of these factors in the problem formulation results in a more accurate reliability assessment of the network, as well as cost reduction. Test Case 2 showed an underestimation of the ECOST as high as \$223,000, and a saving of \$70,000, for the cases with and without considering ageing in the optimization process. Finally, the sensitivity analysis indicated the significance of specific RCS locations, which depend on the customer type and demand of the LPs protected by these RCSs.

Chapter 6. Capacity Value of DNR

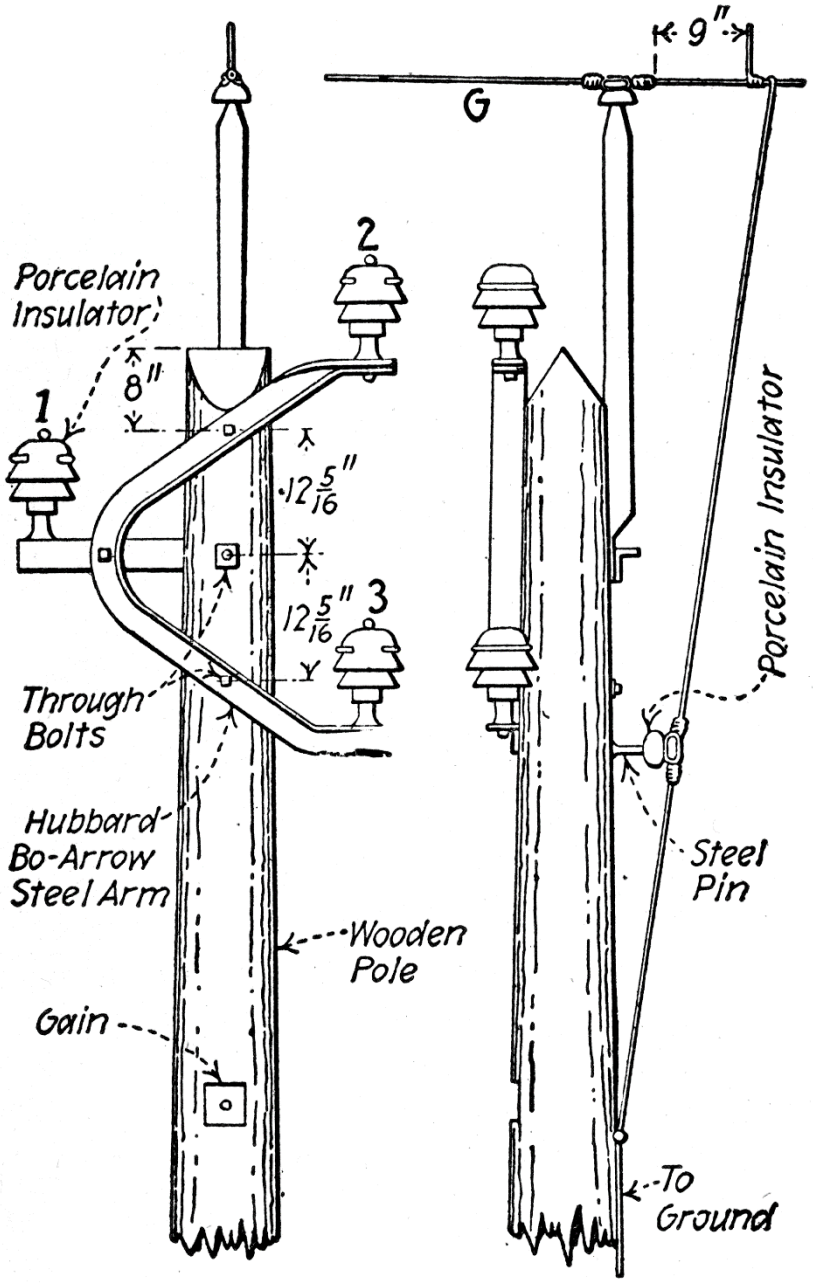

6.1. INTRODUCTION AND LITERATURE REVIEW

The privatization of the electricity sector has put great pressure on power utilities to reduce costs. This means that DNOs should allocate their financial resources in the best possible way, in order to improve the reliability of their networks [7]. This becomes more difficult when the aged asset base of most distribution networks (DNs) is taken into account [3]. At the same time, demand is expected to both increase and significantly change shape due to the upcoming electrification of transport and heat. In the past, utilities had a tendency to handle capacity and reliability problems with capital intensive projects, since there was little pressure to reduce expenditure [7]. Today, the picture is quite different; making better use of the existing network in order to defer network reinforcement seems to be now much more important.

Network reinforcement is required when constraint violations exist in a DN, such as voltage and thermal limits, either during normal or N-1 operation. A number of means can be used to defer network investment such as DG, ESSs, DSR, RTTRs, and DNR. Each of these has a specific contribution to the security of supply of a DN. There are a number of papers that evaluate this contribution to network security and based on that, decisions regarding reinforcement can be made.

One of the main benefits offered by DNR is that it can contribute to network security at low (or even zero) capital expenditure levels [7]. Therefore, it is of great importance to assess this contribution to the security of supply of a DN. The present security of supply standard in the UK (P2/6) [19] states that this contribution should be considered when examining the need for reinforcement. However, this standard does not provide a methodology to quantify this value. Hence, investment decisions might be made much earlier than they are actually needed.

References [21, 29, 112, 113] assess the capacity value of DG and its impact on investment deferral. *Pudaruth et al.* [113] provide a probabilistic approach to determine the capacity credit of DG, using Monte Carlo

simulation in order to take account of the uncertainty. Loss of load probability (LOLP) is used as the reliability index. *Dent et al.* [29] evaluate the capacity value of DG, using the effective load carrying capability (ELCC) capacity credit methodology. ELCC is defined as the additional load that can be accommodated by the DG (or any other solution in general), while maintaining the original risk level. In this paper [29], the employed risk index is the expected power not supplied.

A review of DN security standards in the UK [114] and a paper by *Konstantelos et al.* [23] assess the contribution of ESSs and DSR to network security using ELCC, within a sequential Monte Carlo framework. Chronological simulation is necessary to capture the effect of time-dependent variables, such as energy constraints, temporal demand characteristics, and state of charge. *Greenwood et al.* [22] present a probabilistic method for ESS sizing for a demand peak shaving application and also consider the combination with RTTR in order to defer conventional reinforcement. References [22, 23, 114] consider expected energy not supplied (EENS), as the reliability metric.

Xiao et al. [30] define total supply capability (TSC) as the maximum load that a DN can supply under the N-1 guideline, while satisfying other operational constraints. An optimization-based algorithm is proposed in order to calculate TSC. Based on this approach, [31] and [32] incorporate DNR in the formulation of their optimization problems. In [31], simplified daily load curves are also taken into account and [32] considers N-k transformer contingencies.

However, these papers [30-32] disregard load variation (only [31] considers simplified load profiles) and its associated uncertainty. They also neglect the reliability of the DN (both S/Ss and feeders), which has a direct impact on the availability of the calculated TSC. In addition to that, asset age and condition play an important role in the evaluation of network reliability [11, 12]. In order to be able to quantify the contribution of DNR to the security of

supply of a DN and make decisions about network reinforcement, these factors should be taken into account. Therefore:

1) The first contribution of this chapter is providing a method to quantify the contribution of DNR to security of supply, using a probabilistic and reliability-based analysis; this quantification is implemented using ELCC, within a sequential Monte Carlo framework. This is necessary in order to consider the impact of time-dependent variables, such as switching time and time-varying load as well as their inherent uncertainty. The reliability index used in this work is expected energy not supplied.
2) The second contribution is the condition-based reliability evaluation of the DN (incoming circuits and primary feeder sections), which is based on section 2.3.1; this methodology not only considers current asset health indices, but also their forecast values over the period of interest.

Finally, taking all of the above factors into account, the contribution of DNR to network security can be assessed, which can support decision-making regarding network reinforcement (driven by demand growth and asset condition).

6.2. METHODOLOGY

6.2.1. MODELLING ASSUMPTIONS

It is considered that reconfiguration is performed if there is at least one outage in the incoming circuits such that demand cannot be met by the remaining available capacity. It is clearly stated that the optimization of the load transfer from the failed S/S to its neighbouring ones can be calculated and incorporated in this work by solving the corresponding optimization problem, which is formulated in [115] (for maximum load transfer). However, in order to reduce the computational burden, this chapter focuses on DNR, considering that feeders are interconnected at their endpoints. This means that a high-quality solution can be easily found, as there are

relatively few options. Consequently, load transfer optimization is beyond the scope of this study, as the method is concerned with finding a viable solution, rather than an optimal solution. Optimization depends on the values of demand at time of outage (and on the short-term forecast of demand, as shown later in this chapter). A fast DNR decision is more important than an optimal one.

6.2.2. SECURITY OF SUPPLY AND ELCC

Figure 6.1 shows a conventional reinforcement at a primary S/S, which is typically the addition of a new circuit. This is required when the demand becomes greater than the limit dictated by P2/6; however, this limit neglects the capacity contribution of DNR. Consequently, the capacity credit of this solution should be quantified, which can be achieved by employing the ELCC methodology.

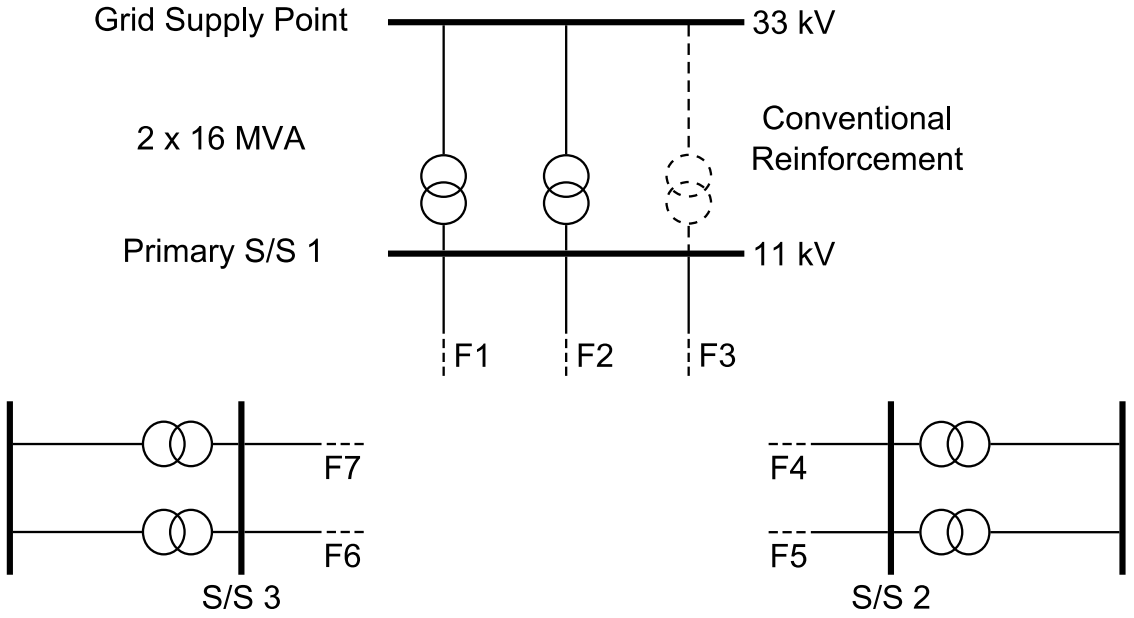

Figure 6.1: The RBTS Bus 4 DN, with conventional network reinforcement at S/S 1 to accommodate increased demand.

The main concept of ELCC [114] for load transfer is presented in Figure 6.2, in which ELCC is considered to be equal to the additional load (ΔD) that can be supplied via load transfer capability, while maintaining the same EENS with the base case (on the left hand side of the figure). The EENS is evaluated for the base case and then this assessment is performed for the

system with load transfer capability (right hand side of the figure) for each year of the study period considering the associated load growth and asset ageing. The year at which the EENS reaches the base case value and the corresponding additional demand, constitute the time that conventional reinforcement can be postponed and the contribution to the security of supply, respectively. In this study, ELCC is expressed in terms of load growth.

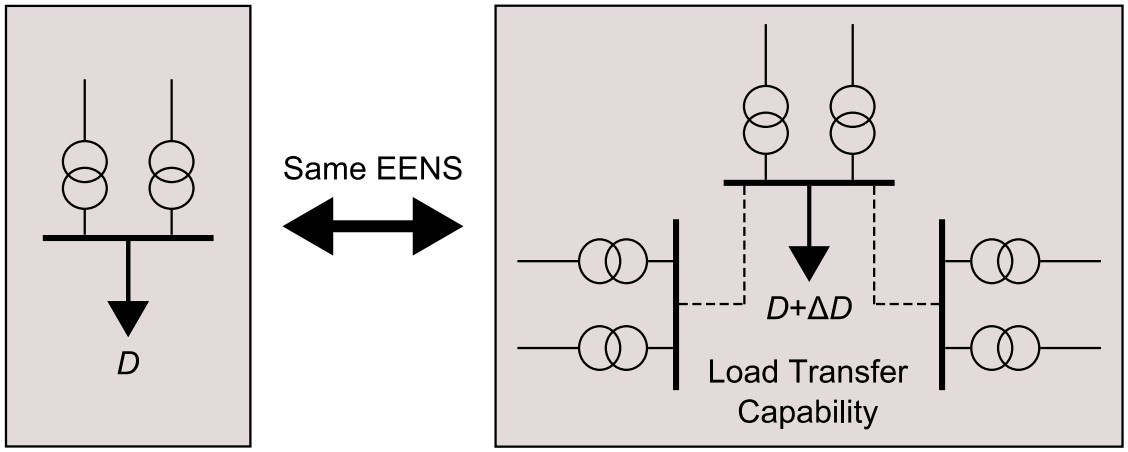

Figure 6.2: The main concept of the ELCC capacity credit methodology.

6.2.3. PROPOSED PROBABILISTIC METHOD

Probabilistic reliability evaluation is implemented using sequential Monte Carlo simulation. The sequential approach simulates the basic intervals of the system lifetime in chronological order. A two state model (up and down) is employed for the components of the network, i.e. lines and transformers. This method creates an artificial operating history (operation/repair sequence) for each component by randomly sampling up and down times.

The proposed method makes use of a substantial amount of historical data being available. The demand profile for an observed day is selected at random from these data; however, the demand profile could also be created by a model. Then, for each time period t of this day, the energy not supplied (ENS_t) is determined using Algorithm 1; switching time is assumed to be one hour in order to make the code more comprehensible. However, some

definitions and explanations should be provided, before describing the algorithm.

The demand group D_t is supplied by two incoming circuits, which have available capacity X_t. The supply to the primary S/S is assumed to be totally reliable. We also consider that the available contribution from the neighbouring S/Ss is Y_t. All the aforementioned variables are random, and we are interested in the loss of load (Z_t) and the ENS_t.

The available capacity of the incoming circuits (X_t) can take the values 0, R_c, and $2R_c$, depending on the availability of each circuit. This can be written as follows:

$$X_t = \begin{cases} 0, & \text{no circuits available} \\ R_c, & \text{one circuit available} \\ 2R_c, & \text{two circuits available} \end{cases} . \tag{6.1}$$

When both incoming circuits are available, it is considered that the loss of load is zero and the network is in its initial configuration. If the network was in a different configuration in the previous time step, then it is set back to its original configuration. The loss of load is also zero if there is: i) an outage of an incoming circuit, ii) demand is lower than the available incoming circuit capacity, and iii) the network has not been reconfigured.

It is assumed that load transfer takes place, if there is at least one outage in the incoming circuits and the demand cannot be met by the remaining available capacity. The load transfer is completed after the switching actions (in the primary DN) have been performed. This time interval is called switching time. During this time period, $Y_t = 0$, and therefore D_t can be supplied only by X_t. The loss of load in this case will be:

$$Z_t = D_t - X_t, \tag{6.2}$$

and the ENS_t will be equal to:

$$ENS_t = \max(Z_t \cdot \Delta t, 0). \tag{6.3}$$

In the reconfigured network, a part of the demand ($D_{1,t}$) continues to be supplied by the S/S under study, while the second part ($D_{2,t}$) is transferred onto the feeders of different S/Ss through NOPs. This can be expressed as:

$$D_t = D_{1,t} + D_{2,t}. \tag{6.4}$$

The network configuration remains fixed until the repair (at the considered S/S) has been completed. During this time, the first part of the demand ($D_{1,t}$) can be supplied only by the available capacity of the S/S (X_t). Hence, the loss of load and the ENS for $D_{1,t}$ are derived as follows:

$$Z_{1,t} = D_{1,t} - X_t, \tag{6.5}$$

$$ENS_{1,t} = \max(Z_{1,t} \cdot \Delta t, 0). \tag{6.6}$$

The second part of the demand group ($D_{2,t}$) is equal to the sum of each demand $D_{2,t}^j$ (explained further below) that is transferred from feeder F_i (of the considered S/S) to an adjacent feeder F_j (of a different S/S), i.e.

$$D_{2,t} = \sum_{j=1}^{N_f} D_{2,t}^j. \tag{6.7}$$

Each $D_{2,t}^j$ (during the repair process) can be supplied only by the available contribution of the adjacent feeder F_j (Y_t^j), which can be defined as:

$$Y_t^j = \max((S_{j,\max} - S_t^j), 0) \cdot \prod_{k \in \Omega_{br}^{F_j}} A_{k,t}. \tag{6.8}$$

In this case, the loss of load and the ENS are:

$$Z_{2,t}^j = D_{2,t}^j - Y_t^j, \tag{6.9}$$

$$ENS_{2,t}^j = \max(Z_{2,t}^j \cdot \Delta t, 0), \tag{6.10}$$

$$ENS_{2,t} = \sum_{j=1}^{N_f} ENS_{2,t}^j. \tag{6.11}$$

The total hourly ENS (after having reconfigured the network and until the repair at the S/S has been completed) is then obtained by:

$$ENS_t = ENS_{1,t} + ENS_{2,t}. \tag{6.12}$$

The network is set to its initial configuration, when both incoming circuits are back in service.

Having evaluated the ENS_t for all time steps, the EENS is derived as follows:

$$EENS = \frac{365}{N_{\text{days}}} \cdot \sum_{t=1}^{N_{\text{hours}}} ENS_t. \tag{6.13}$$

The EENS is calculated for each season separately, because load and line ratings are not constant across the whole year; the final EENS is the weighted sum of the previous results, based on [116].

$$EENS = \frac{3}{12} EENS_{win} + \frac{2}{12} EENS_{spr} + \frac{4}{12} EENS_{sum} + \frac{3}{12} EENS_{aut}. \quad (6.14)$$

Algorithm 1: *ENS* calculation

1. **if** ($X_t = 2R_c$) % *both incoming circuits available*
2. $ENS_t \leftarrow 0$;
3. **elseif** ($D_t < X_t$) and (*reconfiguration* = 0)
4. $ENS_t \leftarrow 0$;
5. **else** % (*one or no circuits available*) and ($D_t > X_t$ or *reconfiguration* = 1)
6. **if** (*reconfiguration* = 0) % *the network was in its initial configuration*
7. % *determine the load transfer according to* X_t (R_c *or zero*)
8. *reconfiguration* ← 1; % *reconfigure the network / load transfer*
9. $ENS_t \leftarrow \max((D_t - X_t) \cdot \Delta t, 0)$; % *during switching time,* $Y_t = 0$
10. **else** % (*reconfiguration* = 1*), the network has been reconfigured*
11. **if** ($X_t = 0$) and ($X_{t-1} = R_c$) % *loss of* 2*nd circuit, after the loss of the* 1*st*
12. % *maximize the load transfer* (*completed at the next time step*)
13. **end**
14. $ENS_{1,t} \leftarrow \max((D_{1,t} - X_t) \cdot \Delta t, 0)$; % *after having reconfigured …*
15. $ENS_{2,t} \leftarrow \sum_{j=1}^{N_t} \max((D_{2,t}^j - Y_t^j) \cdot \Delta t, 0)$; % *the network and until …*
16. $ENS_t \leftarrow ENS_{1,t} + ENS_{2,t}$; % *the repair at the S/S has been completed*
17. **if** ($X_{t+1} = 2R_c$) % *if at the next time step both circuits are available*
18. *reconfiguration* ← 0; % *network is set to its initial configuration*
19. **end**
20. **end**
21. **end**

$D_{2,t}^j$ is the load transferred from feeder F_i to an adjacent feeder F_j via a NOP, at time *t*. The determination of this load transfer is an optimization problem, which is formulated in [115] (for maximum load transfer). This can

be considered in the proposed methodology, but it would impose a huge computational burden. Therefore, in order to investigate the load transfer capability and still be able to handle the computational burden, we choose the RBTS Bus 4 DN, which has been modified for this work and is presented in Figure 6.3. The reason for this choice is that there are no interconnections between buses of the same feeder and between feeders of the same S/S. Only feeders from different S/Ss are connected to each other (at their endpoints). Therefore, there are limited load transfer options, which means that a high-quality solution can be easily found, while still capturing the capability of load transfer.

The load transfer is implemented by opening a normally closed branch and closing a normally open branch. In the case of two feeders interconnected at their endpoints, this leads to a small number of choices: the first option is to transfer the LP closest to the NOP; the second would be the transfer of two buses from one feeder to the other; and the last option is the transfer of all LPs. The operational constraints which must be satisfied after the load transfer are the branch capacity and voltage limits for feeder F_j, which takes up additional load. These are mathematically expressed as:

$$\begin{aligned} &\text{maximize} \quad \sum_{k \in \Omega_{\text{bus}}^{F_i}} P_k \\ &\text{subject to} \quad S_m \le S_{m,\max},\ m \in \Omega_{\text{br}}^{F_j} \\ &\qquad\qquad V_{\min} \le V_n \le V_{\max},\ n \in \Omega_{\text{bus}}^{F_j}, \end{aligned} \tag{6.15}$$

where P_k is the total power of the LP(s) at bus k of feeder F_i that are to be transferred to feeder F_j; S_m is the apparent power flow of branch m (of feeder F_j); $S_{m,\max}$ is the rating of branch m; and V_n is the voltage magnitude of bus n (of feeder F_j).

Different load transfers are considered depending on the number of failed incoming circuits. In the case of a double circuit outage, the optimal reconfiguration is the maximum load transfer. This is the above optimization problem and can be easily solved, because of the limited load transfer possibilities. This is realised by performing these possible load transfers, starting from the last option (transferring all LPs) and checking

for constraint violations, until a feasible solution is found. This way the maximum transferrable load (from each feeder F_i of the S/S under consideration to a specific adjacent feeder F_j) can be determined. For each feeder and for each load transfer, a fast decoupled load flow is run (using MATPOWER [88]) in order to ensure that there is no constraint violation.

In the case of a single circuit outage, the load transfer is approximately equal to the demand that cannot be met by the remaining available capacity of the incoming circuits. This can be incorporated into the optimization problem by adding an extra constraint (6.16). However, since the proposed method is concerned with finding a viable solution, the load transfer in this case is implemented as follows: first, the LP closest to the NOP of feeder F1 is examined if it can be transferred on to feeder F7 or not; second, the corresponding LP for feeder F2; third, on feeder F3; then the second LP of feeder F1, and so on, until the required amount of load has been reached. In this way, the margins of feeders F4, F5, and F7 (which take up additional load) are kept as high as possible; this is important because the reconfiguration of the network is considered fixed until the incoming circuits have been repaired and the demand of the LPs, which have been transferred, vary with time.

$$\sum_{k \in \Omega_{\text{bus}}^{F_i}} P_k \leq D_t - X_t. \tag{6.16}$$

Figure 6.4 illustrates how the proposed method works in three different cases. In the top figure, (a), the available capacity of the incoming circuits is sufficient to supply the demand, despite the circuit outage, and therefore no reconfiguration is required; ENS is zero. In (b), at 17:00, the demand exceeds the available capacity X_t, which leads to loss of load until the failed circuit has been repaired (20:00); this case considers that there is no load transfer capability. In contrast, (c) assumes that reconfiguration can be performed, through which the ENS can be significantly reduced. However the load transfer cannot be implemented until switching operations have been completed, which results in an unavoidable – but substantially reduced – level of ENS.

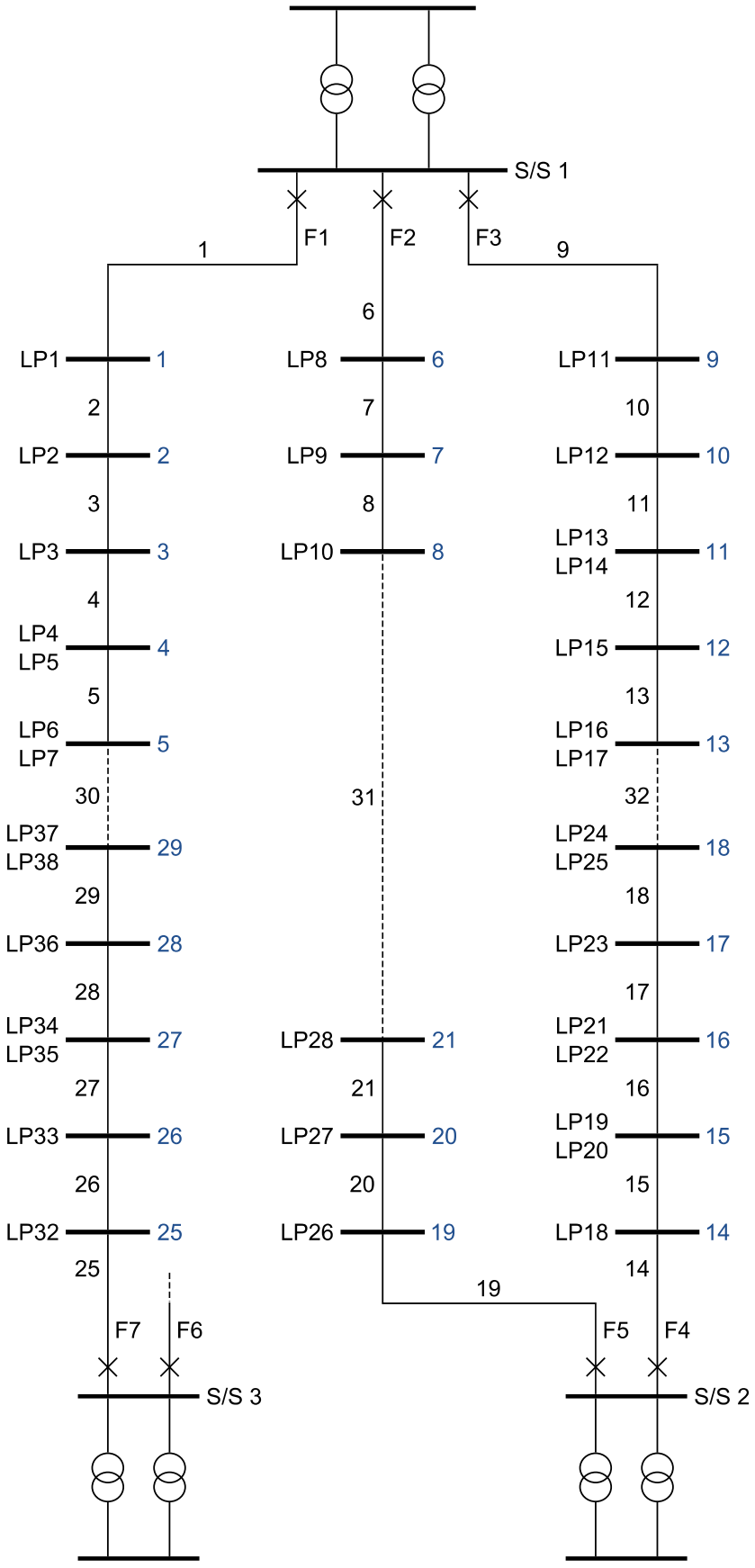

Figure 6.3: The RBTS Bus 4 DN, which has been modified for this chapter: 1) only main feeder sections are considered; 2) feeder F6 is ignored; and 3) feeder F2 is connected only to feeder F5 (through normally open branch 31). Branch numbers are shown in black; bus numbers are shown in blue.

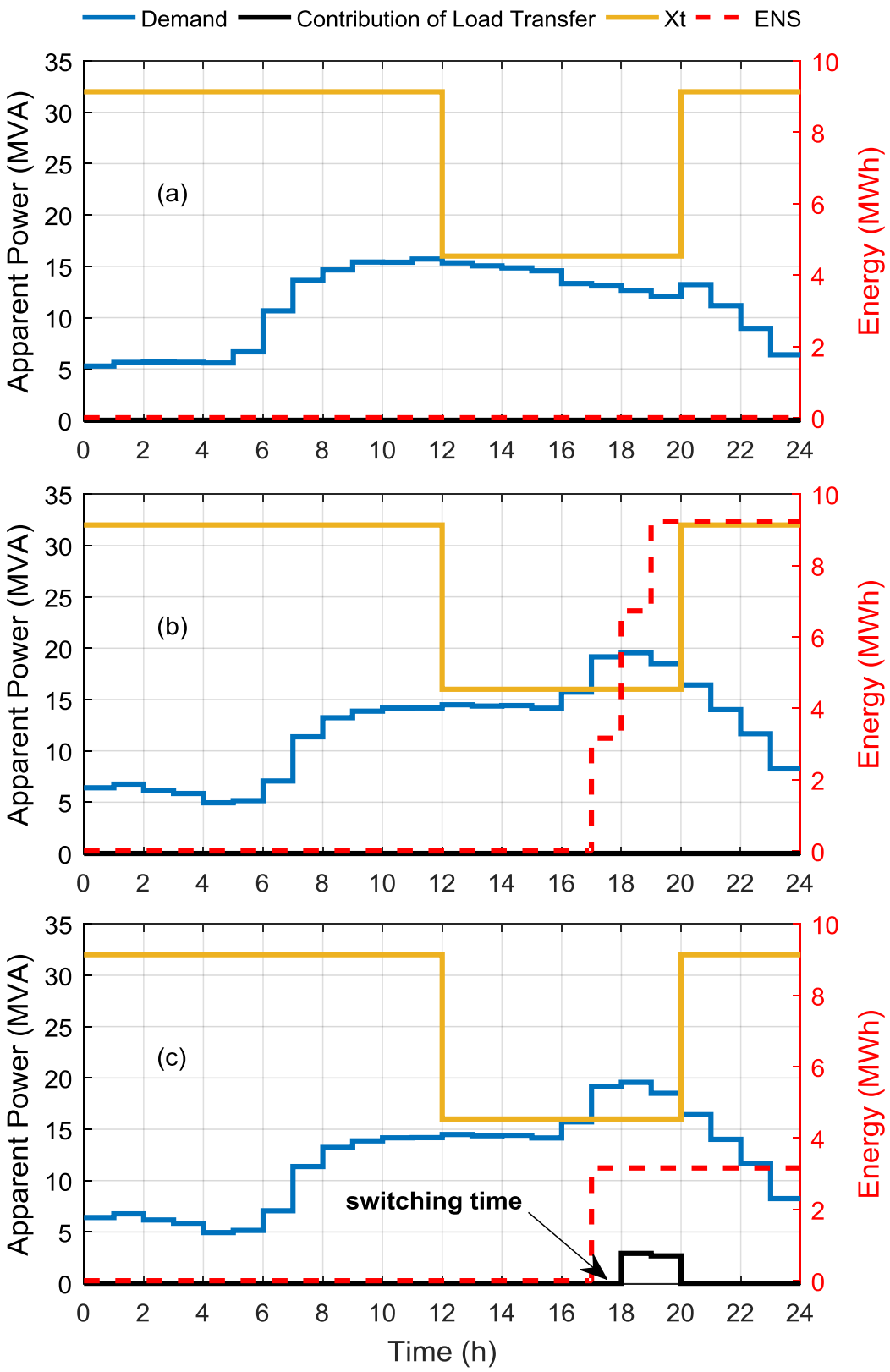

Figure 6.4: Illustrative scenarios to clarify the proposed method. In (a) the demand is lower than the available incoming circuit capacity, and therefore there is no need for reconfiguration; in (b) the demand exceeds the available capacity, resulting in loss of load, since there is no load transfer capability; and (c) illustrates the same case as (b), but with reconfiguration capability, which leads to an improved level of ENS. It should be noted that a single circuit outage occurs at 12:00, and the demand is considered greater than the available capacity of a single incoming circuit (at some time intervals) for demonstration.

6.3. CASE STUDY

6.3.1. ELECTRICITY DEMAND DATA

The demand data are taken from a 33/11 kV S/S from the UK Power Networks' Smarter Network Storage project [117] and are adjusted (see Appendix 5) to match the demand of S/S 1 of the case study network, which is illustrated in Figure 6.3. Historical half-hourly data were available for a period of six years; the data were converted into hourly average values for this study. For the adjusted historical data, with a 16 MVA limit for each S/S transformer, the contribution of DNR would be required (following a first circuit outage) on about 32.4% of winter hours, 11.2% of spring hours, 9% of autumn hours, and 0.14% of summer hours. Figure 6.5 shows the probability of various levels of S/S loading at each hourly interval during a day in each season.

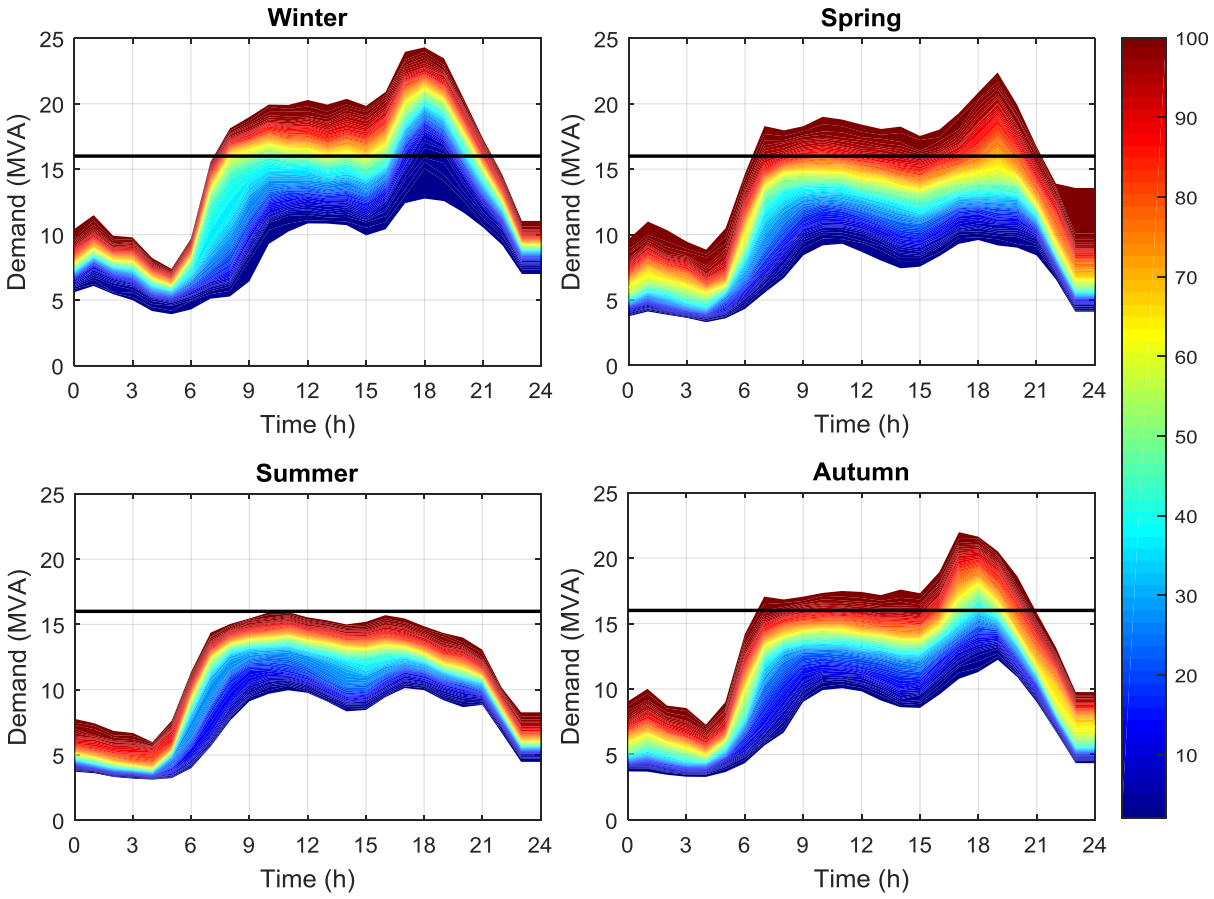

Figure 6.5: Demand quantiles for each season; the limit of each S/S transformer is also shown (black line – 16 MVA), in order to give an indication of the contribution required.

The first branches of the primary DN that will violate the branch rating constraints are the first sections of the feeders that take up additional load after reconfiguration. Therefore, only these branches are checked for a constraint violation following network reconfiguration. For the case study network, this means that branches 14, 19, and 25 are checked for overload. The 65 °C thermal limits (for each season) of these branches are given in Table 6.1 [118]. It has been assumed that feeder F2 can transfer load only to feeder F5. Moreover, the voltage of the low voltage busbar of the S/Ss that experience increased loading after load transfer is allowed up to 1.06 pu.

Table 6.1: Thermal limits of branches 14, 19, and 25 of the case study network (seasonal conductor ratings are not the same because different ambient temperatures are considered for each season)

Season	65 °C Limit (MVA)
Winter	12.55
Spring/Autumn	11.79
Summer	10.65

6.3.2. ASSET CONDITION

6.3.2.1. TRANSFORMERS

The condition of the transformers of S/S 1 is given in Table 2.2. The future HI and the corresponding overall failure rate (according to section 2.3.1) for the next 20 years are illustrated in Figure 6.6. The future HI of the transformers can be calculated as follows:

$$HI_{\mathrm{f}} = 6.17 \cdot e^{0.03723 \cdot year}. \tag{6.17}$$

This case study does not consider any refurbishment or replacement of the assets, which would have an impact on the corresponding HIs. However these interventions can be included in the analysis; in fact, the proposed work can support the planning of these AM decisions.

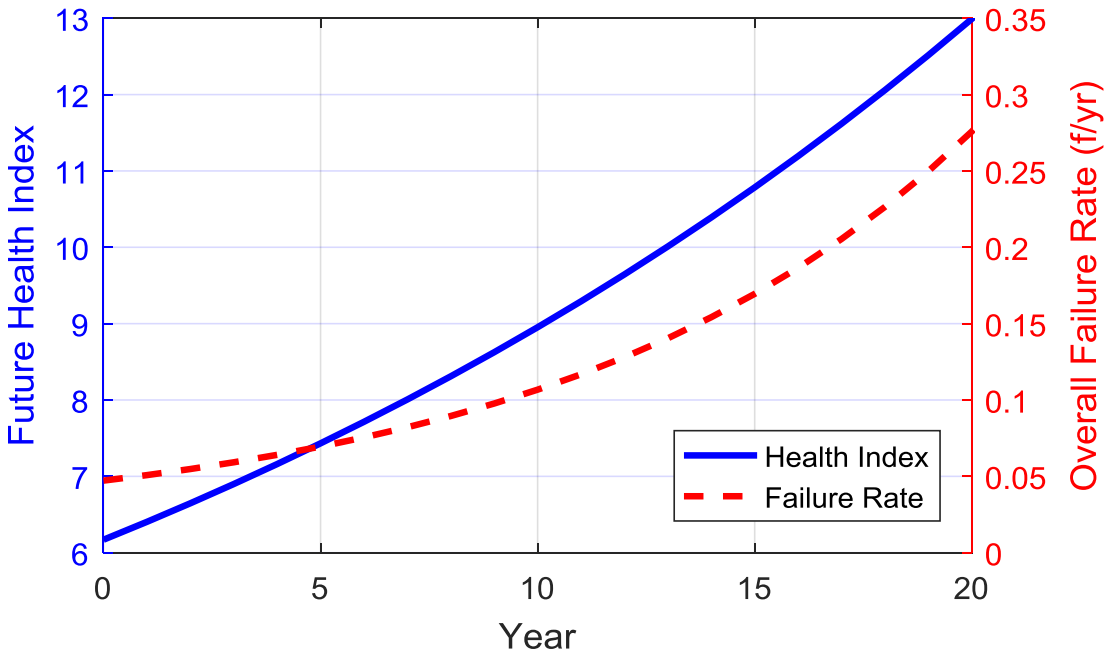

Figure 6.6: Future HI and overall failure rate for the transformers at S/S 1 for the next 20 years.

6.3.2.2. Overhead Lines

Two 33 kV OHLs (11 km each) are assumed to supply S/S 1; their condition is presented in Table 5.3. The same condition-based failure rate has been considered for the 11 kV OHLs in the primary DN. However, the overall failure rates are different, since the percentages of failures related to age or wear (for the two asset types) are not the same. The future HI and the corresponding overall failure rates for the next 20 years are illustrated in Figure 6.7. The future HI of the OHLs is derived as follows:

$$HI_{\mathrm{f}} = 3.14 \cdot e^{0.045144 \cdot year}. \tag{6.18}$$

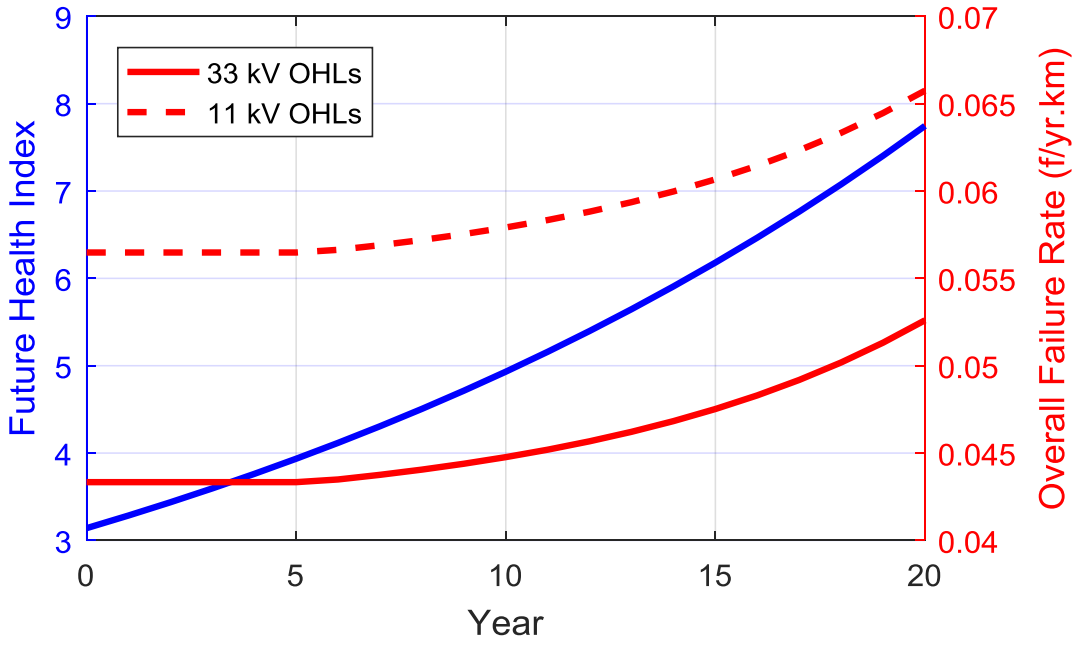

Figure 6.7: Future HI and overall failure rates for the 33 kV OHLs supplying S/S 1 and the 11 kV OHLs in the primary DN for the next 20 years.

6.3.3. Monte Carlo Simulation and Reliability Parameters

The sequential Monte Carlo simulation is run for 100 periods of 10,000 years each. The mean time to failure (MTTF) is derived using the overall failure rate of the asset every year, as follows:

$$MTTF = \frac{8760}{\lambda(year)}. \tag{6.19}$$

Time to failure (TTF) for each asset is exponentially distributed with an MTTF calculated as above. Time to repair (TTR) and time to switch (TTS) are lognormally distributed with mean values taken from Table 4.3 and standard deviations equal to one sixth of their mean values [6].

6.4. RESULTS

The methodology developed in section 6.2 was applied to the case study network shown in Figure 6.3, using the input data described in section 6.3.

The base case corresponds to: 1) no load transfer/DNR capability; 2) zero load growth; and 3) HIs of transformers and OHLs, 6.17 and 3.14, respectively. The EENS for the base case is 2.45 MWh/year. Figure 6.8 shows the EENS with and without considering DNR capability for the next 20 years. This simulation takes the ageing of the assets into account and assumes a load growth rate of 1%/year without compounding, i.e. the demand in year 20 is 20% higher than in the base case.

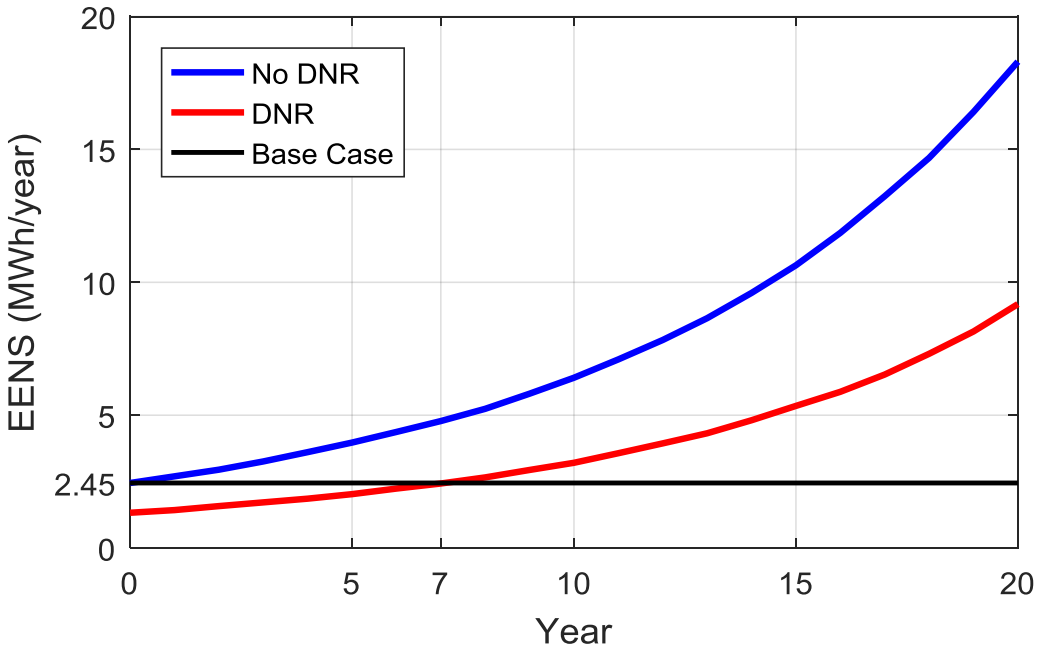

Figure 6.8: EENS with and without DNR capability for the next 20 years; asset ageing is taken into account.

The base case EENS is reached at year 7, which means that the ELCC of DNR (considering asset ageing) is 7% of the initial demand. Figure 6.9 shows the probability distribution of the EENS at this year. The proposed probabilistic method can not only produce the mean value (of the desired reliability index) for each year, but it can also yield the corresponding probability distribution. At year 7, the range for the EENS is from 2.36 to

2.49 MWh/year. Probability distributions can be a valuable tool in order to better inform network reinforcement decisions.

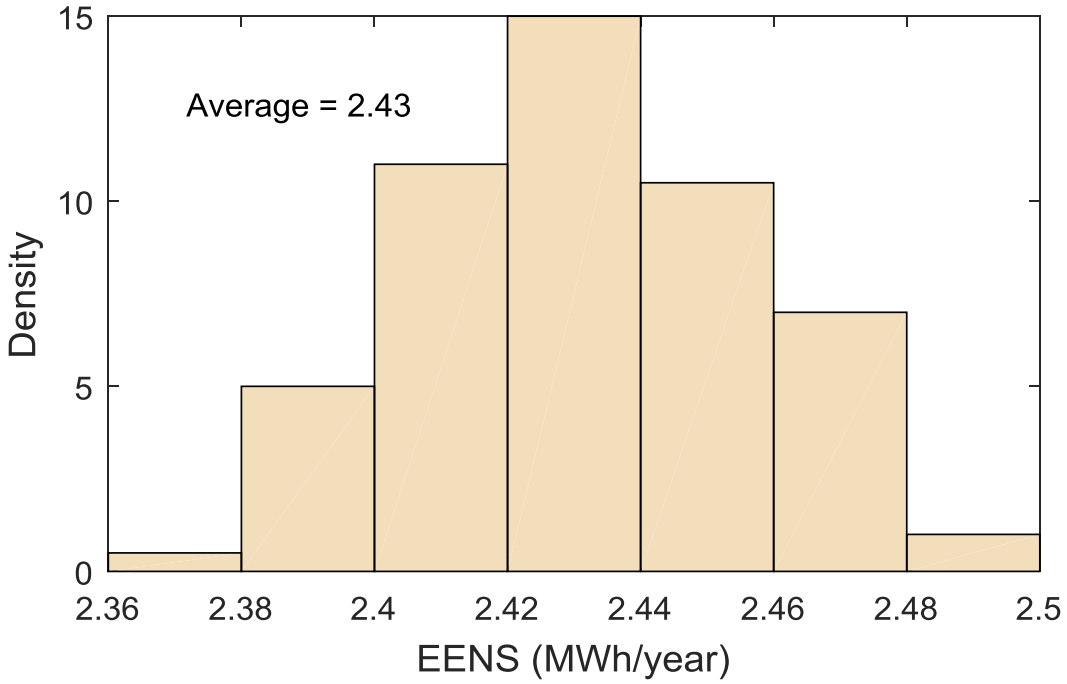

Figure 6.9: EENS probability distribution at year 7; the sum of the areas of the rectangles is equal to one.

Figure 6.10 illustrates the results of Figure 6.8, but without considering the ageing of the assets, i.e. asset HIs remain constant throughout the simulation period, as they were in the base case. In this case, EENS increases at a lower rate, as only load growth has an impact on the deterioration of the reliability of the network. As a result, EENS reaches the base case value at year 9, which indicates an ELCC of 9% of the initial demand. Consequently, neglecting asset ageing can lead to a considerable overestimation of the ELCC, which in turn can negatively influence decisions regarding network investment.

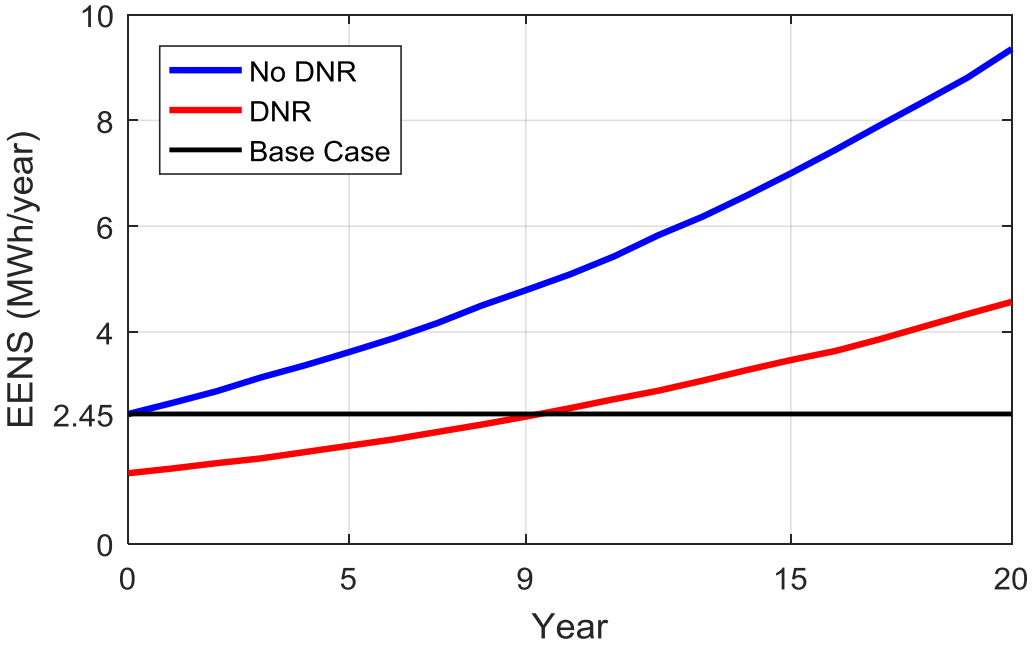

Figure 6.10: EENS with and without DNR capability for the next 20 years; asset ageing is not taken into account.

Finally, a sensitivity analysis was carried out (considering DNR capability) to more thoroughly investigate the impact of load growth and asset condition on the EENS of the network; Figure 6.11 illustrates the corresponding surface plot. It is evident that asset ageing plays a significant role in the determination of network security. For example, when load growth is equal to 20% without considering ageing, EENS is approximately 4.6 MWh/year, whereas – if asset ageing is included – EENS is double. Therefore, it is clear that the combined effect of load growth and asset ageing should be captured by the method which is used to quantify the contribution of load transfer/DNR to the security of supply of the network.

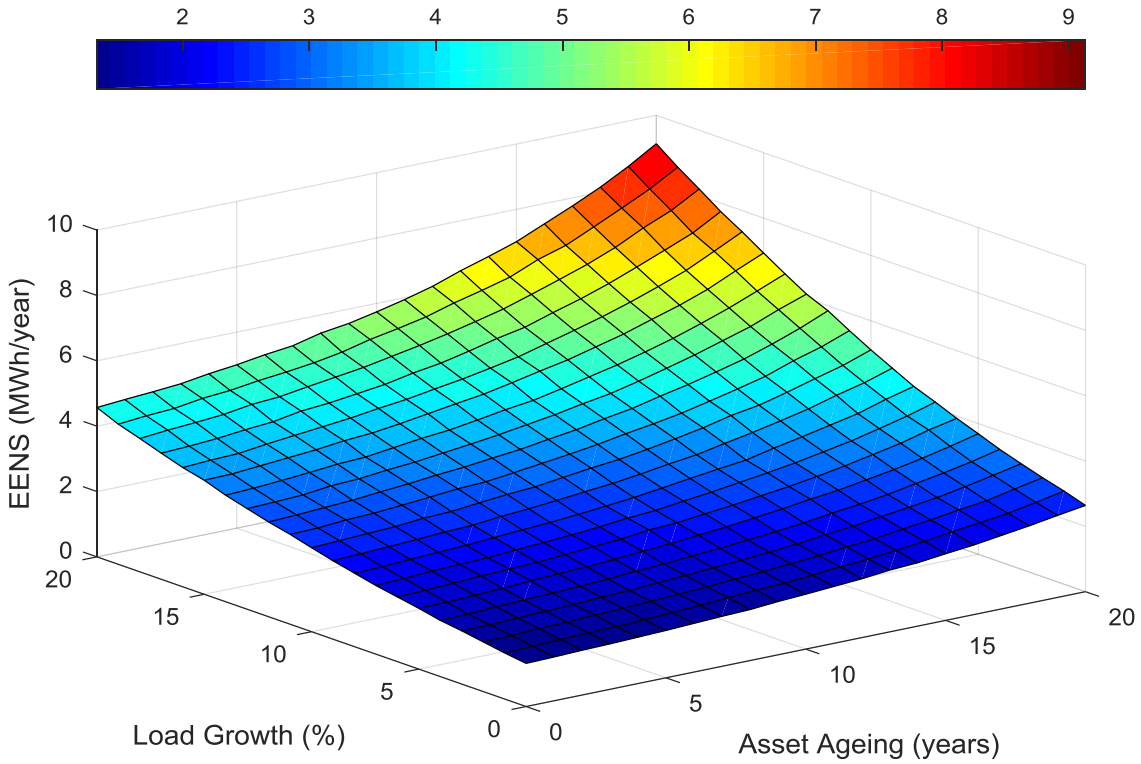

Figure 6.11: Sensitivity analysis of load growth and asset ageing on EENS.

6.5. CONCLUSION

This chapter describes a new method to quantify the contribution of DNR to security of supply in which the impact of asset condition and ageing is investigated. This assessment is implemented using ELCC, within a sequential Monte Carlo framework. The reliability evaluation of the network takes account of asset condition and ageing, by calculating current HIs, as well as their forecast values for the period of study.

The proposed methodology was successfully applied to the modified RBTS Bus 4 DN, showing that:

1) Failure to consider the contribution of DNR to security of supply, can lead to significant overestimation of network risk; for example, at year 7, network risk – with and without considering DNR – was approximately 2.5 and 5 MWh/year, respectively.
2) Disregarding asset condition and ageing resulted in a reinforcement deferral overestimation of two years.

This study can better inform the decision-making process of DNOs regarding network reinforcement in two ways. The first is that the quantification of DNR contribution to security of supply can defer network investment decisions; and the second is that asset condition assessment and ageing should be included in security of supply studies in order to account for the combined effect of load growth and asset ageing.

Finally, the work in this chapter could inform (or even be incorporated in) relevant industry standards and utility internal policies.

Chapter 7. Discussion

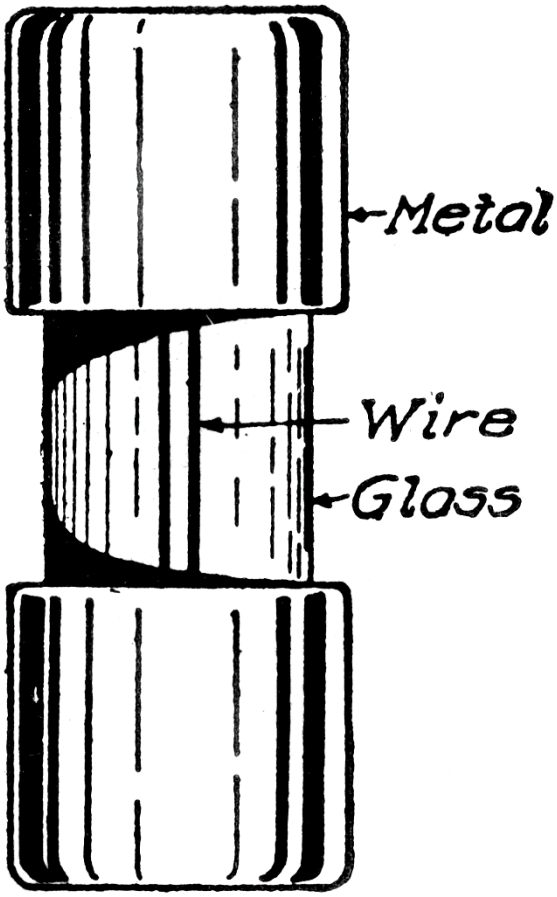

7.1. INTRODUCTION

Chapters 2-6 have presented the research that has been conducted over the duration of the author's PhD. This chapter discusses: 1) the combined impact of the methods described so far; 2) the broader implications of this work, and the potential impact on the electricity industry; and 3) further research that could be carried out in this area.

7.2. RESEARCH INTEGRATION

This section discusses the combined impact of the methods presented in Chapters 2-6. Section 2.3 describes two asset condition assessment and failure rate modelling methodologies; section 2.4 analyzes the effect of the loading of a transformer – which varies in real time – on its condition. These two models can be integrated into a single unified one, which will have the capability to calculate real-time changes in the HIs of the transformers, and therefore will be able to inform NMSs for real-time operations, such as dynamic network reconfiguration. This is also the concept of the – under development – methodology used in [36].

The reconfiguration optimization in Chapter 4 could be used for the optimal load transfer from an S/S to its adjacent ones in Chapter 6. This would require an optimal reconfiguration that would allow the network to transfer the maximum number of LPs – which would be the new objective function – in the case of a double circuit outage.

In the case of a single circuit outage, the load transfer is approximately equal to the difference between the demand of the substation (at the time of the outage) and the remaining available capacity of the incoming circuits. However, because the demand is variable and the configuration of the network is considered fixed after the load transfer, this might result in loss of load due to increase of the remaining demand at the S/S or the overall demand of the adjacent feeders that have taken up additional load. In order to account for this, the optimization algorithm could incorporate a load

forecast in order to minimize the aforementioned loss of load until the repair of the incoming circuit has been completed.

The optimal switch automation in Chapter 5 could improve the speed of the post-fault reconfiguration/load transfer in Chapter 6, which would also increase the contribution of DNR to network security. The RCS placement can also be determined in a way that an optimal schedule of network configurations is defined; RCSs in this case would allow the (frequent) transition from one configuration to the other. For example, the network could be reconfigured in an hourly, daily, weekly, monthly, or seasonal basis, which would depend on load patterns, in order to minimize (primarily) power losses.

The sensitivity analysis in section 5.4.3 shows that there is a priority in the order of the RCS placement in the network. This fact expresses the 'preference' of the method to protect LPs with high interruption costs in the first place. It is also noticed in Chapter 4 that these LPs are more likely to be transferred to adjacent – more reliable – feeders in order to improve their failure rate. Consequently, the two aforementioned methods to increase the reliability level of the LPs with significant outage costs can be jointly considered in order to find the optimal solution.

7.3. Broader Implications

7.3.1. Asset Condition and Network Operation

It has been mentioned earlier in this thesis that the British electricity regulator approved in 2017 a common methodology [11], across all UK DNOs, for the evaluation, forecasting, and regulatory reporting of asset HIs and associated risks. This will encourage DNOs to collect and utilize condition data in a more systematic and organized way. As a consequence, DNOs will have a better knowledge and understanding of the condition of their assets. This knowledge can be used in order to facilitate the application of the proposed methods to a DN. Note that the existence of online condition monitoring systems is not (initially) necessary. A first step

would be to employ available maintenance data in order to derive HIs for all network assets. A default score can be assigned to condition parameters, for which no information is available. The next step would be the utilization of real-time condition monitoring data – if such systems are available – for dynamic network reconfiguration.

The author considers that an integrated asset condition and network operation approach is critical for affordable, reliable, and sustainable electricity networks. In addition, this integration can be more valuable for a number of developing countries, for which their networks operate with very high power losses, frequent outages, and very high temperatures.

In section 2.4, it was shown that transformer condition depends on its hot-spot temperature; this variable is determined by the loading of the asset, as well as the ambient temperature. It is expected that mean temperatures will increase over the next few decades [119], which will accelerate the ageing of the assets. Concurrently, DNOs have limited their expenditure on asset maintenance and replacement [3, 33], which will inevitably increase the average age of the asset base. The utilization of the DNs has also increased with the connection of DGs and will rise even more, as load patterns are changing, in terms of electrification of heat and transport.

All of these facts indicate the criticality of an integrated asset management and network operation approach, which will be further supported by: 1) improved data gathering methods through novel sensor technologies, 2) improved short and long term forecasting capabilities, and 3) increased controllability of assets and networks.

7.3.2. Impact of DNR on Voltage Profile and Feeder Loading

Section 4.4.5 analyzed the impact of network reconfiguration on voltage and feeder loading with and without considering asset condition and S/S reliability. In section 4.4.5.1 (Test Case 2 – RBTS Bus 4 DN), the voltage profile and feeder loading (slightly) deteriorated after the load transfer; in section 4.4.5.2 (Test Case 3 – TPC DN), bus voltages and load balance were

improved. This is related to the structure of the network. The RBTS Bus 4 DN consists of feeders connected to each other only at their endpoints, and the normally open branches interconnect only feeders of different S/Ss; moreover the network is balanced in its original configuration, in terms of feeder lengths and loading (see Appendix 3 and Figure 4.15). A load transfer in this network makes the feeder that takes up the additional LP longer and more heavily loaded; and the feeder whose LP was transferred becomes shorter and its loading is reduced. This way the DN becomes more unbalanced, which means that losses increase, voltage profile deteriorates, and reliability level is also lower.

On the other hand, the TPC DN offered many more reconfiguration options (compared to the RBTS Bus 4 DN), as it had more normally open branches, which connected several points of a feeder to other feeders of both S/Ss. In this network, a load transfer does not necessarily lead to imbalance, because there are more interconnection points between feeders. For example, if LPs 7-10 are transferred from feeder A to feeder H, the latter can transfer a number of LPs to feeder G, and in turn this feeder could transfer load to feeder A; this way a new network configuration can be realized, while maintaining the balance in the network.

It should be noted that the focus of the work presented in this thesis was not to optimize the voltage profile and the load balance of the network, and it is clear that there can be a trade-off between these objectives and, for example, ECOST for failures at S/S and upstream network. However, voltage deviation and load balancing could be incorporated in the optimal DNR problem via a multi-objective formulation.

Taking the above into consideration, the inclusion of asset condition and S/S reliability into DNR may lead to better or worse voltage profile and load balance of the network; however, a greater number of reconfiguration options – in terms of feeder interconnections between each other – can help finding an optimal solution with improved bus voltages and feeder loadings.

7.3.3. ASSET MANAGEMENT DECISIONS

The case study in Chapter 6 considered no maintenance, refurbishment, or replacement of the assets, which would have an impact on their HIs and in turn on their failure rates. These interventions can be incorporated in the methodology presented in Chapter 6, by appropriately modifying the asset HIs; this work could therefore support the decision-making process of asset management.

The interventions can be considered in the analysis by reassessing the relevant condition parameters, depending on the refurbishment activity; for example, if a replacement of bushings takes place on a 33 kV transformer, then the condition parameter 'Bushings Condition' needs to be updated. After evaluating all affected condition parameters, the HI of the asset can be recalculated; based on the updated HI, the new condition-based failure rate can be computed, which will apparently be reduced.

These activities are performed in order to manage the risk of condition-based failures by reducing the probability of failure of the assets. Given a plan of asset refurbishment/replacement activities at specific points in time in the future, one can compare the risk of the network over the study period. This way asset management decisions can be evaluated in terms of capital cost, reliability, and risk; and then the optimal strategy can be selected accordingly.

The proposed research could also be used to evaluate the effect of potential network reinforcement and/or smart grid solutions (such as DG, ESSs, DSR, and RTTRs), along with the capability of DNR/load transfer on the capacity value. Different combinations of these solutions can be examined and – according to given criteria – the most suitable can be selected.

The use of RTTRs would render the capacity of network branches variable, depending on real-time local weather conditions [120]. Because the static rating of the conductors is derived in a conservative way [116], RTTRs would increase the capacity value of DNR. However, RTTR is stochastic,

and would therefore require a probabilistic methodology in order to be taken into account (as the proposed one in this thesis). This fact further supports the recommendation to move to a probabilistic or risk-based standard, as stated in [120]; this is further discussed in the next section.

The quantification of the contribution to network security can also be used to defer conventional network reinforcement. It should be noted again that the main advantage of DNR – compared to the other means – is its ability to contribute to the security of supply of the network for little or no capital investment cost; and this justifies why priority should be given to this solution.

7.3.4. POLICY RECOMMENDATIONS

The reasons mentioned above indicate why it is critical to evaluate the contribution of DNR/load transfer to network security. The present security of supply standard in the UK (Engineering Recommendation P2/6 [19]) mentions that this contribution should be considered when investigating the need for reinforcement. However, this standard does not provide a methodology to assess the capacity value of DNR. In addition to that and to the best of the author's knowledge, DNOs do not use a single comprehensive methodology, which would enable the reconfiguration capability to play a part in a DNO's compliance with P2/6; clearly, this may lead to investment decisions being made much earlier than strictly necessary. Therefore, it is recommended that the proposed work (in Chapter 6) be included in the relevant industry standards, as well as in the internal policies of DNOs.

Another important recommendation is the transition from the current deterministic security of supply standard to a probabilistic or risk-based one. The existing standard endeavours to define fixed values for stochastic quantities based on deterministic rules. However, the variability of smart grid technologies would be more suitable to be assessed probabilistically with a target of an acceptably low risk index, e.g. EENS.

7.4. Further Research

This section presents further research that could be conducted in order to develop and improve the work that has been carried out as part of the author's PhD.

7.4.1. Asset Condition and Network Operation

The condition parameters examined in section 2.3 generally change slowly, i.e. on a time scale of several months or years; this means that asset HIs – based on these condition parameters – change on the same time scale as well. Further research could seek to identify operation variables – except transformer loading, which was considered in section 2.4 – that have a real-time impact on the condition of the asset, and build the appropriate models to quantify this effect. This would allow an even better informed decision-making process for network operations. This concept is illustrated in Figure 7.1.

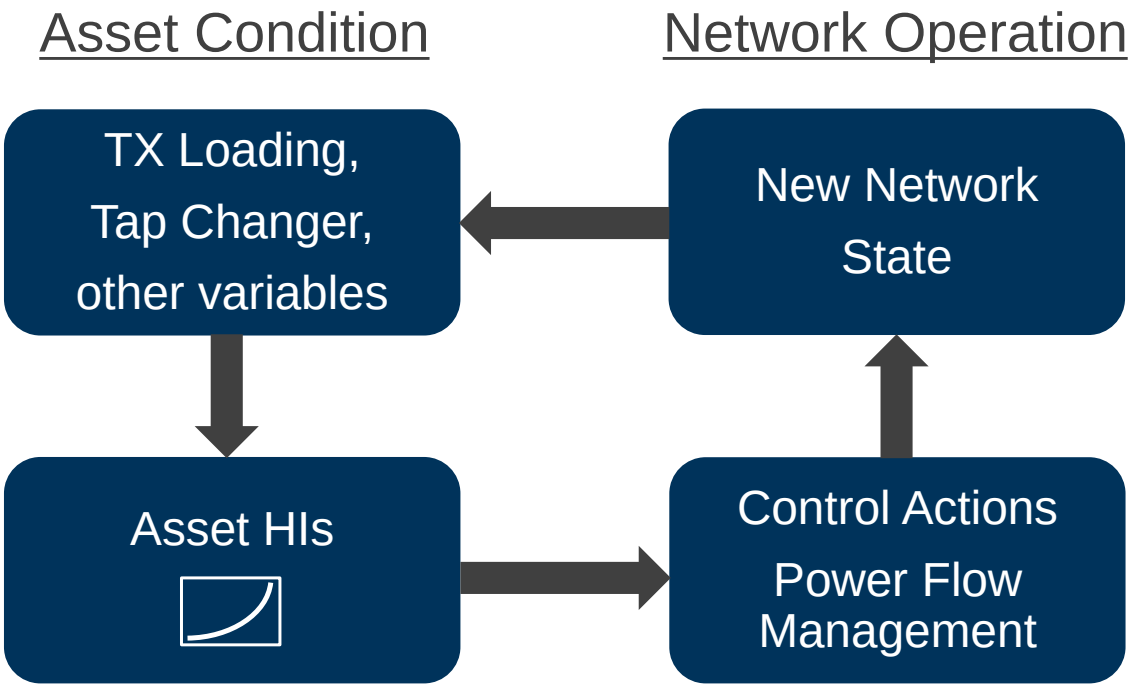

Figure 7.1: Concept of advanced integration of network operation with asset condition information.

Starting from the top right (of the figure) to the bottom right, the process is as follows:

1) Each network state corresponds to specific configuration, power flows, voltages, losses, reliability, risk, etc.
2) Given the above, transformer loadings can be derived and hot-spot temperatures can now be updated, which in turn yield the relative ageing rates and loss of lives; if there are temperature sensors installed on the transformers, then these values can be used instead. Moreover, the number of tap changer operations could be updated and then inform the relevant HI. Generally, any measured condition variable – e.g. partial discharge – can be used to update the HIs of the assets; or inform the NMS to take emergency action to prevent an identified incipient fault or minimize its consequences.
3) The condition variables that have been selected to update the HIs have now been calculated (or measured) and are combined appropriately to produce the HIs of the assets or – if necessary – inform the NMS to take emergency action.
4) The NMS having the above information available can make better informed decisions regarding network operation, such as real-time reconfiguration, in order to reduce overall cost and risk. Finally, this leads to a new network state (top right of the figure), and so on.

The realization of this concept is based on the use of online condition monitoring, as well as advanced communication and computational capabilities, as the aforementioned methods and systems require to gather and analyze data, as well as act on them in real time or near real time.

Furthermore, the asset condition assessment and failure rate modelling methodologies can gradually become more accurate, as more and more data are collected and experience is gained through the use of the methods; this will result in more representative asset HIs and failure rates.

7.4.2. ASSET MANAGEMENT

Time-based maintenance and replacement of the assets is the common practice in DNOs; further work could optimize these decisions based on asset condition and condition-based risk. It was described in section 7.3.3 how a strategy of refurbishment/replacement activities can be incorporated in the analysis in order to manage the risk of condition-based failures. Given a method to do so, one can compare and select between a number of possible options.

7.4.3. DISTRIBUTION NETWORK RECONFIGURATION

The work presented in this thesis (for DNR) did not focus on the optimization method, because the main aim of this study was to demonstrate the value of incorporating asset condition and substation reliability into the DNR problem. As a consequence, optimization per se can be a domain of further research.

The model for DNR considered constant loads and the reliability of the system was evaluated for a yearly period. However, this does not preclude the application of the proposed method to more discrete time periods with appropriate modifications. For example, the network could be reconfigured in an hourly, daily, weekly, monthly, or seasonal basis; optimal schedules of network configurations can then be determined, as well as the optimal frequency at which the network should be reconfigured.

The network configuration schedule could also be based on DG/RTTR forecasts; or on the state of charge of ESSs, if such technologies were used in combination with DNR.

Finally, another possible extension of this work would be to include uncertainty in the DNR problem through the use of robust or stochastic optimization; a significant feature to capture would be the uncertainty of condition-based failure rates of the most critical assets, such as the substation transformers. A sequential Monte Carlo simulation along with

the appropriate load profiles would be able to deal with this problem very accurately; however, that would impose an enormous computational burden.

7.4.4. Capacity Value of DNR

In Chapter 6 an obvious extension would be the investigation of the impact of feeder switch automation on the capacity value of DNR. Furthermore, the economic analysis of the research presented in the relevant chapter could also be examined; this analysis could consider DNR in isolation, or a combination of means (both network and smart grid solutions) such as conventional network reinforcement, DG, ESSs, DSR, and RTTRs. The results of the economic analysis would allow decision-makers to compare between DNR and network reinforcement, or any other smart grid solution; or compare between different combinations of the above-mentioned means.

7.5. Summary

This chapter has described: 1) the combined impact of the methods presented in Chapters 2-6; 2) the broader implications of the research carried out, and how it could impact the electricity industry; and 3) future work that could be conducted in this research area.

Chapter 8. Conclusions

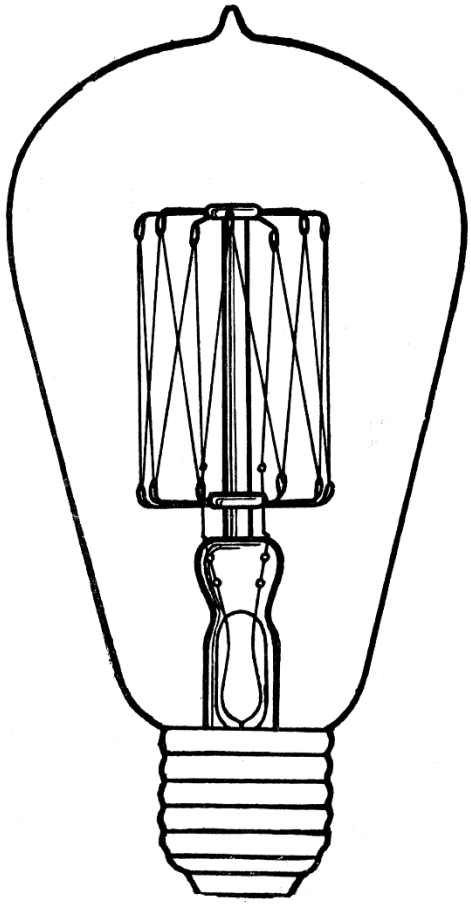

8.1. OVERVIEW

Generally, decisions regarding DN operations are based only on operational parameters of the DN, such as voltages, currents and power flows. Asset condition is a key parameter that is usually not considered by NMSs in their optimization process. Against this background, this thesis sought to quantify the extent to which asset condition information can positively influence network operation and planning, specifically through DNR.

8.2. KEY FINDINGS

The key findings of this research are:

- In section 3.4, the impact of transformer ageing on DNR was examined; the balancing between the relative ageing rates of the transformers at S/Ss X and Y led to a saving of $2,550 for a single day (that an overload occurred). This cost reduction is of significant value, as it corresponds to five times the cost of energy losses for a day.
- Chapter 4 incorporated asset condition and S/S reliability into DNR; the results for both case studies showed that the savings – compared to the formulation that neglects these factors – can be in the order of tens of thousands of U.S. dollars for a single DN. This corresponds approximately to 10% of the annual cost of active power losses, which is a considerable amount of saving. It should also be noted that this can mean hundreds of thousands – or even millions – of U.S. dollars for a single DNO (as it typically has hundreds of primary S/Ss).
- The results of Chapter 5 – which investigated the effect of asset ageing on optimal switch automation – demonstrated an underestimation of the ECOST as high as $223,000, and a saving of $70,000, for the cases with and without considering ageing in the optimization process.
- In Chapter 6, a new method to quantify the contribution of DNR to security of supply was described, which also accounted for the impact of asset condition and ageing. The corresponding results showed that: 1) Failure to consider the contribution of DNR to security of supply, can lead to significant overestimation of network risk; for example, at year 7,

network risk – with and without considering DNR – was approximately 2.5 and 5 MWh/year, respectively. 2) Disregarding asset condition and ageing resulted in a capacity value overestimation of two years.

8.3. FULFILMENT OF RESEARCH OBJECTIVES

This section presents how the main research objectives – defined in 1.6 – have been fulfilled.

1. Describe how asset condition can be translated into HIs and failure rates, which can allow an NMS – or an optimization algorithm – to make better informed decisions.

Asset condition information can influence network decisions through reliability. Condition data can be converted into HIs and failure rates, which in turn can inform NMSs to make improved decisions for network operation. This was realized via appropriate asset condition assessment methodologies and failure rate models (CNAIM [11] and *Brown et al.* [12]), which were selected to satisfy the following criteria: 1) reproducibility; many methodologies were described qualitatively (most of them constituted intellectual property), and thus could not have been implemented, 2) cover all basic asset types; some methods dealt only with a specific asset type (mainly transformers), and 3) relate asset HI to the corresponding condition-based failure rate. Moreover, a technique was proposed in order to derive the overall failure rate of an asset, in case the output of the model was only the condition-based failure rate; through the contribution of failures related to age or wear, using typical national fault statistical data.

2. Develop a method to include asset condition and substation reliability into DNR.

Asset condition and S/S reliability have a material impact on the cost of customer interruptions in DNs. However, these factors are not usually considered within DNR problem formulations, because of the lack of a readily available methodology. This thesis presented such a method, making use of asset HIs, which are now mandatory for DNOs in Great Britain.

Based on these HIs, condition-based failure rate can be calculated for each asset. S/S reliability is a function of asset condition, S/S configuration, and the network upstream of the S/Ss. The reliability of the S/S then has an impact on the reliability indices of each LP it supplies. These factors were combined to deliver a better informed algorithm for DNR, which was verified through its application on two DNs. The annual savings – compared to the formulation that neglects asset condition and S/S reliability – can be in the order of tens of thousands of U.S. dollars for a single DN.

3. Investigate the connection between transformer ageing and network reconfiguration.

Most of the condition parameters (and the associated HIs) that have been examined in this thesis, give an indication of the asset condition on a time scale of years. Transformer loading – a critical operation variable – can significantly affect the condition of the asset on a time scale of hours, especially under overload conditions. The effect of the loading of a transformer on its condition was examined using an appropriate ageing model [44]. This model concentrates on the ageing process of transformer insulation. Its inputs are: 1) the loading of the transformer, and 2) the ambient temperature; the model yields the hot-spot temperature, which in turn determines the relative ageing rate, and based on that finally the transformer loss of life can be derived. The transformer ageing model was incorporated into the DNR problem by including transformer loss of lives (expressed in monetary terms) in the objective function; the saving in this case was $2,550 for a day of an overload occurrence.

4. Examine the impact of asset ageing on optimal switch automation.

Existing literature on optimal distribution switch automation does not address asset condition assessment and ageing, and therefore constant (average) failure rates are assumed for all network components over the study period. Moreover, the feeder type (OHLs/UGCs) plays an important role in the reliability evaluation of the network, when ageing is considered; the UGC failure rate rises much more rapidly than the failure rate of OHLs,

as HI increases (see Figure 2.5). Chapter 5 proposed a new methodology for optimal RCS placement, which incorporates asset condition assessment and ageing; the inclusion of these factors in the problem formulation resulted in a more accurate reliability assessment of the network, as well as cost reduction. The results in section 5.4.2 showed an underestimation of the ECOST as high as $223,000, and a saving of $70,000, for the cases with and without considering ageing in the optimization process. Finally, the sensitivity analysis in section 5.4.3 indicated the significance of specific RCS locations, which depend on the customer type and demand of the LPs protected by these RCSs.

5. Devise a method to quantify the contribution of DNR to the security of supply of the network, considering asset condition and ageing.

Chapter 6 provided a method to quantify the contribution of DNR to the security of supply of a DN, using a probabilistic analysis; the quantification was implemented using ELCC, within a sequential Monte Carlo framework. This was necessary to capture the impact of time-dependent variables, such as switching time and time-varying load, as well as their inherent uncertainty. The second contribution was the condition-based reliability evaluation of the DN (incoming circuits and primary feeders), which was based on section 2.3.1; the proposed methodology not only considered current asset HIs, but also their forecast values over the period of interest. Finally, the incorporation of the combined effect of load growth and asset ageing into the quantification of the capacity value of DNR can lead to a more accurate assessment; this can lead to an improved decision-making process regarding network reinforcement – or a combination of network and smart grid solutions.

8.4. CONCLUSION

The primary contribution of the author has been to incorporate asset condition information into network operation and planning – specifically DNR. Current practice is that DN operations and planning disregard asset condition. This work has described methods, which allow to quantify the

extent to which asset condition data can positively impact DNR and its capacity value. The results have shown reduced cost and improved network reliability, which provide a significant benefit to electricity customers. Therefore, it is recommended that DNOs should include asset condition in DNR problems. It is also suggested that they should include DNR in security of supply studies, using the method developed in this thesis.

References

[1] L. Grigsby, *The Electric Power Engineering Handbook - Power Systems*: CRC Press, 2012.

[2] L. Bertling, R. Allan, and R. Eriksson, "A reliability-centered asset maintenance method for assessing the impact of maintenance in power distribution systems," *IEEE Trans. Power Syst.,* vol. 20, pp. 75-82, Feb. 2005.

[3] U. Zickler, A. Machkine, M. Schwan, A. Schnettler, X. Zhang, and E. Gockenbach, "Asset management in distribution systems considering new knowledge on component reliability and damage costs," in *Power Systems Computation Conference (PSCC)*, Liege, Belgium, 2005.

[4] S. Blake, P. Taylor, and A. Creighton, "Methodologies for the analysis of both short-term and long-term network risk," in *Electricity Distribution - Part 1, 2009. CIRED 2009. 20th International Conference and Exhibition on*, 2009, pp. 1-4.

[5] R. E. Brown and J. J. Burke, "Managing the risk of performance based rates," *IEEE Trans. Power Syst.,* vol. 15, pp. 893-898, May 2000.

[6] R. Billinton and R. N. Allan, *Reliability Evaluation of Power Systems*, 2nd ed. New York: Plenum, 1996.

[7] R. E. Brown, *Electric Power Distribution Reliability*. New York: Marcel Dekker, 2002.

[8] Energy Networks Association, "National Fault and Interruption Reporting Scheme (NaFIRS), National System and Equipment Performance 2009/2010," 2010.

[9] Office of Gas and Electricity Markets (Ofgem), "Electricity Distribution Annual Report for 2010-11," 2012.

[10] I. Sarantakos, D. M. Greenwood, J. Yi, S. R. Blake, and P. C. Taylor, "A method to include component condition and substation reliability into distribution system reconfiguration," *Int. J. Elect. Power Energy Syst.,* vol. 109, pp. 122-138, 2019.

[11] UK DNOs Working Group, "DNO Common Network Asset Indices Methodology," 2017.

[12] R. E. Brown, G. Frimpong, and H. L. Willis, "Failure rate modeling using equipment inspection data," *IEEE Trans. Power Syst.,* vol. 19, pp. 782-787, May 2004.

[13] I. Sarantakos, P. Lyons, S. Blake, P. Taylor, L. Tao, S. Celik, *et al.*, "Incorporating asset management into power system operations," *CIRED - Open Access Proceedings Journal,* vol. 2017, pp. 1227-1231, 2017.

[14] J. Zhu, *Optimization of Power System Operation*, 2nd ed. New Jersey: Wiley-IEEE Press, 2015.

[15] A. Merlin and H. Back, "Search for a Minimal-Loss Operating Spanning Tree Configuration in an Urban Power Distribution System," in *Proc. 5th Power Sys. Comput. Conf. (PSCC)*, Cambridge, UK, 1975.

[16] R. E. Brown, "Distribution reliability assessment and reconfiguration optimization," in *Proc. Transmission and Distribution Conf. Expo.*, 2001.

[17] R. N. Allan, R. Billinton, I. Sjarief, L. Goel, and K. S. So, "A reliability test system for educational purposes – Basic distribution system data and results," *IEEE Trans. Power Syst.,* vol. 6, pp. 813-820, May 1991.

[18] P. M. S. Carvalho, L. A. F. M. Ferreira, and A. J. Cerejo da Silva, "A decomposition approach to optimal remote controlled switch allocation in distribution systems," *IEEE Trans. Power Del.,* vol. 20, pp. 1031-1036, 2005.

[19] Energy Networks Association, "Engineering Recommendation P2/6: Security of Supply," 2006.

[20] Y. G. Hegazy, M. M. A. Salama, and A. Y. Chikhani, "Adequacy assessment of distributed generation systems using Monte Carlo Simulation," *IEEE Trans. Power Syst.,* vol. 18, pp. 48-52, 2003.

[21] D. T. C. Wang, L. F. Ochoa, and G. P. Harrison, "DG Impact on Investment Deferral: Network Planning and Security of Supply," *IEEE Trans. Power Syst.,* vol. 25, pp. 1134-1141, 2010.

[22] D. M. Greenwood, N. S. Wade, P. C. Taylor, P. Papadopoulos, and N. Heyward, "A Probabilistic Method Combining Electrical Energy Storage and Real-Time Thermal Ratings to Defer Network Reinforcement," *IEEE Trans. Sustain. Energy,* vol. 8, pp. 374-384, 2017.

[23] I. Konstantelos, P. Djapic, G. Strbac, P. Papadopoulos, and A. Laguna, "Contribution of energy storage and demand-side response to security of distribution networks," *CIRED - Open Access Proceedings Journal,* vol. 2017, pp. 1650-1654, 2017.

[24] M. Amelin, "Comparison of Capacity Credit Calculation Methods for Conventional Power Plants and Wind Power," *IEEE Trans. Power Syst.,* vol. 24, pp. 685-691, 2009.

[25] A. Keane, M. Milligan, C. J. Dent, B. Hasche, C. D. Annunzio, K. Dragoon*, et al.*, "Capacity Value of Wind Power," *IEEE Trans. Power Syst.,* vol. 26, pp. 564-572, 2011.

[26] Y. Zhou, P. Mancarella, and J. Mutale, "Framework for capacity credit assessment of electrical energy storage and demand response," *IET Gener. Transm. Distrib.,* vol. 10, pp. 2267-2276, 2016.

[27] I. Konstantelos and G. Strbac, "Capacity value of energy storage in distribution networks," *Journal of Energy Storage,* vol. 18, pp. 389-401, 2018.

[28] L. L. Garver, "Effective Load Carrying Capability of Generating Units," *IEEE Trans. Power App. Syst.,* vol. PAS-85, pp. 910-919, 1966.

[29] C. J. Dent, A. Hernandez-Ortiz, S. R. Blake, D. Miller, and D. Roberts, "Defining and Evaluating the Capacity Value of Distributed Generation," *IEEE Trans. Power Syst.,* vol. 30, pp. 2329-2337, 2015.

[30] J. Xiao, F. Li, W. Z. Gu, C. S. Wang, and P. Zhang, "Total supply capability and its extended indices for distribution systems: definition, model calculation and applications," *IET Gener. Transm. Distrib.,* vol. 5, pp. 869-876, 2011.

[31] K. Chen, W. Wu, B. Zhang, S. Djokic, and G. P. Harrison, "A Method to Evaluate Total Supply Capability of Distribution Systems Considering Network Reconfiguration and Daily Load Curves," *IEEE Trans. Power Syst.,* vol. 31, pp. 2096-2104, 2016.

[32] T. Ding, C. Li, C. Zhao, and M. Wang, "Total supply capability considering distribution network reconfiguration under N - k transformer contingency and the decomposition method," *IET Gener. Transm. Distrib.,* vol. 11, pp. 1212-1222, 2017.

[33] X. Zhang, J. Zhang, and E. Gockenbach, "Reliability Centered Asset Management for Medium-Voltage Deteriorating Electrical Equipment Based on Germany Failure Statistics," *IEEE Trans. Power Syst.,* vol. 24, pp. 721-728, 2009.

[34] J. Moubray, *Reliability-centred Maintenance*. Oxford, UK: Butterworth-Heinemann, 1997.

[35] M. Schwan, S. Sánchez, D. Rondon, C. Rodelo, and C. Nabte, "Reliability Centered Asset Management – Case Study for Mexican Sub-Transmission Networks," in *CIDEL Argentina 2010 International Congress on Electricity Distribution*, Argentina, 2010.

[36] *Siemens RCAM Dynamic*. Available: https://www.energy.siemens.com/br/en/services/power-transmission-distribution-smart-grid/condition-monitoring/reliability-centered-asset-management.htm

[37] *ABB Ability Ellipse APM*. Available: http://search.abb.com/library/Download.aspx?DocumentID=9AKK106930A8037&LanguageCode=en&DocumentPartId=&Action=Launch

[38] *EA Technology CBRM*. Available: https://www.eatechnology.com/wp-content/uploads/2017/03/CBRM-brochure.pdf

[39] *GE APM*. Available: https://www.gegridsolutions.com/Services/apm.htm

[40] T. Hjartarson and S. Otal, "Predicting Future Asset Condition Based on Current Health Index and Maintenance Level," in *ESMO 2006 - 2006 IEEE 11th International Conference on Transmission & Distribution Construction, Operation and Live-Line Maintenance*, 2006.

[41] A. Naderian, S. Cress, R. Piercy, F. Wang, and J. Service, "An Approach to Determine the Health Index of Power Transformers," in *2008 IEEE International Symposium on Electrical Insulation*, 2008.

[42] A. Jahromi, R. Piercy, S. Cress, J. Service, and W. Fan, "An approach to power transformer asset management using health index," *Electrical Insulation Magazine, IEEE,* vol. 25, pp. 20-34, 2009.

[43] D. Hughes, T. Pears, and Y. Tian, "Linking engineering knowledge and practical experience to investment planning by means of condition based risk management," in *2008 International Conference on Condition Monitoring and Diagnosis*, 2008.

[44] International Electrotechnical Commission (IEC), "IEC 60076-7 - Loading Guide for Oil-Immersed Power Transformers," 2008.

[45] *Customer-Led Network Revolution*. Available: http://www.networkrevolution.co.uk/

[46] P. Davison, "CLNR Trial Analysis - Real-Time Thermal Rating for Power Transformers," 2014.

[47] M. E. Baran and F. F. Wu, "Network reconfiguration in distribution systems for loss reduction and load balancing," *IEEE Trans. Power Del.,* vol. 4, pp. 1401-1407, Apr. 1989.

[48] S. K. Goswami and S. K. Basu, "A new algorithm for the reconfiguration of distribution feeders for loss minimization," *IEEE Trans. Power Del.,* vol. 7, pp. 1484-1491, 1992.

[49] D. Zhang, Z. Fu, and L. Zhang, "Joint Optimization for Power Loss Reduction in Distribution Systems," *IEEE Trans. Power Syst.,* vol. 23, pp. 161-169, Feb. 2008.

[50] V. Farahani, B. Vahidi, and H. A. Abyaneh, "Reconfiguration and Capacitor Placement Simultaneously for Energy Loss Reduction Based on an Improved Reconfiguration Method," *IEEE Trans. Power Syst.,* vol. 27, pp. 587-595, May 2012.

[51] Y. Ch, S. K. Goswami, and D. Chatterjee, "Effect of network reconfiguration on power quality of distribution system," *Int. J. Elect. Power Energy Syst.,* vol. 83, pp. 87-95, Dec. 2016.

[52] J. Z. Zhu, "Optimal reconfiguration of electrical distribution network using the refined genetic algorithm," *Elect. Power Syst. Res.,* vol. 62, pp. 37-42, 2002/05/28/ 2002.

[53] K. Prasad, R. Ranjan, N. C. Sahoo, and A. Chaturvedi, "Optimal reconfiguration of radial distribution systems using a fuzzy mutated genetic algorithm," *IEEE Trans. Power Del.,* vol. 20, pp. 1211-1213, 2005.

[54] H. D. de Macedo Braz and B. A. de Souza, "Distribution Network Reconfiguration Using Genetic Algorithms With Sequential Encoding: Subtractive and Additive Approaches," *IEEE Trans. Power Syst.,* vol. 26, pp. 582-593, 2011.

[55] A. Mendes, N. Boland, P. Guiney, and C. Riveros, "Switch and Tap-Changer Reconfiguration of Distribution Networks Using Evolutionary Algorithms," *IEEE Trans. Power Syst.,* vol. 28, pp. 85-92, Feb. 2013.

[56] A. M. Eldurssi and R. M. O'Connell, "A Fast Nondominated Sorting Guided Genetic Algorithm for Multi-Objective Power Distribution System Reconfiguration Problem," *IEEE Trans. Power Syst.,* vol. 30, pp. 593-601, Mar. 2015.

[57] Z. Ghofrani-Jahromi, M. Kazemi, and M. Ehsan, "Distribution Switches Upgrade for Loss Reduction and Reliability Improvement," *IEEE Trans. Power Del.,* vol. 30, pp. 684-692, Apr. 2015.

[58] A. M. Tahboub, V. R. Pandi, and H. H. Zeineldin, "Distribution System Reconfiguration for Annual Energy Loss Reduction Considering Variable Distributed Generation Profiles," *IEEE Trans. Power Del.,* vol. 30, pp. 1677-1685, Aug. 2015.

[59] A. Asrari, S. Lotfifard, and M. Ansari, "Reconfiguration of Smart Distribution Systems With Time Varying Loads Using Parallel Computing," *IEEE Trans. Smart Grid,* vol. 7, pp. 2713-2723, Nov. 2016.

[60] Y. Liu and X. Gu, "Skeleton-Network Reconfiguration Based on Topological Characteristics of Scale-Free Networks and Discrete

Particle Swarm Optimization," *IEEE Trans. Power Syst.,* vol. 22, pp. 1267-1274, 2007.

[61] B. Amanulla, S. Chakrabarti, and S. N. Singh, "Reconfiguration of Power Distribution Systems Considering Reliability and Power Loss," *IEEE Trans. Power Del.,* vol. 27, pp. 918-926, Apr. 2012.

[62] W. Guan, Y. Tan, H. Zhang, and J. Song, "Distribution system feeder reconfiguration considering different model of DG sources," *Int. J. Elect. Power Energy Syst.,* vol. 68, pp. 210-221, Jun. 2015.

[63] S. M. M. Larimi, M. R. Haghifam, and A. Moradkhani, "Risk-based reconfiguration of active electric distribution networks," *IET Gener. Transm. Distrib.,* vol. 10, pp. 1006-1015, 2016.

[64] Z. Li, S. Jazebi, and F. de León, "Determination of the Optimal Switching Frequency for Distribution System Reconfiguration," *IEEE Trans. Power Del.,* vol. 32, pp. 2060-2069, Aug. 2017.

[65] Y. J. Jeon, J. C. Kim, J. O. Kim, J. R. Shin, and K. Y. Lee, "An efficient simulated annealing algorithm for network reconfiguration in large-scale distribution systems," *IEEE Trans. Power Del.,* vol. 17, pp. 1070-1078, 2002.

[66] V. Parada, J. A. Ferland, M. Arias, and K. Daniels, "Optimization of electrical distribution feeders using simulated annealing," *IEEE Trans. Power Del.,* vol. 19, pp. 1135-1141, 2004.

[67] H. Kim, Y. Ko, and K. H. Jung, "Artificial neural-network based feeder reconfiguration for loss reduction in distribution systems," *IEEE Trans. Power Del.,* vol. 8, pp. 1356-1366, 1993.

[68] H. Salazar, R. Gallego, and R. Romero, "Artificial neural networks and clustering techniques applied in the reconfiguration of distribution systems," *IEEE Trans. Power Del.,* vol. 21, pp. 1735-1742, 2006.

[69] C.-T. Su, C.-F. Chang, and J.-P. Chiou, "Distribution network reconfiguration for loss reduction by ant colony search algorithm," *Elect. Power Syst. Res.,* vol. 75, pp. 190-199, Aug. 2005.

[70] C. F. Chang, "Reconfiguration and Capacitor Placement for Loss Reduction of Distribution Systems by Ant Colony Search Algorithm," *IEEE Trans. Power Syst.,* vol. 23, pp. 1747-1755, Nov. 2008.

[71] A. Ahuja, A. Pahwa, B. K. Panigrahi, and S. Das, "Pheromone-Based Crossover Operator Applied to Distribution System Reconfiguration," *IEEE Trans. Power Syst.,* vol. 28, pp. 4144-4151, Nov. 2013.

[72] T. T. Nguyen and A. V. Truong, "Distribution network reconfiguration for power loss minimization and voltage profile improvement using

cuckoo search algorithm," *Int. J. Elect. Power Energy Syst.,* vol. 68, pp. 233-242, Jun. 2015.

[73] T. T. Nguyen, A. V. Truong, and T. A. Phung, "A novel method based on adaptive cuckoo search for optimal network reconfiguration and distributed generation allocation in distribution network," *Int. J. Elect. Power Energy Syst.,* vol. 78, pp. 801-815, Jun. 2016.

[74] D. Sudha Rani, N. Subrahmanyam, and M. Sydulu, "Multi-Objective Invasive Weed Optimization – An application to optimal network reconfiguration in radial distribution systems," *Int. J. Elect. Power Energy Syst.,* vol. 73, pp. 932-942, Dec. 2015.

[75] A. Lotfipour and H. Afrakhte, "A discrete Teaching–Learning-Based Optimization algorithm to solve distribution system reconfiguration in presence of distributed generation," *Int. J. Elect. Power Energy Syst.,* vol. 82, pp. 264-273, Nov. 2016.

[76] H. P. Schmidt, N. Ida, N. Kagan, and J. C. Guaraldo, "Fast Reconfiguration of Distribution Systems Considering Loss Minimization," *IEEE Trans. Power Syst.,* vol. 20, pp. 1311-1319, Aug. 2005.

[77] W. Cao, J. Wu, N. Jenkins, C. Wang, and T. Green, "Benefits analysis of Soft Open Points for electrical distribution network operation," *Appl. Energy,* vol. 165, pp. 36-47, Mar. 2016.

[78] Q. Qi and J. Wu, "Increasing Distributed Generation Penetration Using Network Reconfiguration and Soft Open Points," *Energy Procedia,* vol. 105, pp. 2169-2174, May 2017.

[79] K. Deep, K. P. Singh, M. L. Kansal, and C. Mohan, "A real coded genetic algorithm for solving integer and mixed integer optimization problems," *Applied Mathematics and Computation,* vol. 212, pp. 505-518, 2009/06/15/ 2009.

[80] L. Tang, F. Yang, and X. Feng, "A novel method for distribution system feeder reconfiguration using black-box optimization," in *Proc. IEEE Power Energy Soc. Gen. Meeting*, Vancouver, BC, Canada, 2013.

[81] N. G. Paterakis, A. Mazza, S. F. Santos, O. Erdinç, G. Chicco, A. G. Bakirtzis*, et al.*, "Multi-Objective Reconfiguration of Radial Distribution Systems Using Reliability Indices," *IEEE Trans. Power Syst.,* vol. 31, pp. 1048-1062, Mar. 2016.

[82] S. A. Yin and C. N. Lu, "Distribution Feeder Scheduling Considering Variable Load Profile and Outage Costs," *IEEE Trans. Power Syst.,* vol. 24, pp. 652-660, May 2009.

[83] P. Zhang, W. Li, and S. Wang, "Reliability-oriented distribution network reconfiguration considering uncertainties of data by interval

analysis," *Int. J. Elect. Power Energy Syst.,* vol. 34, pp. 138-144, Jan. 2012.

[84] A. Kavousi-Fard and T. Niknam, "Optimal Distribution Feeder Reconfiguration for Reliability Improvement Considering Uncertainty," *IEEE Trans. Power Del.,* vol. 29, pp. 1344-1353, Jun. 2014.

[85] L. Goel and R. Billinton, "Evaluation of interrupted energy assessment rates in distribution systems," *IEEE Trans. Power Del.,* vol. 6, pp. 1876-1882, Oct. 1991.

[86] S. R. Blake, "Methodologies for the Evaluation and Mitigation of Distribution Network Risk," Doctoral thesis, Durham University, UK, 2010.

[87] S. R. Blake, P. C. Taylor, D. C. Miller, and M. Black, "Incorporating health indices into a composite distribution network risk model to evaluate asset replacement major projects," in *Reliability of Transmission and Distribution Networks (RTDN 2011), IET Conference on*, 2011, pp. 1-6.

[88] R. D. Zimmerman, C. E. Murillo-Sánchez, and R. J. Thomas, "MATPOWER: Steady-State Operations, Planning, and Analysis Tools for Power Systems Research and Education," *IEEE Trans. Power Syst.,* vol. 26, pp. 12-19, 2011.

[89] L. M. O. Queiroz, M. A. Roselli, C. Cavellucci, and C. Lyra, "Energy Losses Estimation in Power Distribution Systems," *IEEE Trans. Power Syst.,* vol. 27, pp. 1879-1887, 2012.

[90] *Statutory Instruments, The Electricity Safety, Quality and Continuity Regulations 2002, No. 2665*, 2002.

[91] Elexon. *Load Profiles*. Available: https://www.elexon.co.uk/operations-settlement/profiling/

[92] R. Billinton and R. N. Allan, *Reliability Evaluation of Engineering Systems*, 2nd ed. New York: Plenum, 1992.

[93] R. Billinton, S. Kumar, N. Chowdhury, K. Chu, K. Debnath, L. Goel, *et al.*, "A reliability test system for educational purposes-Basic data," *IEEE Trans. Power Syst.,* vol. 4, pp. 1238-1244, Aug. 1989.

[94] MathWorks. (2018). *Mixed Integer Optimization*. Available: https://uk.mathworks.com/help/gads/mixed-integer-optimization.html

[95] C.-T. Su and C.-S. Lee, "Network reconfiguration of distribution systems using improved mixed-integer hybrid differential evolution," *IEEE Trans. Power Del.,* vol. 18, pp. 1022-1027, 2003.

[96] R. Billinton and S. Jonnavithula, "Optimal switching device placement in radial distribution systems," *IEEE Trans. Power Del.,* vol. 11, pp. 1646-1651, 1996.

[97] G. Levitin, S. Mazal-Tov, and D. Elmakis, "Genetic algorithm for optimal sectionalizing in radial distribution systems with alternative supply," *Elect. Power Syst. Res.,* vol. 35, pp. 149-155, 1995.

[98] M. R. Haghifam, "Optimal allocation of tie points in radial distribution systems using a genetic algorithm," *Eur. Trans. Elect. Power,* vol. 14, pp. 85-96, 2004.

[99] L. S. de Assis, J. F. V. González, F. L. Usberti, C. Lyra, C. Cavellucci, and F. J. Von Zuben, "Switch Allocation Problems in Power Distribution Systems," *IEEE Trans. Power Syst.,* vol. 30, pp. 246-253, 2015.

[100] A. Moradi and M. Fotuhi-Firuzabad, "Optimal Switch Placement in Distribution Systems Using Trinary Particle Swarm Optimization Algorithm," *IEEE Transactions on Power Delivery,* vol. 23, pp. 271-279, 2008.

[101] J.-H. Teng and Y.-H. Liu, "A novel ACS-based optimum switch relocation method," *IEEE Trans. Power Syst.,* vol. 18, pp. 113-120, 2003.

[102] H. Falaghi, M. Haghifam, and C. Singh, "Ant Colony Optimization-Based Method for Placement of Sectionalizing Switches in Distribution Networks Using a Fuzzy Multiobjective Approach," *IEEE Trans. Power Del.,* vol. 24, pp. 268-276, 2009.

[103] W. Tippachon and D. Rerkpreedapong, "Multiobjective optimal placement of switches and protective devices in electric power distribution systems using ant colony optimization," *Elect. Power Syst. Res.,* vol. 79, pp. 1171-1178, 2009/07/01/ 2009.

[104] C.-S. Chen, C.-H. Lin, H.-J. Chuang, C.-S. Li, M.-Y. Huang, and C.-W. Huang, "Optimal placement of line switches for distribution automation systems using immune algorithm," *IEEE Transactions on Power Systems,* vol. 21, pp. 1209-1217, 2006.

[105] V. Calderaro, V. Lattarulo, A. Piccolo, and P. Siano, "Optimal Switch Placement by Alliance Algorithm for Improving Microgrids Reliability," *IEEE Trans. Ind. Informat.,* vol. 8, pp. 925-934, 2012.

[106] A. Abiri-Jahromi, M. Fotuhi-Firuzabad, M. Parvania, and M. Mosleh, "Optimized Sectionalizing Switch Placement Strategy in Distribution Systems," *IEEE Trans. Power Del.,* vol. 27, pp. 362-370, 2012.

[107] J. Luth, "Four rules to help locate protective devices," *Elect. World,* pp. 36-37, 1991.

[108] P. Wang and R. Billinton, "Demand-side optimal selection of switching devices in radial distribution system planning," *IEE Proc. Gener. Transm. Distrib.,* vol. 145, pp. 409-414, 1998.

[109] G. Celli and F. Pilo, "Optimal sectionalizing switches allocation in distribution networks," *IEEE Trans. Power Del.,* vol. 14, pp. 1167-1172, 1999.

[110] A. Heidari, V. G. Agelidis, M. Kia, J. Pou, J. Aghaei, M. Shafie-Khah, *et al.*, "Reliability Optimization of Automated Distribution Networks With Probability Customer Interruption Cost Model in the Presence of DG Units," *IEEE Trans. Smart Grid,* vol. 8, pp. 305-315, 2017.

[111] A. S. Bouhouras, G. T. Andreou, D. P. Labridis, and A. G. Bakirtzis, "Selective Automation Upgrade in Distribution Networks Towards a Smarter Grid," *IEEE Trans. Smart Grid,* vol. 1, pp. 278-285, 2010.

[112] H. A. Gil and G. Joos, "On the Quantification of the Network Capacity Deferral Value of Distributed Generation," *IEEE Trans. Power Syst.,* vol. 21, pp. 1592-1599, 2006.

[113] G. R. Pudaruth and F. Li, "Locational Capacity Credit Evaluation," *IEEE Trans. Power Syst.,* vol. 24, pp. 1072-1079, 2009.

[114] Imperial College London, "Review of Distribution Network Security Standards," 2015.

[115] M. R. Dorostkar-Ghamsari, M. Fotuhi-Firuzabad, A. Safdarian, A. S. Hoshyarzade, and M. Lehtonen, "Improve capacity utilization of substation transformers via distribution network reconfiguration and load transfer," in *2016 IEEE 16th International Conference on Environment and Electrical Engineering (EEEIC)*, 2016, pp. 1-6.

[116] Energy Networks Association, "Engineering Recommendation P27: Current rating guide for high voltage overhead lines operating in the UK distribution system," 1986.

[117] D. Greenwood, N. Wade, N. Heyward, P. Mehta, P. Taylor, and P. Papadopoulos, "Scheduling power and energy resources on the smarter network storage project," in *23rd Int. Conf. Exhibition on Electricity Distribution (CIRED)*, Lyon, France, 2015.

[118] National Grid, "Current Ratings for Overhead Lines," 2001.

[119] *UK Climate Projections, 2018, UKCP18*. Available: https://www.metoffice.gov.uk/research/collaboration/ukcp

[120] D. M. Greenwood, "Quantifying the Benefits and Risks of Real-Time Thermal Ratings in Electrical Networks," PhD Thesis, Newcastle University, UK, 2014.

[121] A. Kembhavi. (2007). *Data Scaling*. Available: https://uk.mathworks.com/matlabcentral/fileexchange/15561-data-scaling?focused=5092233&tab=function

Appendix 1: IEEE 33-Bus Network

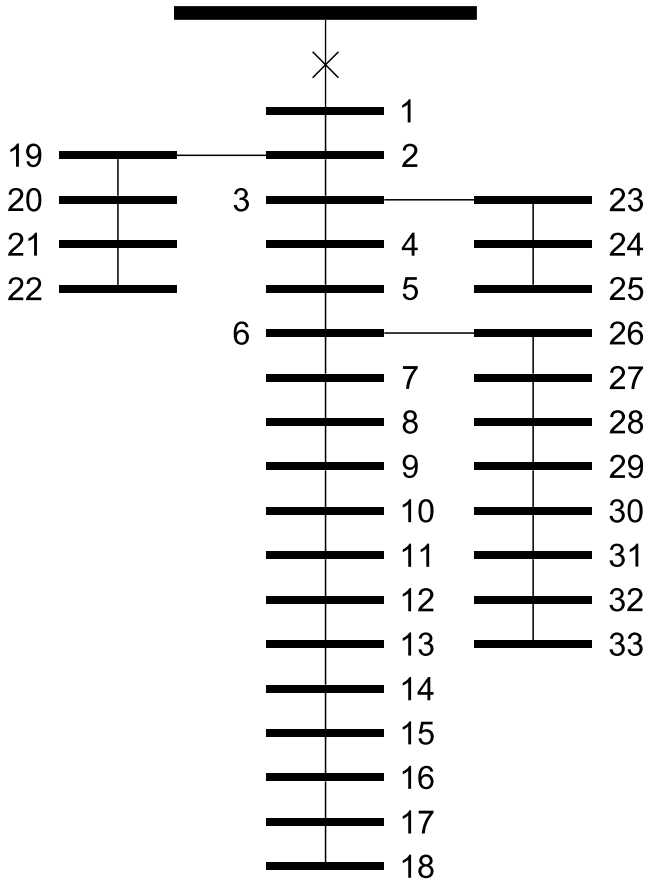

Figure A1.1: Diagram of the IEEE 33-bus network.

Table A1.1: Load data of the IEEE 33-bus network

Bus	P (MW)	Q (MVAr)	Bus	P (MW)	Q (MVAr)
1	0.000	0.000	18	0.090	0.040
2	0.100	0.060	19	0.090	0.040
3	0.090	0.040	20	0.090	0.040
4	0.120	0.080	21	0.090	0.040
5	0.060	0.030	22	0.090	0.040
6	0.060	0.020	23	0.090	0.050
7	0.200	0.100	24	0.420	0.200
8	0.200	0.100	25	0.420	0.200
9	0.060	0.020	26	0.060	0.025
10	0.060	0.020	27	0.060	0.025
11	0.045	0.030	28	0.060	0.020
12	0.060	0.035	29	0.120	0.070
13	0.060	0.035	30	0.200	0.600
14	0.120	0.080	31	0.150	0.070
15	0.060	0.010	32	0.210	0.100
16	0.060	0.020	33	0.060	0.040
17	0.060	0.020			

Table A1.2: Branch data of the IEEE 33-bus network

Branch No.	*From* Bus	*To* Bus	R (Ω)	X (Ω)	R (pu)	X (pu)
1	1	2	0.0922	0.0470	0.0575	0.0293
2	2	3	0.4930	0.2511	0.3076	0.1567
3	3	4	0.3660	0.1864	0.2284	0.1163
4	4	5	0.3811	0.1941	0.2378	0.1211
5	5	6	0.8190	0.7070	0.5110	0.4411
6	6	7	0.1872	0.6188	0.1168	0.3861
7	7	8	0.7114	0.2351	0.4439	0.1467
8	8	9	1.0300	0.7400	0.6426	0.4617
9	9	10	1.0440	0.7400	0.6514	0.4617
10	10	11	0.1966	0.0650	0.1227	0.0406
11	11	12	0.3744	0.1238	0.2336	0.0772
12	12	13	1.4680	1.1550	0.9159	0.7206
13	13	14	0.5416	0.7129	0.3379	0.4448
14	14	15	0.5910	0.5260	0.3687	0.3282
15	15	16	0.7463	0.5450	0.4656	0.3400
16	16	17	1.2890	1.7210	0.8042	1.0738
17	17	18	0.7320	0.5740	0.4567	0.3581
18	2	19	0.1640	0.1565	0.1023	0.0976
19	19	20	1.5042	1.3554	0.9385	0.8457
20	20	21	0.4095	0.4784	0.2555	0.2985
21	21	22	0.7089	0.9373	0.4423	0.5848
22	3	23	0.4512	0.3083	0.2815	0.1924
23	23	24	0.8980	0.7091	0.5603	0.4424
24	24	25	0.8960	0.7011	0.5590	0.4374
25	6	26	0.2030	0.1034	0.1267	0.0645
26	26	27	0.2842	0.1447	0.1773	0.0903
27	27	28	1.0590	0.9337	0.6607	0.5826
28	28	29	0.8042	0.7006	0.5018	0.4371
29	29	30	0.5075	0.2585	0.3166	0.1613
30	30	31	0.9744	0.9630	0.6080	0.6008
31	31	32	0.3105	0.3619	0.1937	0.2258
32	32	33	0.3410	0.5302	0.2128	0.3308

Table A1.3: Power flow results of the IEEE 33-bus network – voltage magnitudes

Bus	V	Bus	V	Bus	V
1	1.000	12	0.927	23	0.979
2	0.997	13	0.921	24	0.973
3	0.983	14	0.919	25	0.969
4	0.975	15	0.917	26	0.948
5	0.968	16	0.916	27	0.945
6	0.950	17	0.914	28	0.934
7	0.946	18	0.913	29	0.926
8	0.941	19	0.997	30	0.922
9	0.935	20	0.993	31	0.918
10	0.929	21	0.992	32	0.917
11	0.928	22	0.992	33	0.917

Appendix 2: Substation Reliability Analysis

Table A2.1: Reliability analysis for substation configuration (a)

Failure event	λ (f/yr)	r (h)	*ECOST* (k$/yr)
First-order total outages			
7	1.00×10^{-3}	2.00	0.1121
Second-order total outages			
1 + 4	9.66×10^{-5}	4.00	0.0199
1 + 5	9.06×10^{-6}	5.22	0.0026
1 + 6	1.89×10^{-6}	2.67	0.0002
2 + 4	9.06×10^{-6}	5.22	0.0026
2 + 5	7.71×10^{-7}	7.50	0.0003
2 + 6	1.95×10^{-7}	3.16	0.0000
3 + 4	1.89×10^{-6}	2.67	0.0002
3 + 5	1.95×10^{-7}	3.16	0.0000
3 + 6	3.29×10^{-8}	2.00	0.0000
Subtotal	1.20×10^{-4}	4.16	0.0261
Second-order total outages (m)	1.12×10^{-2}	7.56	5.2791
Active failures			
3A	4.00×10^{-3}	1.00	0.2520
6A	4.00×10^{-3}	1.00	0.2520
F4 CB	4.00×10^{-3}	1.00	0.2520
F5 CB	4.00×10^{-3}	1.00	0.2520
Subtotal	1.60×10^{-2}	1.00	1.0081
Active failures and stuck CB			
1A + 3S	1.15×10^{-2}	1.00	0.7246
2A + 3S	7.50×10^{-4}	1.00	0.0473
4A + 6S	1.15×10^{-2}	1.00	0.7246
5A + 6S	7.50×10^{-4}	1.00	0.0473
(31, 33, 36, 39, 41)A + F4 CB S	1.24×10^{-2}	1.00	0.7781
(44, 46, 48)A + F5 CB S	7.00×10^{-3}	1.00	0.4410
Subtotal	4.39×10^{-2}	1.00	2.7628
Total	7.22×10^{-2}	2.04	9.1878

Table A2.2: Reliability analysis for substation configuration (b)

Failure event	λ (f/yr)	r (h)	*ECOST* (k$/yr)
Load L1 (Feeder F4)			
First-order total outages			
7	0.001	2.00	0.0324
1	0.230	1.00	3.4851
2	0.015	1.00	0.2273
3	0.006	1.00	0.0909
Subtotal	0.252	1.004	3.8357
Second-order total outages	(0.00012)	4.16	0.0094
Second-order total outages (m)	(0.0112)	7.56	2.1886
Active failures			
9A	0.004	1.00	0.0606
F4 CB	0.004	1.00	0.0606
Subtotal	0.008	1.00	0.1212
Active failures and stuck CB			
(31, 33, 36, 39, 41)A + F4 CB S	0.01235	1.00	0.1871
Total	0.2724	1.26	6.3257
Load L2 (Feeder F5)			
First-order total outages			
8	0.001	2.00	0.0796
4	0.230	1.00	11.0054
5	0.015	1.00	0.7177
6	0.006	1.00	0.2871
Subtotal	0.252	1.004	12.0898
Second-order total outages	(0.00012)	4.16	0.0167
Second-order total outages (m)	(0.0112)	7.56	3.1030
Active failures			
9A	0.004	1.00	0.1914
F5 CB	0.004	1.00	0.1914
Subtotal	0.008	1.00	0.3828
Active failures and stuck CB			
(44, 46, 48)A + F5 CB S	0.007	1.00	0.3350
Total	0.267	1.27	15.9273

It should be noted that the second-order failure rates (in parentheses) in Table A2.2 are excluded from the calculation of the total failure rates; the second-order outages are used only for their ECOST contribution.

Appendix 3: RBTS Bus 4 Distribution Network

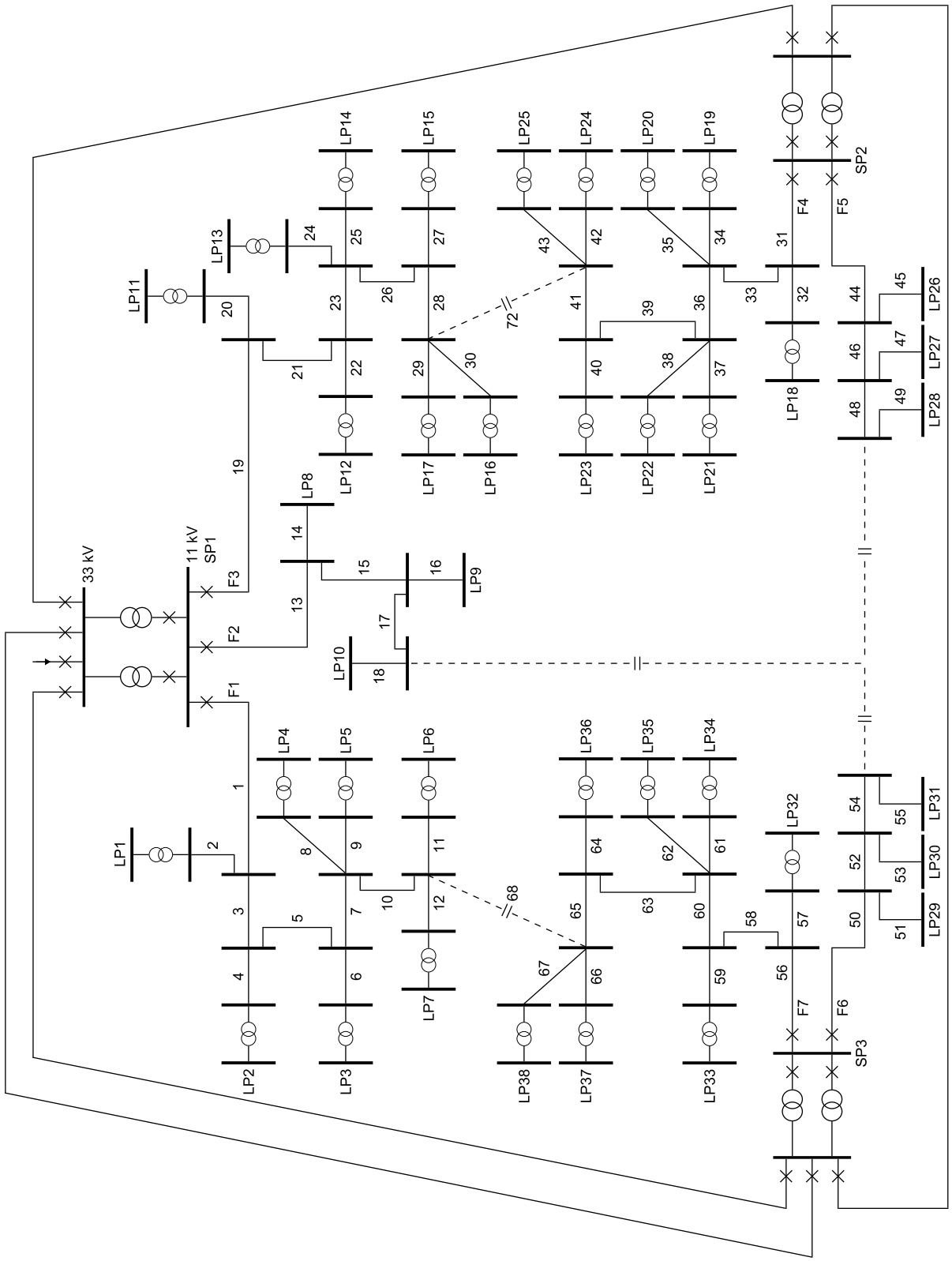

Figure A3.1: Diagram of the RBTS Bus 4 DN (same as Figure 4.2; reproduced here for convenience).

Table A3.1: Feeder types and lengths

Feeder Type	Length (km)	Feeder Section Numbers
1	0.60	2, 6, 10, 14, 17, 21, 25, 28, 30, 34, 38, 41, 43, 46, 49, 51, 55, 58, 61, 64, 67
2	0.75	1, 4, 7, 9, 12, 16, 19, 22, 24, 27, 29, 32, 35, 37, 40, 42, 45, 48, 50, 53, 56, 60, 63, 65
3	0.80	3, 5, 8, 11, 13, 15, 18, 20, 23, 26, 31, 33, 36, 39, 44, 47, 52, 54, 57, 59, 62, 66

Table A3.2: Customer data

Number of LPs	LPs	Customer Type	Load Level per LP (MW) Average	Peak
15	1-4, 11-13, 18-21, 32-35	Residential	0.545	0.8869
7	5, 14, 15, 22, 23, 36, 37	Residential	0.500	0.8137
7	8, 10, 26-30	**Industrial**	1.000	1.6300
2	9, 31	**Industrial**	1.500	2.4450
7	6, 7, 16, 17, 24, 25, 38	Commercial	0.415	0.6714
Total	–	–	24.58	40.000

LPs 8-10 and 26-31 (shown in bold in Table A3.2) have been considered to be industrial, since there was no available CDF for their original type (small users in [17]).

Appendix 4: TPC Distribution Network

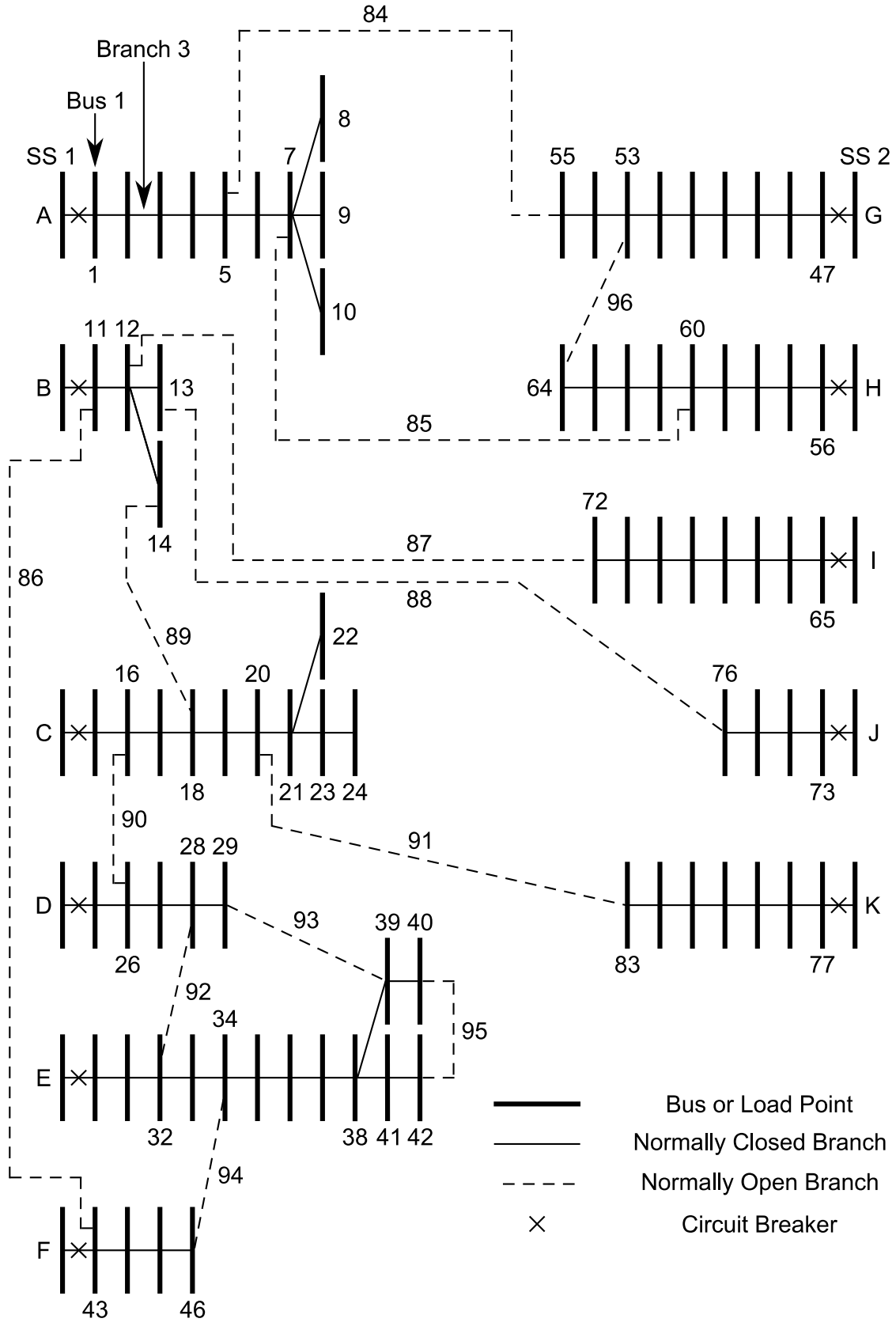

Figure A4.1: Diagram of the TPC DN.

Table A4.1: Load data of the TPC DN

Bus	*P* (MW)	*Q* (MVAr)	Bus	*P* (MW)	*Q* (MVAr)
A-K	0.00	0.00	42	0.05	0.03
1	0.00	0.00	43	0.00	0.00
2	0.10	0.05	44	0.03	0.02
3	0.30	0.20	45	0.80	0.70
4	0.35	0.25	46	0.20	0.15
5	0.22	0.10	47	0.00	0.00
6	1.10	0.80	48	0.00	0.00
7	0.40	0.32	49	0.00	0.00
8	0.30	0.20	50	0.20	0.16
9	0.30	0.23	51	0.80	0.60
10	0.30	0.26	52	0.50	0.30
11	0.00	0.00	53	0.50	0.35
12	1.20	0.80	54	0.50	0.30
13	0.80	0.60	55	0.20	0.08
14	0.70	0.50	56	0.00	0.00
15	0.00	0.00	57	0.03	0.02
16	0.30	0.15	58	0.60	0.42
17	0.50	0.35	59	0.00	0.00
18	0.70	0.40	60	0.02	0.01
19	1.20	1.00	61	0.02	0.01
20	0.30	0.30	62	0.20	0.13
21	0.40	0.35	63	0.30	0.24
22	0.05	0.02	64	0.30	0.20
23	0.05	0.02	65	0.00	0.00
24	0.05	0.01	66	0.05	0.03
25	0.05	0.03	67	0.00	0.00
26	0.10	0.06	68	0.40	0.36
27	0.10	0.07	69	0.00	0.00
28	1.80	1.30	70	0.00	0.00
29	0.20	0.12	71	2.00	1.50
30	0.00	0.00	72	0.20	0.15
31	1.80	1.60	73	0.00	0.00
32	0.20	0.15	74	0.00	0.00
33	0.20	0.10	75	1.20	0.95
34	0.80	0.60	76	0.30	0.18
35	0.10	0.06	77	0.00	0.00
36	0.10	0.06	78	0.40	0.36
37	0.02	0.01	79	2.00	1.30
38	0.02	0.01	80	0.20	0.14
39	0.02	0.01	81	0.50	0.36
40	0.02	0.01	82	0.10	0.03
41	0.20	0.16	83	0.40	0.36

Table A4.2: Branch data of the TPC DN

Branch No.	*From* Bus	*To* Bus	*R* (Ω)	*X* (Ω)	*R* (pu)	*X* (pu)
1	A	1	0.1944	0.6624	0.1496	0.5097
2	1	2	0.2096	0.4304	0.1613	0.3312
3	2	3	0.2358	0.4842	0.1814	0.3726
4	3	4	0.0917	0.1883	0.0706	0.1449
5	4	5	0.2096	0.4304	0.1613	0.3312
6	5	6	0.0393	0.0807	0.0302	0.0621
7	6	7	0.0405	0.1380	0.0312	0.1062
8	7	8	0.1048	0.2152	0.0806	0.1656
9	7	9	0.2358	0.4842	0.1814	0.3726
10	7	10	0.1048	0.2152	0.0806	0.1656
11	B	11	0.0786	0.1614	0.0605	0.1242
12	11	12	0.3406	0.6944	0.2621	0.5343
13	12	13	0.0262	0.0538	0.0202	0.0414
14	12	14	0.0786	0.1614	0.0605	0.1242
15	C	15	0.1134	0.3864	0.0873	0.2973
16	15	16	0.0524	0.1076	0.0403	0.0828
17	16	17	0.0524	0.1076	0.0403	0.0828
18	17	18	0.1572	0.3228	0.1210	0.2484
19	18	19	0.0393	0.0807	0.0302	0.0621
20	19	20	0.1703	0.3497	0.1310	0.2691
21	20	21	0.2358	0.4842	0.1814	0.3726
22	21	22	0.1572	0.3228	0.1210	0.2484
23	21	23	0.1965	0.4035	0.1512	0.3105
24	23	24	0.1310	0.2690	0.1008	0.2070
25	D	25	0.0567	0.1932	0.0436	0.1487
26	25	26	0.1048	0.2152	0.0806	0.1656
27	26	27	0.2489	0.5111	0.1915	0.3933
28	27	28	0.0486	0.1656	0.0374	0.1274
29	28	29	0.1310	0.2690	0.1008	0.2070
30	E	30	0.1965	0.3960	0.1512	0.3047
31	30	31	0.1310	0.2690	0.1008	0.2070
32	31	32	0.1310	0.2690	0.1008	0.2070
33	32	33	0.0262	0.0538	0.0202	0.0414
34	33	34	0.1703	0.3497	0.1310	0.2691
35	34	35	0.0524	0.1076	0.0403	0.0828
36	35	36	0.4978	1.0222	0.3830	0.7865
37	36	37	0.0393	0.0807	0.0302	0.0621
38	37	38	0.0393	0.0807	0.0302	0.0621

39	38	39	0.0786	0.1614	0.0605	0.1242
40	39	40	0.2096	0.4304	0.1613	0.3312
41	38	41	0.1965	0.4035	0.1512	0.3105
42	41	42	0.2096	0.4304	0.1613	0.3312
43	F	43	0.0486	0.1656	0.0374	0.1274
44	43	44	0.0393	0.0807	0.0302	0.0621
45	44	45	0.1310	0.2690	0.1008	0.2070
46	45	46	0.2358	0.4842	0.1814	0.3726
47	G	47	0.2430	0.8280	0.1870	0.6371
48	47	48	0.0655	0.1345	0.0504	0.1035
49	48	49	0.0655	0.1345	0.0504	0.1035
50	49	50	0.0393	0.0807	0.0302	0.0621
51	50	51	0.0786	0.1614	0.0605	0.1242
52	51	52	0.0393	0.0807	0.0302	0.0621
53	52	53	0.0786	0.1614	0.0605	0.1242
54	53	54	0.0524	0.1076	0.0403	0.0828
55	54	55	0.1310	0.2690	0.1008	0.2070
56	H	56	0.2268	0.7728	0.1745	0.5946
57	56	57	0.5371	1.1029	0.4133	0.8486
58	57	58	0.0524	0.1076	0.0403	0.0828
59	58	59	0.0405	0.1380	0.0312	0.1062
60	59	60	0.0393	0.0807	0.0302	0.0621
61	60	61	0.0262	0.0538	0.0202	0.0414
62	61	62	0.1048	0.2152	0.0806	0.1656
63	62	63	0.2358	0.4842	0.1814	0.3726
64	63	64	0.0243	0.0828	0.0187	0.0637
65	I	65	0.0486	0.1656	0.0374	0.1274
66	65	66	0.1703	0.3497	0.1310	0.2691
67	66	67	0.1215	0.4140	0.0935	0.3186
68	67	68	0.2187	0.7452	0.1683	0.5734
69	68	69	0.0486	0.1656	0.0374	0.1274
70	69	70	0.0729	0.2484	0.0561	0.1911
71	70	71	0.0567	0.1932	0.0436	0.1487
72	71	72	0.0262	0.0528	0.0202	0.0406
73	J	73	0.3240	1.1040	0.2493	0.8495
74	73	74	0.0324	0.1104	0.0249	0.0849
75	74	75	0.0567	0.1932	0.0436	0.1487
76	75	76	0.0486	0.1656	0.0374	0.1274
77	K	77	0.2511	0.8556	0.1932	0.6584
78	77	78	0.1296	0.4416	0.0997	0.3398
79	78	79	0.0486	0.1656	0.0374	0.1274

80	79	80	0.1310	0.2640	0.1008	0.2031
81	80	81	0.1310	0.2640	0.1008	0.2031
82	81	82	0.0917	0.1883	0.0706	0.1449
83	82	83	0.3144	0.6456	0.2419	0.4968
84	5	55	0.1310	0.2690	0.1008	0.2070
85	7	60	0.1310	0.2690	0.1008	0.2070
86	11	43	0.1310	0.2690	0.1008	0.2070
87	12	72	0.3406	0.6994	0.2621	0.5382
88	13	76	0.4585	0.9415	0.3528	0.7245
89	14	18	0.5371	1.0824	0.4133	0.8329
90	16	26	0.0917	0.1883	0.0706	0.1449
91	20	83	0.0786	0.1614	0.0605	0.1242
92	28	32	0.0524	0.1076	0.0403	0.0828
93	29	39	0.0786	0.1614	0.0605	0.1242
94	34	46	0.0262	0.0538	0.0202	0.0414
95	40	42	0.1965	0.4035	0.1512	0.3105
96	53	64	0.0393	0.0807	0.0302	0.0621

Appendix 5: Demand Adjustment & Disaggregation

This appendix describes the process to adjust and disaggregate the demand data used in Chapter 6. The original demand data are taken from a 33/11 kV S/S from the UK Power Networks' Smarter Network Storage project [117]. These are historical half-hourly data for a period of six years. The data are converted into hourly average values for this study. Then, the demand data are adjusted to match the demand of S/S 1 of the case study network (see Figure 6.3), according to the code below, which is based on [121].

```
for i = 1:N_days
    datain = Demand_data_original(i,:);
    day_max = max(datain);
    day_min = min(datain);
    maxval = day_max/1.6;
    minval = day_min/3;
    % data scaling
    dataout = datain - min(datain(:));
    dataout = (dataout/range(dataout(:)))*(maxval-minval);
    dataout = dataout + minval;
    Demand_data_adjusted(i,:) = dataout;
end
```

The adjusted demand data have an average value of 11.22 MVA and a maximum value of 24.91 MVA. These are illustrated in Figure 6.5.

As far as the disaggregation is concerned, it is implemented as follows:

$$P_k(t) = D(t) \cdot \alpha_{type}(t) \cdot \beta_k,\ k = 1,2,\ldots,13, \qquad \text{(A5.1)}$$

where $P_k(t)$ is the power of the LP(s) (of S/S 1) at bus k at time t; $D(t)$ is the total demand at the substation at time t; $\alpha_{type}(t)$ is a time-varying coefficient, which expresses the share of the load type of the LP in the total demand at time t; and β_k is a time-invariant coefficient, which expresses the share of the LP in the total demand of this type. These coefficients are explained below.

First, using load profiles for each customer type (taken from [91]; see Figure 3.4 for residential), the total S/S demand is derived, which is illustrated in Figure A5.1. It is noted that all commercial customers were considered as residential in order to better match the shape of the input demand data.

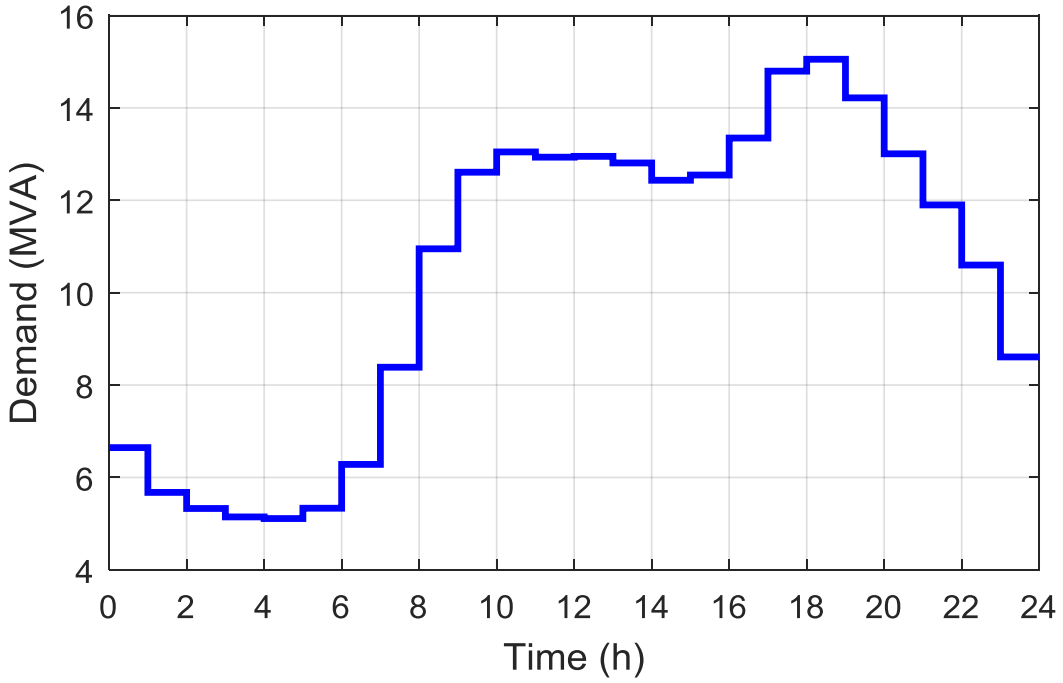

Figure A5.1: S/S 1 demand profile used to derive the time-varying coefficients $\alpha_{type}(t)$ for demand disaggregation in Chapter 6.

Considering the demand illustrated in Figure A5.1, as a typical load profile for S/S 1, the contribution of each customer type (and losses) at each time step t is calculated as follows:

$$\alpha_{type}(t) = \frac{D_{type}(t)}{D(t)}, \tag{A5.2}$$

where $D_{type}(t)$ is the demand of residential or industrial customers (or losses) at time t; and $D(t)$ is the total demand at the substation at time t (shown in Figure A5.1). Table A5.1 shows the derived values for $\alpha_{type}(t)$.

The second coefficient can be computed as:

$$\beta_k = \frac{P_{k,\,\mathrm{avg}}}{P_{type,\,\mathrm{avg}}}, \tag{A5.3}$$

where $P_{k,\,\mathrm{avg}}$ is the average active power of the LP(s) at bus k; and $P_{type,\,\mathrm{avg}}$ is the average active power of the total demand of all LPs of this type. The values for β_k are shown in Table A5.2.

Table A5.1: The shares of the demand of residential customers (a_{res}), industrial customers (a_{ind}), and losses (a_{loss}) in total S/S demand at each hour of the day ($a_{type}(t)$ values)

Hour	$\alpha_{res}(t)$	$\alpha_{ind}(t)$	$\alpha_{loss}(t)$	Hour	$\alpha_{res}(t)$	$\alpha_{ind}(t)$	$\alpha_{loss}(t)$
0	0.719	0.252	0.029	12	0.529	0.438	0.033
1	0.668	0.305	0.027	13	0.539	0.428	0.033
2	0.638	0.334	0.028	14	0.537	0.430	0.033
3	0.626	0.347	0.027	15	0.552	0.415	0.033
4	0.624	0.347	0.029	16	0.598	0.368	0.034
5	0.634	0.338	0.028	17	0.683	0.280	0.037
6	0.658	0.314	0.028	18	0.755	0.206	0.039
7	0.683	0.286	0.031	19	0.783	0.179	0.038
8	0.651	0.316	0.033	20	0.784	0.179	0.037
9	0.579	0.388	0.033	21	0.784	0.179	0.037
10	0.541	0.425	0.034	22	0.786	0.179	0.035
11	0.526	0.441	0.033	23	0.765	0.203	0.032

Table A5.2: The shares of the LP(s) at bus k in the total demand of this type (β_k values)

Bus	β_k	Bus	β_k
1	0.078	8	0.286
2	0.078	9	0.078
3	0.078	10	0.078
4	0.150	11	0.150
5	0.119	12	0.072
6	0.286	13	0.119
7	0.428		

It was described how the total demand of S/S 1 was disaggregated into the demand at each bus k (of S/S 1) at each time period t. The demand at each bus of the other two S/Ss of the network is considered to be proportional to the average power of the buses of S/S 1 of the same type. For example, the demand of bus 14 (LP 18) is considered equal to the demand of bus 1 (LP1), as they both have an average power of 0.545 MW and their type is residential. The data for the case study network can be found in [17].